

# **LIVE LOAD MODELS FOR HIGHWAY BRIDGES BASED ON PROVINCIAL TRAFFIC DATA**

by

**Diego G. Padilha**

B.Sc.E. (Civil Engineering), University of New Brunswick, 2017

A Thesis Submitted in Partial Fulfillment

of the Requirements for the Degree of

**Master of Science in Engineering**

in the Graduate Academic Unit of Civil Engineering

Supervisor: Kaveh Arjomandi, Ph.D, P.Eng, Department of Civil Engineering

Examining Board: Jeff Rankin, Ph.D, P.Eng, Department of Civil Engineering  
Othman Nasir, Ph.D, P.Eng, Department of Civil Engineering  
Shabnam Jabari, Ph.D, P.Eng, Department of Geodesy and  
Geomatics Engineering

UNIVERSITY OF NEW BRUNSWICK

June 2019

© Diego G. Padilha, 2019

## **ABSTRACT**

This thesis assesses the site-specific live load spectra in New Brunswick and the adequacy of the Canadian Highway Bridges Design Code (CAN/CSA-S6-14) CL-625-ONT live load model, which is used by the New Brunswick Department of Transportation and Infrastructure (NBDTI) for design and evaluation of highway bridges. In the past few decades, the heavy traffic loads have significantly increased and as presented in this thesis, the CL-625-ONT does not sufficiently represent the alterations in the local traffic conditions. As a result, two idealized live load models were developed to reflect the following: (1) normal traffic enforced by provincial laws and regulations; (2) nonconforming vehicles that are allowed to operate in the provincial highway bridge network under special permits. The proposed models were developed using a multi-objective optimization-based approach. The live load is quantified using an extensive Weigh-In-Motion (WIM) database from five sites in New Brunswick and a database containing permit applications that were approved by the NBDTI between 2014 and 2018. Four bridge configurations were considered in this study based on the provincial bridge inventory with spans ranging from 2m to 80m. The proposed live load models can further assist the NBDTI for the design and evaluation of medium and short span highway bridges in New Brunswick, as the findings presented in this thesis show that the CL-625-ONT load model is no longer representative of the current local traffic conditions.

## **ACKNOWLEDGEMENTS**

I am truly grateful to my parents, Walderes Padilha and Hudson Padilha, and my siblings, Bruno, Igor, Adriana and Socorro, for their endless love, support and inspiration since day one and for always pushing me to pursue my goals and be a better person each day.

I would like to express my deepest appreciation to my supervisor, Dr. Kaveh Arjomandi, for his continuous encouragement, guidance and indispensable support from my undergraduate research journey throughout my graduate studies. It has been an honor and a privilege to have him as a mentor. My appreciation is extended to Tracy MacDonald for her expertise, mentorship and encouragement during this research. I have learned tremendously from her. This study would not have been possible without their guidance and commitment to the profession.

Also, I would like to thank Haider Razak, Mohamad Salaheddine, and to all my friends for their constant support and motivation during this great adventure. Their positivity and friendship kept me focused and resilient. Thanks to my former coach Miles Pinsent, who brought me all the way from Brazil providing me with the opportunity to pursue my studies at UNB, and gave me indispensable support during my academic and athletic careers.

Thanks to the New Brunswick Department of Transportation and Infrastructure (NBDTI), and the Department of Civil Engineering at UNB for the study and research opportunities they provided, and to all the staff and colleagues for their incredible contributions. Finally, I would like to acknowledge the financial assistance provided by the NBDTI and The Natural Sciences and Engineering Research Council of Canada.

## Table of Contents

ABSTRACT.....	ii
ACKNOWLEDGEMENTS.....	iii
Table of Contents .....	iv
List of Tables.....	vii
List of Figures.....	viii
1 Introduction .....	1
1.1 Problem Statement.....	5
1.2 Research Objectives .....	6
1.3 Organization of the Thesis.....	6
1.4 Contribution of the Candidate .....	7
References .....	9
2 Methods of Analysis.....	11
2.1 Multi-Objective Optimization .....	11
2.1.1 MOO Algorithm.....	13
2.1.2 Problem Formulation .....	15
2.2 Bridge Idealization .....	16
2.3 Structural Analysis .....	17
2.3.1 Direct Stiffness Method for Beam Analysis .....	18
2.3.1.1 Element Stiffness Matrix.....	19
2.3.1.2 Forces and Displacements .....	20
2.3.1.3 MATLAB Code Validation.....	21
Notations.....	23
References .....	25

3	WIM-Based Live Load Model for Bridges Using Provincial Traffic Data.....	27
	Abstract.....	28
	3.1 Introduction .....	29
	3.2 New Brunswick Traffic WIM Data .....	35
	3.3 Moving Load Simulation.....	42
	3.4 Proposed Live Load Model .....	49
	3.5 Performance of CL-625-ONT .....	53
	3.6 Conclusions .....	54
	Notations.....	56
	References .....	58
4	Permit Vehicle Live Load Model for Evaluation of Highway Bridges in the Province of New Brunswick.....	61
	Abstract.....	62
	4.1 Introduction .....	63
	4.2 Development of Permit Live Load Models .....	67
	4.3 Statistical Analysis of New Brunswick Permit Database.....	70
	4.4 Permit Live Load Development .....	76
	4.4.1 Permit Vehicle Group .....	76
	4.4.2 Permit Truck Load Simulation.....	78
	4.5 Proposed Model.....	83
	4.6 Standard CL-625-ONT Performance.....	87
	4.7 Conclusions .....	88
	Notations.....	90
	References .....	91
5	Summary and Conclusions .....	94
6	Recommendations for Future Work .....	96

References.....	97
Appendix A: Direct Stiffness Method for Moving Load Analysis.....	103
Appendix B: WIM Quality Assurance.....	121
Appendix C: Raw WIM Database Sample .....	126
Appendix D: Raw Permit Database Sample .....	130
Curriculum Vitae	

## List of Tables

Table 1.1: Bridges in New Brunswick with BCI less than 60 .....	3
Table 3.1: Distribution of WIM trucks based on NOA .....	40
Table 3.2: Distribution of WIM trucks based on GVW .....	41
Table 3.3: Maximum load effects extrapolated for a 75-year lifespan .....	48
Table 4.1: Overall length, axle load, and gross vehicle weight limits in New Brunswick	66
Table 4.2: Distribution of New Brunswick bridge inventory in terms of number of spans .....	73
Table A.1: Variables used in the code. ....	104

## List of Figures

Figure 1.1: Distribution of the New Brunswick bridge inventory based on age .....	4
Figure 2.1: 2D beam kinematic degrees of freedom.....	18
Figure 3.1: CAN/CSA-S6-14 live load standards: (a) CL-625; (b) CL-625-ONT .....	31
Figure 3.2: New Brunswick Weigh-In-Motion stations (Retrieved from GeoNB 2018) .	36
Figure 3.3: NB WIM data cumulative distribution function for: (a) GVW; (b) axle load	38
Figure 3.4: Distribution of filtered WIM vehicles: (a) NOA; (b) GVW .....	39
Figure 3.5: Distribution of WIM data: (a) axle load; (b) axle spacing .....	42
Figure 3.6: Load effects distribution of WIM vehicles: (a) positive moment; (b) negative moment; (c) shear force .....	44
Figure 3.7: Statistical properties of maximum load effects of WIM vehicles: (a) negative moment; (b) positive moment; (c) shear force.....	46
Figure 3.8: Upper tail extrapolation of negative moment for 50m FF bridge configuration on normal probability plot .....	47
Figure 3.9: Load envelope: (a) shear; (b) moment .....	49
Figure 3.10: CL-810-NB idealized live load model .....	50
Figure 3.11: CL-810-NB performance indicator: (a) negative moment; (b) positive moment; (c) shear force .....	51
Figure 3.12: Comparison between NB normal traffic and OBF and MOL .....	52
Figure 3.13: CAN/CSA-S6-14 CL-625-ONT truck load performance (a) negative moment; (b) positive moment; (c) shear force.....	54
Figure 4.1: Typical vehicle dimensions controlled by NB – Motor Vehicle act (2001) ..	64
Figure 4.2: CAN/CSA-S6-14 live load models: (a) CL-625; (b) CL-625-ONT.....	68
Figure 4.3: NB permit database cumulative distribution functions for: (a) GVW; (b) axle load.....	72
Figure 4.4: Cumulative distribution function of New Brunswick bridge inventory.....	73
Figure 4.5: Distribution of permit vehicles: (a) NOA; (b) GVW .....	75

Figure 4.6: Permit vehicles axle load and spacing numbering .....	77
Figure 4.7: Distribution of New Brunswick permits: (a) axle load; (b) axle spacing.....	78
Figure 4.8: Load effects distribution of permit vehicles: (a) positive moment; (b) negative moment; (c) shear force .....	80
Figure 4.9: Statistical properties of load effects due to permits: (a) negative moment; (b) positive moment; (c) shear force.....	82
Figure 4.10: Load effects envelope: (a) shear; (b) moment.....	83
Figure 4.11: NB P10-1300 idealized permit live load model .....	84
Figure 4.12: Performance of NB P10-1300: (a) negative moment; (b) positive moment; (c) shear force .....	86
Figure 4.13: Comparison between NB permits and OBF and MOL .....	87
Figure 4.14: Performance of CL-625-ONT truck load model: (a) negative moment; (b) positive moment; (c) shear force.....	88
Figure A.1: Beam layout.....	107
Figure A.2: System parameters.....	108
Figure A.3: Boundary conditions.....	109
Figure A.4: Element stiffness matrix .....	110
Figure A.5: Global stiffness matrix .....	111
Figure A.6: Moving load layout.....	111
Figure A.7: Defining series of moving point loads.....	112
Figure A.8: Applying external loads.....	113
Figure A.9: Nodal displacement and support reactions .....	114
Figure A.10: Element forces .....	115
Figure A.11: Maximum load effect envelope.....	116
Figure A.12: Load effect diagrams .....	117
Figure A.13: Beam problem validation .....	118
Figure A.14: Moving load.....	119

Figure A.15: MATLAB results.....	119
Figure A.16: SAP2000 results .....	120
Figure B.1: WIM quality assurance of Deerwood Site.....	123
Figure B.2: WIM quality assurance of Longscreek Site.....	124
Figure B.3: WIM quality assurance of Waweig Site .....	124
Figure B.4: WIM assurance of Salisbury Eastbound.....	125
Figure B.5: WIM assurance of Salisbury Westbound .....	125
Figure C.1: WIM raw data from Waweig site. Columns 1 – 12.....	127
Figure C.2: WIM raw data from Waweig site. Columns 13 – 20.....	128
Figure C.3: WIM raw data from Waweig site. Columns 21 – 28.....	128
Figure C.4: WIM raw data from Waweig site. Columns 29 – 35.....	129
Figure C.5: WIM raw data from Waweig site. Columns 36 – 37.....	129
Figure D.1: Permit database. Columns 1 – 8 .....	131
Figure D.2: Permit database. Columns 9 – 21 .....	131
Figure D.3: Permit database. Columns 22 – 30 .....	132

# 1 Introduction

Bridges are key elements of the world's infrastructure that contribute to the growth and development of communities by providing critical links for the movement of goods, people, and services. These structures are designed to withstand the simultaneous actions of various load types including dead, live, wind, seismic, and thermal loads for an intended 75-year service life (CAN/CSA-S6-14). In Canada, highway bridge design loads are specified by the CAN/CSA-S6-14, where the structural components must comply with the Ultimate Limit States (ULS), Serviceability Limit States (SLS), and Fatigue Limit States (FLS). The ULS consists of the limit states associated with the structural safety, where the factored resistance must always exceed the total factored load effects. The SLS comprises of the limit states related to the life and appearance of the bridge accounting for vibrations, deflections, and cracks. The FLS consists of the limit states associated with the development of permanently induced damage as a result of cyclic transitory loads. In contrast to long span bridges, in which their design is governed by the dead load, for short and medium span bridges, the live load often governs (Tonias and Zhao 1995). This load type is highly site-specific and can vary substantially over time depending upon factors such as the population growth, the economy, and the dominant industry.

The significant increase in truck weights and volumes on the highway infrastructure over the past few decades has drawn the attention of numerous researchers across the world to assess the performance of the standard live load models outlined by codes of practice as well as to accurately model the actual live load imposed upon bridge structures (Nowak

1994; Kozikowski 2009, Taplin et al. 2013; Novak 1999; Nowak and Hong 1991; Davis et al. 2007). Many highway bridges in New Brunswick were designed and built several decades ago in accordance with the live load models specified by the Canadian Highway Bridge Design Code (CAN/CSA-S6) at the time. However, these codes legacy estimations of traffic are no longer representative of the normal traffic loads present in the province today. In addition, several permits are issued every year by the New Brunswick Department of Transportation and Infrastructure (NBDTI) to allow the operation of vehicles that do not comply with the provincial enforced truck size and weight regulations. This has become a major concern for the safety of the highway network, since the primary structural components of many operating bridges might be carrying loads substantially larger than their design capacity, thus, compromising the integrity of these structures.

The performance and functionality of a highway bridge diminish over time as the structure experiences numerous loadings, extreme events and harsh environmental conditions. In addition, the increase in live load can significantly impact the lifespan of these structures. In New Brunswick, highway bridges are inspected on a regular basis with different frequency depending upon age, structure type, and condition reported by provincial bridge inspectors. Each bridge component is assessed and quantitatively rated to calculate an overall Bridge Condition Index (BCI), which ranges from 0 to 100, with BCI of 100 being exceptional. According to the Bridge Integration System (BRDG 2018), used by the NBDTI for management purposes, there are 178 bridges in the province rated with a BCI of 60 or less. This does not necessarily mean the risk of structural failure; however, it is an indicator that significant maintenance work needs to be done in the near future to ensure

the safety of these structures. Table 1.1 summarizes the distribution of these structures among all the districts of New Brunswick. Fredericton contains the majority of them, representing 39.9% of the inventory.

Table 1.1: Bridges in New Brunswick with BCI less than 60

<b>District Number</b>	<b>District Name</b>	<b>Bridge Count</b>	<b>(%)</b>
1	Bathurst	15	8.4
2	Miramichi	14	7.9
3	Moncton	27	15.2
4	Saint John	31	17.4
5	Fredericton	71	39.9
6	Edmunston	20	11.2

The provincial bridge inventory is suffering from aging, as most jurisdictions around the world. Prior to 1970, most bridges in the province were designed and built for a 50-year service life and different live load models. Figure 1.1 summarizes New Brunswick’s bridge inventory based on the age of the structures, indicating that 26.78% of the bridges have already exceeded their 50-year lifespan, and a significant number of structures will be reaching their intended service life in the near future.

In this thesis, two main studies were undertaken. First, an extensive Weigh-In-Motion (WIM) database representative of the normal traffic conditions in New Brunswick collected from five sites in the province between 2014 and 2018 was analyzed. The maximum load effects of the WIM vehicles were calculated by extrapolation for a 75-year service life using probabilistic methods. A new idealized live load model, NB-810-NB, was developed to accurately account for the normal traffic load increase in the province

since the CL-625-ONT truck load model significantly underestimates the bridge responses due to the local traffic conditions.

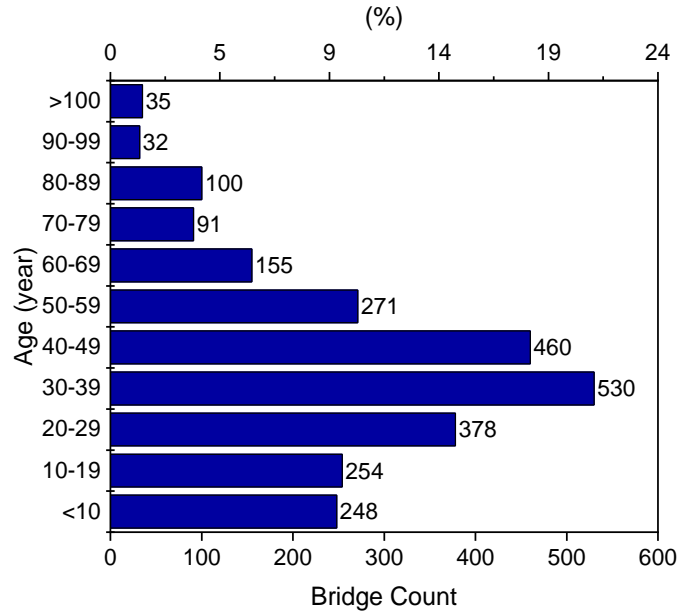


Figure 1.1: Distribution of the New Brunswick bridge inventory based on age

The province of New Brunswick currently does not use a standard permit live load model specific to the local nonconforming vehicle configurations. Hence, the significantly heavier loads that are permitted in the provincial infrastructure must be assessed individually on a case by case basis. This leads to an extremely time-consuming task and generates a substantial amount of workload for the NBDTI, where a large number of permits are processed. In the second topic of study, a truck database containing permit applications that were approved by the provincial authorities between 2014 and 2018 was also analyzed. A new permit live load model, NB P10-1300, was developed to assist the department for the evaluation of highway bridges in their designated heavy haul corridor, therefore, enhancing their efficiency for load rating practices.

## **1.1 Problem Statement**

The heavy truck loads across the Province of New Brunswick have changed substantially over the years, which has become a major concern to the integrity of the provincial highway bridge network as well as to the public safety. In addition, numerous permits are issued yearly, for overweight nonconforming vehicles to commute throughout the province. As the trucking industry has grown along with the increase in truck weights, numerous bridges may now be subjected to overstress. Furthermore, the provincial bridge inventory is suffering from aging, where 26.78% of the bridges have already exceeded their intended lifespan, and a significant amount of structures will be reaching their service life in the near future.

The NBDTI uses the CAN/CSA-S6-14 CL-625-ONT truck load model to represent the legal live loads considered for design and evaluation of bridges in New Brunswick. This load model was developed back in the 90's and it needs to be updated according to the current heavy truck demand imposed upon the bridge structures in the province. This is to ensure an adequate level of safety for bridges designed and evaluated today under the local requirements. Hence, it is deemed necessary the development of idealized legal and permit live load models which take into consideration these load changes and can potentially provide the NBDTI with the necessary tools for design and rating practices of the bridge infrastructure in New Brunswick.

## **1.2 Research Objectives**

The purpose of this study is to assess the site-specific traffic load demands to which highway bridges in New Brunswick are subjected and evaluate the adequacy of the currently used live load models to envelope the maximum load effects due to the local heavy truck loads. A WIM database representative of normal traffic collected from five sites across the province and a database containing permit applications approved by the NBDTI between 2014 and 2018 were used. Two new idealized live load models were developed to effectively reflect the actual traffic conditions in the province: (1) CL-810-NB; and (2) NB P10-1300.

## **1.3 Organization of the Thesis**

This thesis is presented in accordance with the articles-format and consists of two independent journal articles. Furthermore, introductory, theoretical background, and concluding chapters are included herein along with four appendices.

Chapter one is an introduction of the thesis providing an overview of the studies conducted along with the problem statement and the statement of objectives. The contributions and scope of the research are also included in this chapter.

Chapter two presents a brief summary of the fundamental theories adopted in this study, the multi-objective optimization algorithm used for the development of the proposed models, and the structural analysis method that was used to perform the moving load analysis.

Chapter three outlines the development of an idealized live load model for design and evaluation of medium and short span highway bridges in New Brunswick using a WIM database obtained from five sites in the province which represents the normal traffic. This chapter will be submitted to a journal in the field of bridge engineering as a research article.

Chapter four presents the development of a permit live load model for load rating practices of medium and short span bridges in New Brunswick using a database containing permit applications approved by the New Brunswick Department of Transportation and Infrastructure. This chapter will be submitted to a journal in the field of bridge engineering as a research article.

Chapter five consists of the summary and general conclusions of this study. Recommendations for future work and contributions to the professional practice are also outlined in this chapter.

#### **1.4 Contribution of the Candidate**

The two articles presented in this thesis were co-authored by the candidate's supervisor, Dr. Kaveh Arjomandi, and the industrial mentor from the NBDTI, Tracy MacDonald. The research topic was proposed by Tracy MacDonald and Dr. Arjomandi: live load models for design and rating practices of highway bridges in New Brunswick, whom provided the continuous guidance and implausible support for the completion of this research. The candidate identified the research problem outlined in each article, developed the necessary

analytical tools, analyzed the data, developed the proposed models and wrote the manuscripts under the supervision of Dr. Arjomandi.

## References

- Bridge Integration System – BRDG (2018). Information and Technology – *Production Internet Applications*. New Brunswick Department of Transportation and Infrastructure.
- CSA (Canadian Standards Association). (2014). Canadian highway bridge design code. *CAN/CSA-S6-14*.
- Davis, J., Nassif, H. H., Nawy, E. G., Najm, H. S., & Tsakalagos, T. (2007). Live-load models for design and fatigue evaluation of highway bridges. *Language*, 10.
- Kozikowski, M. (2009). WIM based live load model for bridge reliability. *Civil Engineering Dissertations and Student Research*, 2.
- Nowak, A. S. (1999). Calibration of LRFD Bridge Design Code (No. Project C12-33 FY'88-'92).
- Nowak, A. S. (1994). Load model for bridge design code. *Canadian Journal of Civil Engineering*, 21(1), 36-49.
- Nowak, A. S., & Hong, Y. K. (1991). Bridge live-load models. *Journal of Structural Engineering*, 117(9), 2757-2767.
- Taplin, G., Deery, M., van Geldermalsen, T., Gilbert, J., & Grace, R. (2013). A new vehicle loading standard for road bridges in New Zealand (No. 539).

Tonias, D. E., & Zhao, J. J. (1995). Bridge engineering: design, rehabilitation, and maintenance of modern highway bridges. New York, NY: McGraw-Hill.

## **2 Methods of Analysis**

This chapter provides a brief summary of the fundamental theories adopted in this thesis for the optimization algorithm used for the development of the proposed live load models and the structural analysis methods used to perform the moving load analysis of the New Brunswick database vehicles.

### **2.1 Multi-Objective Optimization**

Multi-Objective Optimization (MOO) deals with complex optimization problems that involve multiple decision criteria (Wang et al. 2009). MOO has been widely used in solving real world's problems in numerous fields such as engineering, computer science, economics, finance, and aerospace. For instance, Fathi and Afshar (2010) adopted a multi-objective Genetic Algorithm optimization model for a finance-based construction project scheduling. The goal of their studies was to search for the most suitable line of credit option for cash acquisition to optimize the initial construction schedule and limit the maximum negative cash flow based on the specific credit limit. Zavala et al. (2016) used the multi-objective metaheuristic optimization-based approach to solve a highway bridge design problem with the main objectives of minimizing the overall structural weight of a cable-stayed bridge while maximizing its stiffness.

Chen and Liu (1994) used the MOO goal-attainment method for the optimization of reactive power (VAR) planning under several operating and load constraints. The optimization objectives of their studies were to reduce the active power loss cost, minimize

the investment cost of VAR sources, enhance the system security and reduce the voltage deviation of the system. In another study, Cortes-Borda et al. (2015) adopted a multi-objective input-output approach that seeks to optimize the total economic output and the total life cycle of CO<sub>2</sub> emissions simultaneously and to identify the most significant economic sectors which contribute to global warming. In summary, the ultimate goal of MOO is to search for the most optimal solutions of an optimization problem containing more than a single objective function that need to be optimized simultaneously while satisfying certain predetermined constraints (Huang & Masud 1979). Nonetheless, in contrast to single objective optimization problems, where a unique optimal solution is feasible, for MOO there is always a tradeoff between the attainment of one objective and degradation of another, and the most suitable solution for the given problem shall be ultimately chosen by the decision maker. A general mathematical formulation of MOO can be expressed according the following Equation (2.1):

$$\min_{X \in \mathbb{R}} [f_i(x), f_{i+1}(x), \dots, f_n(x)], \text{ for } i = 1, 2, \dots, n \quad \text{s. t. } x \in X; \quad (2.1)$$

where  $X$  is the feasible set of decision vectors,  $F(x) = [f_i(x), f_{i+1}(x), \dots, f_n(x)]$  is the objective vector containing  $n$  objective functions that may be subject to certain constraints, and  $x = [x_j, x_{j+1}, \dots, x_m]$  is the vector of  $m$  decision variables. Therefore, the objective of MOO is to find a particular optimal set of values  $x^* = [x_j^*, x_{j+1}^*, \dots, x_m^*]$  that yields the optimal set of objective functions,  $F(x)^* = [f_i(x)^*, f_{i+1}(x)^*, \dots, f_n(x)^*]$ , while satisfying the specified constraints.

To the knowledge of the author, there is no available published literature on the application of MOO-based methods for the development of live load models for highway bridges. Instead, systematic iterative approaches have been used in the past. The latter leads to an extremely time-consuming task, since the iterations are performed with constant increments. In addition, this approach is highly sensitive to the initial search vector. As a result, an optimal solution may be achieved only after numerous iterations.

### **2.1.1 MOO Algorithm**

For the purpose of this study, the *fgoalattain* built-in solver available in the MATLAB Optimization Toolbox™ (MATLAB and Statistics Toolbox 2018) is used. The *fgoalattain* solver is used to solve optimization problems containing multiple objective functions that need to be optimized simultaneously. This algorithm is based on the goal-attainment method proposed by Gembicki & Haimes (1975), which is a powerful tool to search for the most optimal solution in nonlinear MOO problems by computing the non-inferior points. This method uses gradient-based Sequential Quadratic Programming (SQP), which represents the foundation of nonlinear programming methods. The formulation for the goal-attainment method is similar to the general representation of MOO algorithms described previously in Equation (2.1). However, three additional components are incorporated to the system: the unrestricted scalar variable  $\beta$ , the weighting vector  $w$ , and the design goal vector  $G(x)^*$ , which is associated with the nonlinear objective function  $G(x)$ . The ultimate goal of this method is to minimize  $\beta$  subject to a set of specified constraints as formulated in Equation (2.2).

$$\begin{array}{l} \text{Min } \beta \\ \beta \in \mathbb{R}, x \in \Omega \end{array} \text{ subject to } \begin{cases} G(x) - w \cdot \beta \leq G(x)^* \\ c(x) \leq 0 \\ ceq(x) = 0 \\ A \cdot x \leq b \\ Aeq \cdot x = beq \\ lb \leq x \leq ub \end{cases} \quad (2.2)$$

where the nonlinear objective function  $G(x)$  is given by:

$$G(x) = [g(x)_i, g(x)_{i+1}, \dots, g(x)_n]^T, \quad \text{for } i = 1, 2, \dots, n \quad (2.3)$$

The design goal vector  $G(x)^*$  is expressed by:

$$G(x)^* = [g(x)_i^*, g(x)_{i+1}^*, \dots, g(x)_n^*]^T, \quad \text{for } i = 1, 2, \dots, n \quad (2.4)$$

The decision function is:

$$x = [x_j, x_{j+1}, \dots, x_m]^T, \quad \text{for } j = 1, 2, \dots, m \quad (2.5)$$

where the weighting vector  $w = [w_i, w_{i+1}, \dots, w_n]^T$  controls the under- of over-achievement of  $G(x)^*$  and determines the optimization direction of search. The arrays of nonlinear inequality and equality constraints are  $c$  and  $ceq$ , respectively, which compute the nonlinear inequalities and equalities at  $x$ . The linear inequality and equality constraint matrices are  $A$  and  $Aeq$ , respectively. The corresponding linear inequality and equality constraint vectors are  $b$  and  $beq$ , respectively. The lower and upper bounds of the decision function are  $lb$  and  $ub$ , respectively, and  $\Omega$  is a feasible solution region that satisfies the specified constraints. In other words, the goal-attainment method seeks to minimize the difference between  $G(x)$  and  $G(x)^*$  by minimizing  $\beta$  and finding an  $x$  optimum.

### 2.1.2 Problem Formulation

Prior to performing the MOO using the MATLAB Optimization Toolbox™ *fgoalattain* solver, the problem needed to be properly formulated. The objective function  $G(x)$  was coded on MATLAB using the direct stiffness method for beam analysis, which is described in the next section. This function accepts the decision function  $x$  as input and returns a nonlinear objective function comprised of the maximum load effects due to  $x$  including negative moment  $M_i^-$ , positive moment  $M_i^+$ , and shear  $V_i$ . The design goal vector  $G(x)^*$  contains the respective maximum load effects threshold (TH), which are obtained from the moving load analysis of the database vehicle that need to be overachieved by  $G(x)$ , where  $p$  is the number of span lengths of interest. These functions must be in the form of a single vector as expressed in Equation 2.6.

$$G(x) = \begin{Bmatrix} M_i^+ \\ M_{i+1}^+ \\ \vdots \\ M_p^+ \\ M_i^- \\ M_{i+1}^- \\ \vdots \\ M_p^- \\ V_i \\ V_{i+1} \\ \vdots \\ V_p \end{Bmatrix}; G(x)^* = \begin{Bmatrix} M_i^+(\text{TH}) \\ M_{i+1}^+(\text{TH}) \\ \vdots \\ M_p^+(\text{TH}) \\ M_i^-(\text{TH}) \\ M_{i+1}^-(\text{TH}) \\ \vdots \\ M_p^-(\text{TH}) \\ V_i(\text{TH}) \\ V_{i+1}(\text{TH}) \\ \vdots \\ V_p(\text{TH}) \end{Bmatrix}; x \in \Omega, i = 1, 2, \dots, p \quad (2.6)$$

where  $x$  consists of the vehicle parameters that need to be optimized including  $k$  axle loads ( $AL_j$  to  $AL_k$ ) and  $k-1$  axle spacing ( $S_j$  to  $S_{k-1}$ ) as given in Equation 2.7.

$$x = [AL_j, \dots, AL_k, S_j, \dots, S_{k-1}]^T, \quad j = 1, 2, \dots, k \quad (2.7)$$

An initial search vector  $x_0$  must be defined as a start searching point, which is determined as the most governing vehicle configuration within the database. The weighting vector was set as ones for all  $n$  objectives in order to establish the same relative importance factor for all goals simultaneously. Furthermore, the *EqualityGoalCount* option was enabled on MATLAB for all objectives to force them the closest possible to the goals. The lower and upper bounds of  $x$  is given in Equation 2.8 and 2.9, respectively. These bounds were used to limit the magnitude of  $x$ .

$$lb = [AL_j^{lb}, \dots, AL_k^{lb}, S_j^{lb}, \dots, S_{k-1}^{lb}]^T \quad (2.8)$$

$$ub = [AL_j^{ub}, \dots, AL_k^{ub}, S_j^{ub}, \dots, S_{k-1}^{ub}]^T \quad (2.9)$$

## 2.2 Bridge Idealization

The beam analogy method was used for determining the longitudinal distribution of the load effects due to the one-lane moving load. In this method, the bridge is treated as a 2D beam. The load effects are then reduced by applying the Lateral Distribution Factor (LDF), also known as the truck load fraction, which can be either calculated in accordance with Chapter 5 of the CAN/CSA-S6-14 or using refined methods and computer modeling. The *LDF* is a function of number of lanes, girder spacing, number of girders, and bridge width. This factor determines the contribution of each girder to carry the live load that is transferred from the deck to the superstructure, as no girder will bear the full load by itself.

The multiple presence of vehicles on a bridge was not considered in this study, as the CAN/CSA-S6-14 states that the alternative live load model shall be also evaluated with its axle loads reduced by eighty percent, superimposed with the lane load specified in Chapters 3 and 14 for design and evaluation, respectively, which accounts for the traffic jam loading scenario.

### **2.3 Structural Analysis**

Displacement methods can be used to analyze structures, in which equilibrium equations are formulated in order to calculate the unknown joint displacements (Hibbeler 2015). The moment-distribution displacement and the slope-deflection methods have been widely used for analyzing simple structural systems by hand calculations. However, these methods are not ideal for analyzing complex statically indeterminate structures that require high computational efforts. In case of complex structures, the direct stiffness method is widely used. The latter is a matrix displacement analysis method which yields the displacement and forces directly and equilibrium equations are formulated into a single matrix relationship (Przemieniecki 1985). The main advantage of this method is the ability to analyze statically determinate and indeterminate structures equally, as it uses the kinematic redundancy rather than static. Matrix methods represent a powerful design tool in structural engineering, and most structural analysis software use the matrix analysis direct stiffness method.

### 2.3.1 Direct Stiffness Method for Beam Analysis

The first step required for the direct stiffness method is to define the structural system by subdividing the structure into a series of discrete finite elements and identifying their geometry such as the node numbers and coordinates, their connectivity, material and section properties, support conditions, and external applied loads. For two-dimensional beam analysis, the finite elements are represented by each of the members that comprise the beam, and the nodes represent the joints. The global  $(x, y)$  and local  $(x', y')$  coordinates are collinear. Each element has four kinematic degrees of freedom (DOF), as shown in Figure 2.1, where there is a vertical displacement  $v_i$  and a rotation  $\theta_i$  at each node, corresponding to a force  $f_i$ , and a moment  $m_i$ , respectively. All forces and displacements represented in this figure are acting in the positive direction. External loads must be applied at the joints, and members shall be prismatic. Hence, the nodes must be identified where the member cross-section changes, at support locations, where members are connected together, where external loads are applied and at specific locations of interest.

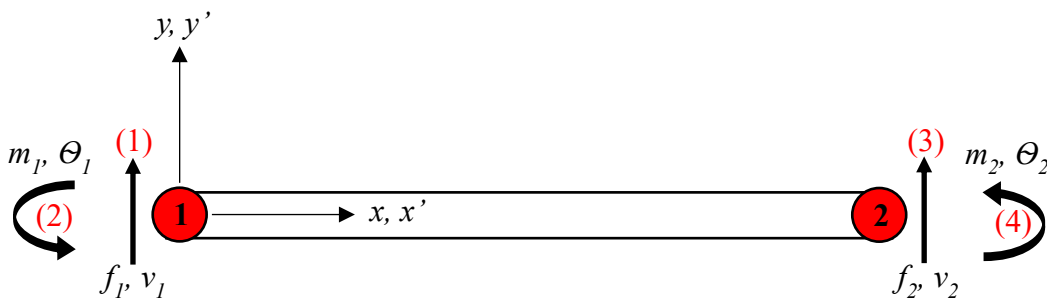


Figure 2.1: 2D beam kinematic degrees of freedom

The force equilibrium equations can then be formulated at each node by determining the force-displacement properties of each element. Once these relationships are determined, the stiffness matrix for each element  $k^{(i)}$ , can be calculated and then assembled together into a global stiffness matrix  $K$  that represents the structural system. The unknown nodal displacements can be calculated for any applied load, and force-displacement relations for each member can be used to determine the support reactions and internal shear and moment at the nodes of the structure. The following procedure describes the direct stiffness method:

- i. Identifying the nodes and elements of the beam
- ii. Identifying the kinematic DOF at each node
- iii. Calculating the stiffness method for each element  $k^{(i)}$
- iv. Assembling element stiffness matrices into a global stiffness matrix  $K$
- v. Defining the boundary conditions
- vi. Calculating nodal displacements, support reactions and internal member forces

### **2.3.1.1 Element Stiffness Matrix**

The element stiffness matrix  $k^{(i)}$ , comprises of sixteen stiffness coefficients  $k_{ij}$  that corresponds to the force required  $f_i$ , at the  $i^{th}$  DOF to produce a unit displacement  $d_j$ , at the  $j^{th}$  DOF, while all other displacements are prevented. The DOF numbering is represented inside brackets in Figure 2.1, where the vertical displacement and rotation at the joint 1 represent the first and second DOFs, respectively, and the displacement and rotation at

joint 2 represent the third and fourth DOFs, respectively. In this study, the Timoshenko beam theory (Timoshenko 1921) was used to calculate  $k^{(i)}$ , which accounts for shear deformations and is given by Equation 2.10:

$$k^{(i)} = \frac{EI}{L^3(1 + \beta_s)} \begin{bmatrix} 12 & 6L & -12 & 6L \\ 6L & L^2(4 + \beta_s) & -6L & L^2(2 - \beta_s) \\ -12 & -6L & 12 & -6L \\ 6L & L^2(2 - \beta_s) & -6L & L^2(4 + \beta_s) \end{bmatrix} \quad (2.10)$$

Where the coefficient  $\beta_s$  is a function of the modulus of elasticity  $E$ , moment of inertia  $I$ , shear modulus  $G$ , cross-sectional area  $A$ , shape factor  $f_s$ , and the element length  $L$ . This coefficient is calculated according to Equation 2.11.

$$\beta_s = \frac{12EI f_s}{GAL^2} \quad (2.11)$$

The load-displacement relationship can then be used to express all DOFs in a matrix form for each element as shown in Equation 2.12:

$$\begin{Bmatrix} f_1 \\ m_1 \\ f_2 \\ m_2 \end{Bmatrix} = \frac{EI}{L^3(1 + \beta_s)} \begin{bmatrix} \mathbf{v}_1 & \boldsymbol{\theta}_1 & \mathbf{v}_2 & \boldsymbol{\theta}_2 \\ 12 & 6L & -12 & 6L \\ 6L & L^2(4 + \beta_s) & -6L & L^2(2 - \beta_s) \\ -12 & -6L & 12 & -6L \\ 6L & L^2(2 - \beta_s) & -6L & L^2(4 + \beta_s) \end{bmatrix} \begin{Bmatrix} v_1 \\ \theta_1 \\ v_2 \\ \theta_2 \end{Bmatrix} \quad (2.12)$$

### 2.3.1.2 Forces and Displacements

Once each element stiffness matrix has been determined in the global coordinate system, they must be assembled into the global stiffness matrix  $K$ , using superposition. Each  $k^{(i)}$  must be placed at same global coordinate of the  $K$  matrix. This matrix relates the global

force vector  $F$ , to the global displacement vector  $D$  (Equation 2.13) and is a square matrix of an order equal to the total number of DOF of the system.

$$\{F\} = [K]\{D\} \quad (2.13)$$

Where  $F$  and  $D$  consist of the known and unknown externally applied loads and displacements, respectively. Equation 2.13 can be portioned as given in Equation 2.14 to group the known and the unknown DOFs together.

$$\begin{Bmatrix} F_{Known} \\ F_{Unknown} \end{Bmatrix} = \begin{bmatrix} K_{11} & K_{12} \\ K_{21} & K_{22} \end{bmatrix} \begin{Bmatrix} D_{Unknown} \\ D_{Known} \end{Bmatrix} \quad (2.14)$$

Expanding Equation 2.14 yields the two following equations:

$$F_{Known} = K_{11}D_{Unknown} + K_{12}D_{Known} \quad (2.15)$$

$$F_{Unknown} = K_{21}D_{Unknown} + K_{22}D_{Known} \quad (2.16)$$

Therefore,  $D_{Unknown}$  can be determined directly from Equation 2.15, and the support reactions  $F_{Unknown}$  can be consecutively calculated according to Equation 2.16. Finally, the internal forces including shear and bending moment can then be calculated using Equation 2.12.

### 2.3.1.3 MATLAB Code Validation

The direct stiffness method was implemented into a MATLAB code to perform the moving load analysis of the truck database used in this study. The beams are subdivided into a series of discrete finite elements. Each element is 0.1m long. The trucks are simulated as

moving loads where the axle loads move incrementally over each joint along the beam, and the maximum shear force and bending moment are calculated at each joint. The maximum load effect envelopes are then assembled as the truck exits the beam. The MATLAB code was validated using the SAP2000 software version 18.2 (SAP2000 2018). The MATLAB code manual and its validation can be found in Appendix A of this thesis.

## Notations

The following symbols are used in this chapter:

$A$  = Beam cross sectional area; Linear inequality constraints matrix;

$A_{eq}$  = Linear equality constraints matrix;

$AL$  = Vehicle axle load;

$b$  = Linear inequality constraints vector;

$b_{eq}$  = Linear equality constraints vector;

$c$  = Nonlinear inequality constraints;

$c_{eq}$  = Nonlinear equality constraints;

$D$  = Global displacement vector;

$DOF$  = Degree of freedom;

$E$  = Beam modulus of elasticity;

$f$  = Shear force;

$F$  = Global force vector;

$f_s$  = Shape factor;

$F(x)$  = Objective function;

$F(x)^*$  = Optimal objective function;

$G$  = Shear modulus;

$G(x)$  = Nonlinear objective function;

$G(x)^*$  = Design goal vector;

$I$  = Beam moment of inertia;

$k$  = Number of axles on a vehicle

$K$  = Global stiffness matrix;

$k_{ij}$  = Stiffness coefficient;

$k^{(i)}$  = Element stiffness matrix

$L$  = Finite element length;

$lb$  = Lower bound of decision function;

$LDF$  = Lateral distribution factor;

$m$  = Number of decision variables; moment;

$M_i^-, M_i^+$  = Negative and positive moment;  
 $MOO$  = Multi-objective optimization;  
 $n$  = Number of objective functions;  
 $p$  = Number of span lengths of interest;  
 $S$  = Axle spacing;  
 $SQP$  = Sequential quadratic programming;  
 $TH$  = Threshold;  
 $ub$  = Upper bound of decision function;  
 $VAR$  = Optimization of reactive power;  
 $v$  = Vertical displacement;  
 $V_i$  = Shear;  
 $w$  = Weighting vector;  
 $x$  = Decision function; global coordinate;  
 $X$  = Feasible set of decision functions;  
 $x_0$  = Initial search vector;  
 $x'$  = Local coordinate;  
 $x^*$  = Optimal decision vector;  
 $y$  = Global coordinate;  
 $y'$  = Local coordinate;  
 $\beta$  = Unrestricted scalar variable;  
 $\beta_s$  = Timoshenko coefficient;  
 $\Theta$  = Rotation;  
 $\Omega$  = Feasible solution region;

## References

- Chen, Y. L., & Liu, C. C. (1994). Multiobjective VAR planning using the goal-attainment method. *IEE Proceedings-Generation, Transmission and Distribution*, 141(3), 227-232.
- Cortés-Borda, D., Ruiz-Hernández, A., Guillén-Gosálbez, G., Llop, M., Guimerà, R., & Sales-Pardo, M. (2015). Identifying strategies for mitigating the global warming impact of the EU-25 economy using a multi-objective input–output approach. *Energy Policy*, 77, 21-30.
- Fathi, H., & Afshar, A. (2010). GA-based multi-objective optimization of finance-based construction project scheduling. *KSCE Journal of Civil Engineering*, 14(5), 627-638.
- Gembicki, F., & Haimes, Y. (1975). Approach to performance and sensitivity multiobjective optimization: The goal attainment method. *IEEE Transactions on Automatic control*, 20(6), 769-771.
- Hibbeler, R. C. (2015). *Structural analysis ninth edition*. Pearson Prentice Hall.
- Hwang, C. L., & Masud, A. S. M. (2012). *Multiple objective decision making methods and applications: a state-of-the-art survey* (Vol. 164). Springer Science & Business Media.
- MATLAB and Statistics Toolbox Release 2018a (2018), The MathWorks, Inc., Natick, Massachusetts, United States.
- Przemieniecki, J. S. (1985). *Theory of matrix structural analysis*. Courier Corporation.

SAP2000. (2018). Integrated finite element analysis and design of structures, Computers and Structures, Berkeley, CA.

Timoshenko, S. P. (1921). On the correction for shear of the differential equation for transverse vibrations of prismatic bars. *Phil. Mag.*, 41, 744-746.

Wang, J. J., Jing, Y. Y., Zhang, C. F., & Zhao, J. H. (2009). Review on multi-criteria decision analysis aid in sustainable energy decision-making. *Renewable and sustainable energy reviews*, 13(9), 2263-2278.

Zavala, G., Nebro, A. J., Luna, F., & Coello, C. A. C. (2016). Structural design using multi-objective metaheuristics. Comparative study and application to a real-world problem. *Structural and Multidisciplinary Optimization*, 53(3), 545-566.

### **3 WIM-Based Live Load Model for Bridges Using Provincial Traffic Data**

**Diego Padilha<sup>1</sup>; Kaveh Arjomandi, Ph.D., P.Eng.<sup>2</sup>; and Tracy MacDonald, P.Eng.<sup>3</sup>**

<sup>1</sup>Research Assistant, Department of Civil Engineering, University of New Brunswick, Fredericton, NB, E3B 5A3, Canada. E-mail: dpadilha@unb.ca.

<sup>2</sup>Associate Professor, Department of Civil Engineering, University of New Brunswick, Fredericton, NB, E3B 5A3, Canada (corresponding author). E-mail: kaveh.arjomandi@unb.ca.

<sup>3</sup>Bridge Engineer, New Brunswick Department of Transportation and Infrastructure, Fredericton, NB, E3B 5H1, Canada. E-mail: tracy.macdonald@gnb.ca.

## **Abstract**

Highway bridges must be designed to withstand the simultaneous actions of various load types including dead, live, thermal, wind, and seismic loads. In Canada, bridge design loads are specified by the Canadian Highway Bridge Design Code (CAN/CSA-S6-14). This paper focuses on the idealized bridge live loads recommended by CAN/CSA-S6-14 for the design and evaluation of highway bridges. Live load is highly site-specific, and its spectra has significantly changed over the past few decades. In this study, an updated live load model is developed for the design and evaluation of medium and short span highway bridges that accounts for the current traffic conditions in New Brunswick. The proposed model was developed using a multi-objective optimization-based approach and an extensive WIM database recorded between 2014 and 2018 in five sites across the province. Based on the provincial bridge inventory, four bridge configurations spanning from 2m to 80m were considered in this study. A High-Performance Computing (HPC) clustering was used to perform the moving load analysis and optimization. Statistical methods were employed to account for the maximum load effects in a 75-year service life. The performance of the currently used design live load model (CAN/CSA-S6-14 CL-625-ONT) by the New Brunswick Department of Transportation and Infrastructure (NBDTI) in design and evaluation of bridges is also described herein. Finally, it is shown that the proposed model accurately represents the live loads across the province that are insufficiently estimated by the currently used load models.

### 3.1 Introduction

Bridges are core components of the world's highway infrastructure that contribute to the growth and development of communities by providing critical links for the movement of goods, people, and services. As per the Canadian Highway Bridge Design Code (CAN/CSA-S6-14), the bridge design loads are categorized into permanent, transitory and exceptional loads. The dead loads are a type of permanent loads that account for the weight of all structural and non-structural components of the bridge. The dominant transitory loads are live loads that represent the critical vehicular loadings and vary in their position and magnitude. Bridges may also be subjected to exceptional loads such as seismic or collision loads. In contrast to long span bridges in which the dead load is more critical than the live load; for short and medium span bridges, live load is generally the governing loading case (Tonias and Zhao 1995). This load type is highly site-specific and is represented by code provisions in the form of idealized live load models to reflect the most governing load effects caused by the heavy truck loads. Trucks are available in a variety of axle configurations and Gross Vehicle Weight (GVW). As a result, quantifying economical and safe live load spectra imposed upon the highway bridges becomes extremely challenging.

Prior to the mid 70's, the design live load was developed using truck surveys collected from stationary weigh stations. Later, with the advancement of technology, Weigh-in-motion (WIM) systems were implemented on many jurisdictions across the world to enforce and monitor the local traffic loads in real time (Nowak and Rakoczy 2013; Miao and Chan 2002; Gindy and Nassif 2015; Sivakumar and Sheikh 2017; Getachew and

Obrien 2007). The latter allows a more accurate estimation of unbiased live load than one could obtain from conventional static weigh stations as some heavily loaded trucks could simply avoid the respective routes.

Many Canadian highway bridges were designed and built several decades ago in accordance with the standard live load models specified by the CAN/CSA-S6 at the time. These CAN/CSA-S6 legacy estimations of traffic do not necessarily reflect the equivalent heavy truck loads currently imposed upon bridge structures in the country. In addition, the advancement in the automobile industry has led to the development of modern trucks that are capable of transporting substantially heavier loads than in the past few decades. Although these vehicles are equipped to haul larger volumes of goods and therefore contribute to the economy and reduce emissions, they pose major risks to the safety of the highway bridge network. The increase in truck capacities and axle loads may lead to overstress of the primary structural components, thus, diminishing the life expectancy of the bridge structures. In order to enhance the safety of the highway network and control the legal allowable vehicular loading, different jurisdictions enforce truck weight and size regulations in accordance with their bridge inventory (Luskin and Walton 2001). Vehicles that do not comply with the enforced laws are required to apply for a permit to operate on the highway infrastructure.

Upon the creation of the Memorandum of Understanding on Vehicle Weights and Dimensions (MOU) signed by all provinces in Canada, which contains a set of regulations for interprovincial transportation, the CAN/CSA-S6-14 established the CL-625 loading

model (Figure 3.1a) as the minimum live load requirements for the design of a national highway network. However, the CAN/CSA-S6-14 also provides flexibility for the provinces to develop an alternative live load model based on the site-specific vehicles and traffic conditions that better reflect the normal traffic within their respective jurisdictions. Currently, all bridges in New Brunswick are designed and evaluated in accordance with the CAN/CSA-S6-14 using the Ontario loading model CL-625-ONT (Figure 3.1b), which is a slightly modified version of the CL-625 with heavier tandem axles.

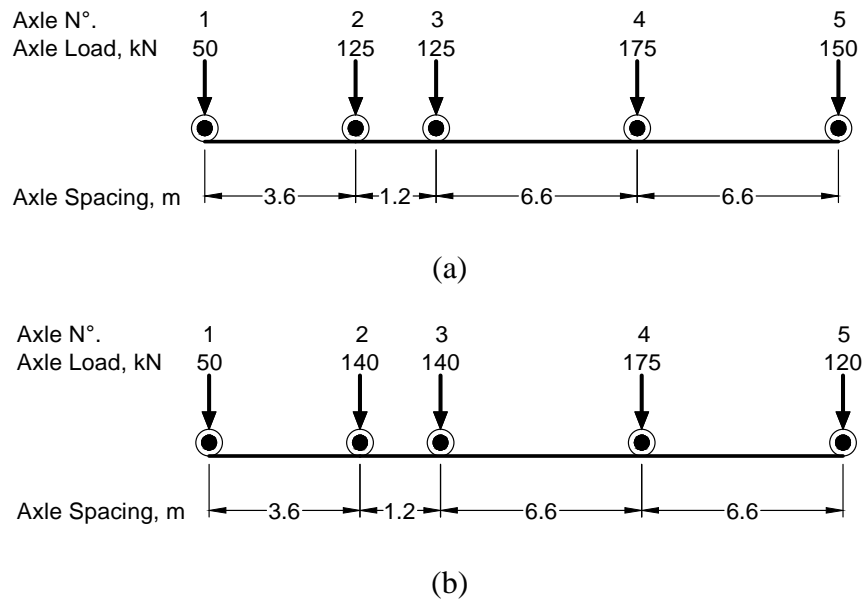


Figure 3.1: CAN/CSA-S6-14 live load standards: (a) CL-625; (b) CL-625-ONT

The significant increase in truck weights and volumes on the highway infrastructure over the past few decades has drawn the attention of many researchers across the world to assess the performance of the standard live load models outlined by code provisions, as well as to accurately model the actual heavy truck loads imposed upon bridge structures. Live loads like most phenomena in life are defined as random variables, which cannot be expressed as an absolute value. Due to the uncertainties associated with the predictions of this load

type, probabilistic methods are used to determine its variation and extrapolation techniques are carried out to forecast future trends.

Local traffic data have been widely used by several researchers for the development and calibration of highway bridge live load models across the world. For instance, Taplin et al. (2013) analyzed WIM records from five regions of New Zealand to develop a new vehicle loading standard for design and evaluation of bridge structures in the country. The findings of his study were used to update the legacy model that was introduced in 1972 and was no longer representative of the local traffic. In another study, Kozikowski (2009) examined WIM data from different sites across the United States (US) that were collected between 2005 and 2007. In his study, a comparison between the most up-to-date and the original truck data was carried out indicating that on average the vehicles from the WIM database are lighter than the Ontario trucks. Based on his findings, it was concluded that the existing live load model HL-93 outlined by the American Association of State Highway and Transportation Officials (AASHTO) at the time was still adequate for representing the local traffic across the US, except for New York, where extremely heavy loads were present and calibration was deemed necessary.

Nowak (1994) analyzed a traffic database containing two truck surveys conducted in Ontario in 1975 and 1988, respectively. These truck surveys contained over 11,000 heavily loaded trucks. The load effects including shear and moment for spans ranging from 9m to 60m were extrapolated for a 50-year lifespan using the normal probability plot method. In his study, a new calibrated live load model was proposed, in which the tandem axle load

of the Ontario truck load model at the time (OHBDC-1983) was increased to reflect the actual traffic demand present in the province. In another study, Nowak (1999) used truck surveys and WIM data collected in the US for modeling bridge live loads. The maximum load effects were calculated by extrapolation for a 75-year return period using the normal probability plot technique with the assumption that the legal load limits and the truck population remained unchangeable during the 75-year service life. The maximum load effects were evaluated against the load effects caused by the AASHTO HS-20 loading standard, and it was found that the actual load effects experienced by highway bridges in the US were of a magnitude up to 1.8 times greater than the HS-20 load effects. A new live load model was introduced to account for the up-to-date load effects imposed upon the American highway network.

Calibration of live loads may also result in lighter truck load models. Leahy et al. (2016) evaluated WIM database from a site in The Netherlands to study the traffic load characteristics in the European Union. Based on the findings of their study, the European Load Model 1 (LM1), used for the design of highway bridges, was observed to be overly conservative and a new model was proposed by applying reduction scale factors to the axle loads of the LM1. A general calibration approach has been used for the development of highway bridge live load models in the previously mentioned studies. The site-specific truck database was evaluated on different bridge configurations in order to calculate the maximum load effects including shear and moment. The load effects were compared with the ones due to the current standard load model, and probabilistic techniques were used to calculate the maximum load effects by extrapolations for the bridge intended service life.

Finally, based on the performance of the standard load model to envelope the maximum load effects due to the database vehicles, calibration was carried out to the existing model in order to accurately represent the local traffic conditions.

In this study, the performance of the current live load model (CL-625-ONT) used by the NBDTI is evaluated against the normal traffic load spectra observed in the province today. WIM data collected from the NBDTI in five sites across New Brunswick between 2014 and 2018 were analyzed. A data quality check was first performed on the vehicle database to ensure the reliability of the WIM data. The statistical properties of the traffic database are described in detail. For the purpose of this research, the database was filtered and vehicles that do not comply with the provincial truck size and weight regulations such as permit trucks and mobile cranes were removed from the analysis. The heaviest 5% vehicles in each class defined by the Federal Highway Administration (FHWA) were further analyzed. Based on the provincial bridge inventory, four bridge configurations spanning from 2m to 80m were considered. Parallel processing computer algorithms were used to perform the moving load analysis and the optimization for the development of the proposed live load model. The future estimation of the maximum load effects was also calculated by extrapolating the analysis results for a 75-year intended service life. The statistical properties of the maximum load effects due to site-specific traffic loads are also discussed. An idealized live load model was developed for design and evaluation of medium and short span bridges in the province that accurately reflect the up-to-date site-specific normal traffic.

### **3.2 New Brunswick Traffic WIM Data**

Five sites in New Brunswick are equipped with WIM systems and managed by the NBDTI. These sites are located along the Routes 1 and 2 as depicted in Figure 3.2: (1) Deerwood, (2) Longscreek, (3) Waweig, (4) Salisbury Eastbound, and (5) Salisbury Westbound. The WIM stations house tracking sensors such as piezoelectric sensors, single load-cell WIM scales, and inductive loops embedded on the pavement. The stations are also equipped with License Plate Cameras (LPC) and Side View Cameras (SVC) that are used to monitor the traffic loads at highway speed in real time, and to identify any vehicle configuration that do not comply with the provincial size and weight regulations. The LPCs are used to capture the license plate while the SVCs record an overview photo of vehicles travelling in a lane. The inductive loops trigger the passage of the vehicles through the system while the WIM scales and piezoelectric sensors record parameters that are used to quantify the live load spectra such as the axle weight, the axle spacing, the Number of Axles (NOA) and the GVW (Hanson et al. 2010). Nonconforming vehicles are directed to exit the highway and to report to an inspection station with a static scale for further weighing assessment. In the data recorded by the WIM stations, the vehicles are categorized according to the classification system established by the FHWA. Only vehicles from class 4 (buses) to class 13 (seven or more axle multi-trailer trucks) are recorded. Classes 1-3 are discarded by the WIM system since they represent passenger vehicles and their load effects have negligible influence compared to the other vehicle classes.

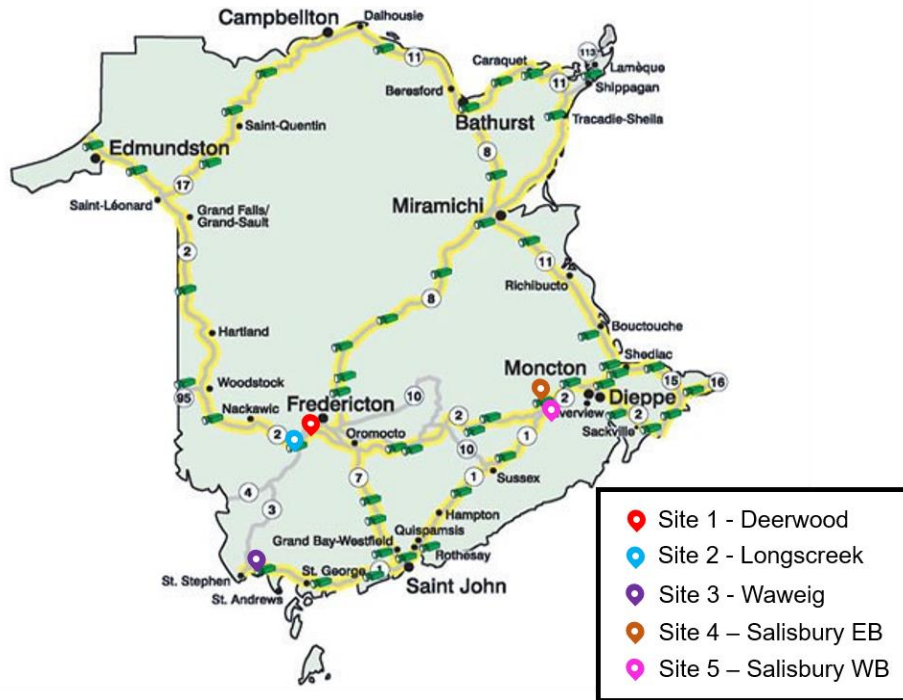


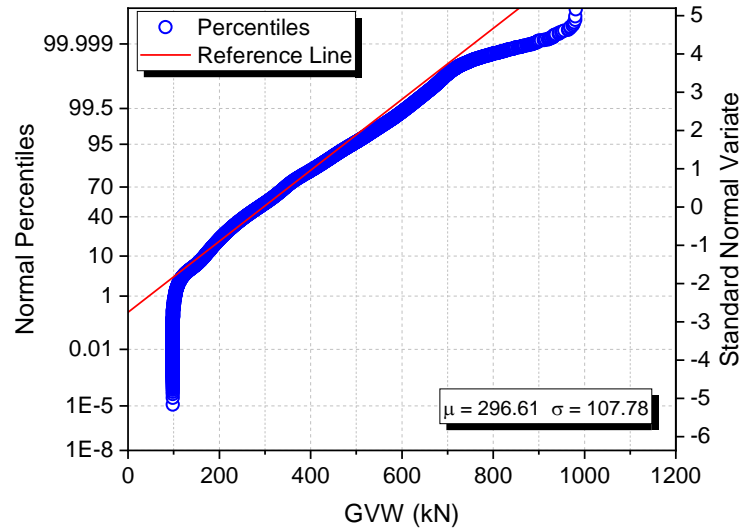
Figure 3.2: New Brunswick Weigh-In-Motion stations (Retrieved from GeoNB 2018)

In this study, a traffic database containing 5,258,500 vehicles obtained from the five WIM stations across the province of New Brunswick from 2014 to 2018 was analyzed. Figure 3.3 illustrates the cumulative distribution function (CDF) of the WIM database on a normal probability plot in terms of (a) GVW and (b) axle load. As seen in Figure 3.3a, 99.67% of the vehicles have a maximum GVW of 625kN, with a mean value of 296.61kN and a standard deviation of 107.78kN. This also indicates that the vehicles exceeding the legal provincial GVW limit (613.13kN) only represent 0.46% of the database, with the heaviest vehicle configuration weighing 981kN. Figure 3.3b reveals that 99.99% of the vehicles have a maximum axle load of 150kN, and only 3.10% of these vehicles exceed the provincial enforced axle load limit (89.27kN). As seen in this figure, the mean value for an individual axle load is 61.29kN with a standard variation of 15.68kN. Furthermore, the

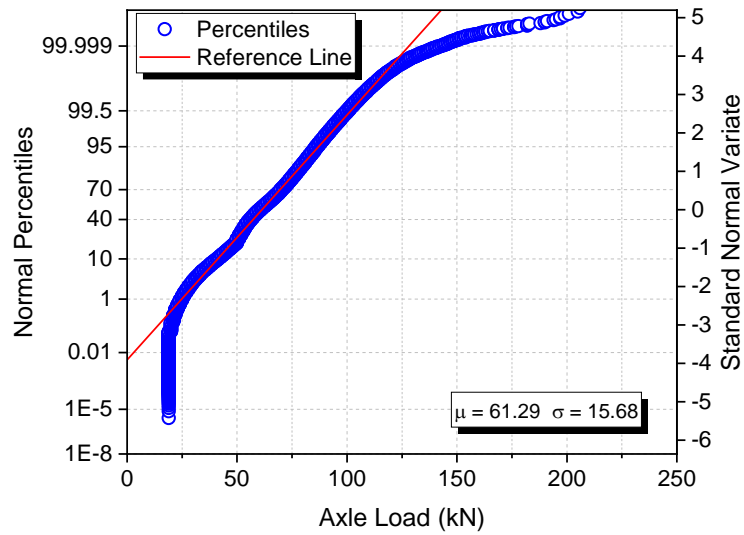
presence of some extremely heavy axle loads in the province with the heaviest being mobile cranes weighing 207kN is evident. These extreme loads represent less than  $1.9 \times 10^{-5}$  % of the WIM records and are considered to be special escorted vehicles that shall not operate simultaneously with normal traffic.

The WIM system records the traffic loads in real time as the vehicles move over the tracking sensors, and calibration must be conducted on a regular basis to ensure the proper operation of the system. Several factors may affect the calibration of a WIM system including the effects from temperature, calibration drift over, improper installation, poor maintenance, and stiffness of flexible asphalt (Southgate 2001). Prior to proceeding to the analysis of the WIM records studied herein, a data quality check was performed using a calibration assurance technique proposed by Southgate (2001).

Upon completing the data quality check, the WIM database was filtered in order to discard any incorrect or impractical information that could impact the analysis results. Trucks with inconsistencies in the number of axles and spacing were removed from the database. In this analysis, the WIM database was grouped based on the NOA. The database was further filtered to limit the maximum GVW to 625kN, the maximum axle load to 150kN, and the minimum axle spacing to 1.0m. These criteria removed erroneous measurements and permit vehicles that represented 0.34% of the database. Finally, the 5% heaviest filtered vehicles were used for further analysis. This criterion was employed to optimize the computational efforts required to analyze the entire database. A total of 172,328 vehicles complied using the applied filters and proceeded to the truck moving load simulation.



(a)



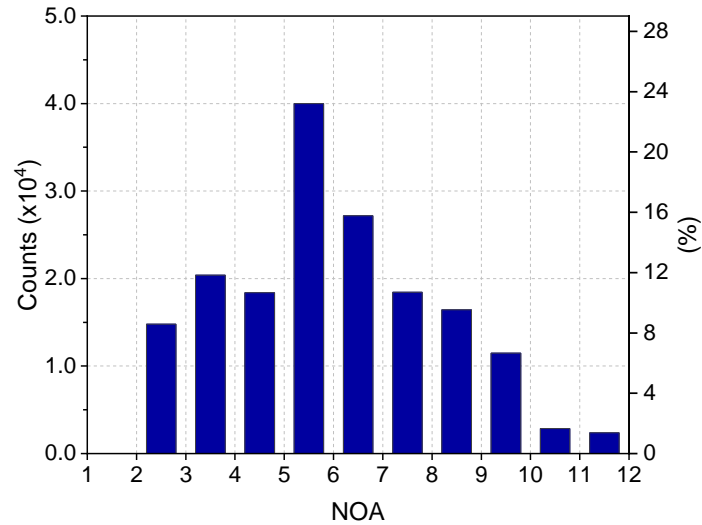
(b)

Figure 3.3: NB WIM data cumulative distribution function for: (a) GVW; (b) axle load

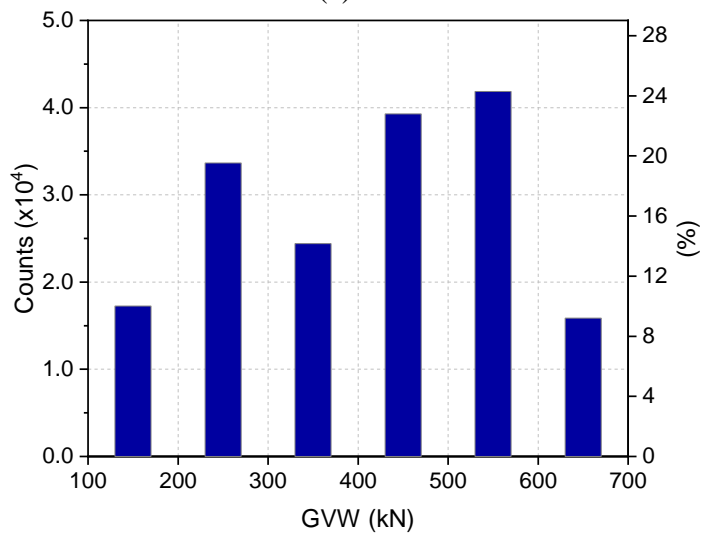
Figure 3.4 presents the distribution of the filtered vehicles based on the NOA and GVW.

Figure 3.4a illustrates that the five-axle truck configuration is the dominant vehicle class representing 23.21% of the filtered database. These vehicles are equivalent to the Class 9 in the FHWA, representing the most commonly used five-axle single-trailer trucks for

haulage in North America. This category of vehicles was the basis for the development of the CAN/CSA-S6-14 CL-625 loading standard.



(a)



(b)

Figure 3.4: Distribution of filtered WIM vehicles: (a) NOA; (b) GVW

Tables 3.1 and 3.2 summarize the distribution of the WIM database in terms of NOA and GVW, respectively, prior to and after filtering. As seen in Table 3.1, all vehicles containing 12 axles were not included in the analysis, as these vehicles were considered to be permit

vehicles after filtering the database. Furthermore, Table 3.2 illustrates that the majority of the filtered vehicles (47.28%) weigh between 400kN and 600kN, and 8.9% of the vehicles weigh between 600kN and 625kN.

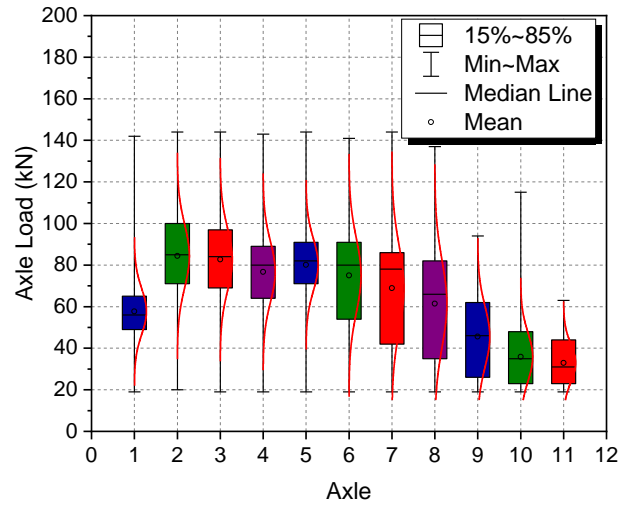
Table 3.1: Distribution of WIM trucks based on NOA

NOA	Raw Data		Filtered Data	
	Count	%	Count	%
2	115,346	2.19	14,797	8.59
3	300,624	5.72	20,380	11.83
4	75,305	1.43	18,389	10.67
5	2,687,043	51.10	39,998	23.21
6	1,670,918	31.78	27,164	15.76
7	195,581	3.72	18,445	10.70
8	167,282	3.18	16,440	9.54
9	39,239	0.75	11,472	6.66
10	4,251	0.08	2,863	1.66
11	2,864	0.05	2,380	1.38
12	47	0.00	-	-
Total	5,258,500		172,328	

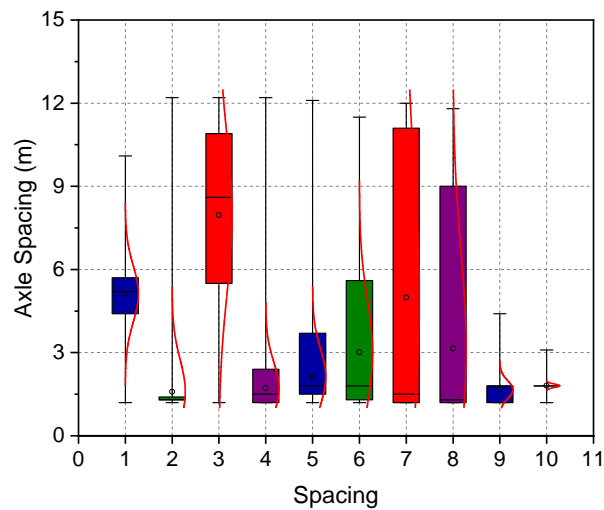
Table 3.2: Distribution of WIM trucks based on GVW

GVW (kN)	Raw Data		Filtered Data	
	Count	%	Count	%
<100	29,161	0.55	-	-
100-200	1,020,747	19.41	17,359	10.07
200-300	1,796,735	34.17	33,682	19.55
300-400	1,516,997	28.85	24,477	14.20
400-500	661,087	12.57	39,267	22.79
500-600	200,098	3.81	42,210	24.49
600-700	32,334	0.61	15,333	8.90
700-800	1,180	0.02	-	-
800-900	125	0.00	-	-
>900	36	0.00	-	-
Total	5,258,500		172,328	

Figure 3.5 presents the distribution of the axle loads and axle spacing of the filtered WIM vehicles. As seen in Figure 3.5a, the steering axle and the axles 9, 10 and 11 are lighter on average, with a mean value varying between 33kN and 58kN. The remaining axles are heavier on average with a mean value ranging between 61kN and 84kN. It is also evident that the axles 1 – 8 have the highest variation, with axle loads ranging from 19kN to 144kN, whereas the axle 11 varies the least with axle loads ranging from 19 to 63kN. Figure 3.5b illustrates that on average, the axle spacing 3 is the longest with a mean value of 8.0m. This also indicates that the spacing 2, 4, 9 and 10 are on average tandems with a mean value smaller than 1.8m. Furthermore, spacing 3, 7 and 8 have the highest variation with the axle spacing ranging from 1.0m to 12.2m.



(a)



(b)

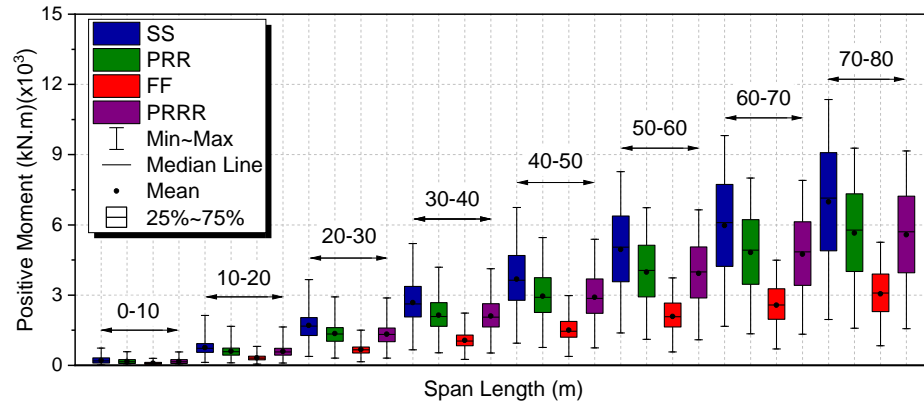
Figure 3.5: Distribution of WIM data: (a) axle load; (b) axle spacing

### 3.3 Moving Load Simulation

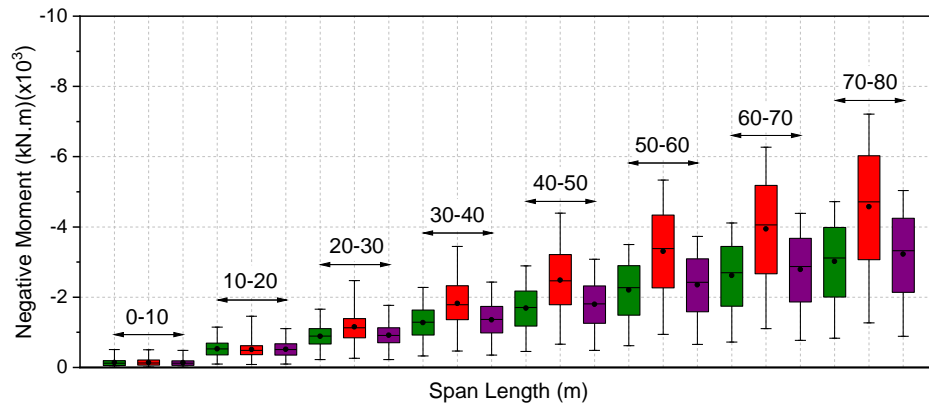
The load analysis of the WIM data was performed using the direct stiffness method for beam analysis. This method was implemented in a MATLAB code, where the vehicles were simulated as moving loads driving across the bridge configurations of interest and the corresponding maximum load effects including shear force, positive and negative moment

were calculated. A High-Performance Computing (HPC) clustering was deemed necessary to carry out the computationally expensive moving load simulations. The HPC clustering consists of a cluster of nodes (computers) that are networked together to provide high-performance data processing in parallel means through efficiently distributing the workload among the nodes. For this study, the CEDAR and GRANHAM networks that are part of the Compute Canada clusters, were used. Four bridge configurations were considered according to the provincial bridge inventory: simply supported span (SS), two-equal continuous spans (PRR), three-equal continuous spans (PRRR) and a single span with fixed supports at both ends (FF). Bridge spans ranged from 2m to 80m with the following increments: 2m from 2m to 20m, 5m from 20m to 50m and 10m from 50m to 80m.

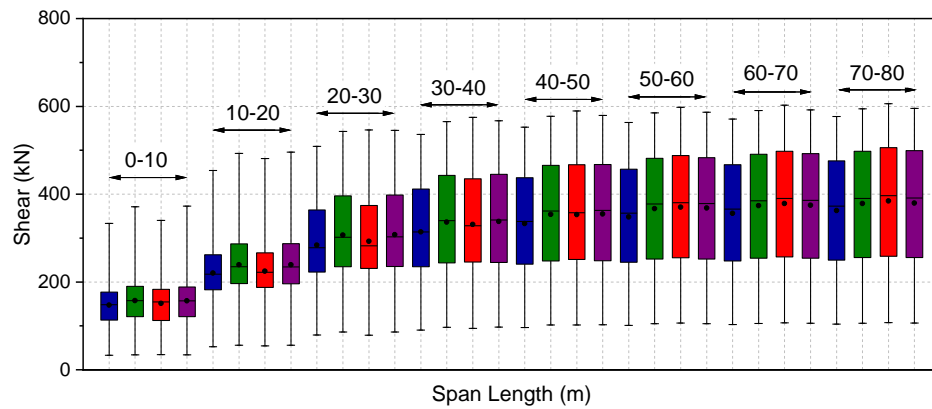
Figure 3.6 shows the distribution of the load effects obtained from the moving load analysis of the filtered WIM database at 10m span increments for all bridge configurations considered in this study. This figure illustrates that different boundary conditions behave differently depending upon the span length and the vehicles configuration. Figure 3.6a shows that the SS configuration governs for positive moment for all spans as this boundary condition allows the free rotation and have no moment restraint at the support locations. Conversely, the FF configuration has the least positive moment effects as bending moment is transferred from the beam to the supports. The latter will also reduce the deflection as the inflection points, where there is zero moment, move from the support line to some distance along the beam.



(a)



(b)



(c)

Figure 3.6: Load effects distribution of WIM vehicles: (a) positive moment; (b) negative moment; (c) shear force

Figure 3.6b shows that for negative moment the PRR configuration governs for shorter spans up to 10m, whereas the FF configuration has the most critical effects for longer spans.

In terms of shear force, it can be observed in Figure 3.6c that conversely to positive moment, the SS configuration has the least critical shear effects. This also indicates, that PRR and PRRR configurations often governs for shorter spans up to 20m, whereas the FF configuration governs for longer spans.

Figure 3.7 presents the statistical properties of the maximum load effects due to the WIM vehicles. As seen in this figure, the maximum negative moment varies between 509kN.m and 7210kN.m, the positive moment varies between 734kN.m and 11351kN.m, and the shear force varies between 373kN and 606kN for 10m and 80m spans, respectively. The observations obtained from Figure 3.7 confirm that the moment effects have significant more variation compared with the shear effects. This is due to the relationship between the moment arm created by the bridge span coupled with the weights of the axle group, whereas for shear force the axle group that is simultaneously present on the bridge dictates the most critical load effects.

The normal probability plot method was used in this study to extrapolate the maximum load effects for a 75-year service life. The horizontal axis of the normal probability plot is represented by the ratio of the load effects (i.e. shear, positive moment or negative moment) due to the WIM vehicles over the load effects caused by the standard CL-625-ONT truck load model. The left vertical axis corresponds to the redefined cumulative probability,  $p_i = F_x(x)$ , and the vertical axis on the right side corresponds to its respective standard normal variate,  $z = \Phi^{-1}(p_i)$ , where  $\Phi^{-1}$  is the inverse of the standard normal distribution function. More details about this method can be found in Nowak and Collins (2012). The highest  $z$  value is associated with a return period  $T$ , over which the data was recorded. For

this study, T is 4 years. The total number of vehicles, N, is equal to the number of trucks recorded during the period T. Therefore, for a 75-year return period,  $N_{75}$ , is estimated as 98,596,875 trucks and the cumulative probability corresponding to this return period is

$$p_{75} = \frac{N}{N+1} = 99.999999 \times 10^{-2} \text{ and } z_{75} = \Phi^{-1}(p_{75}) = 5.6096.$$

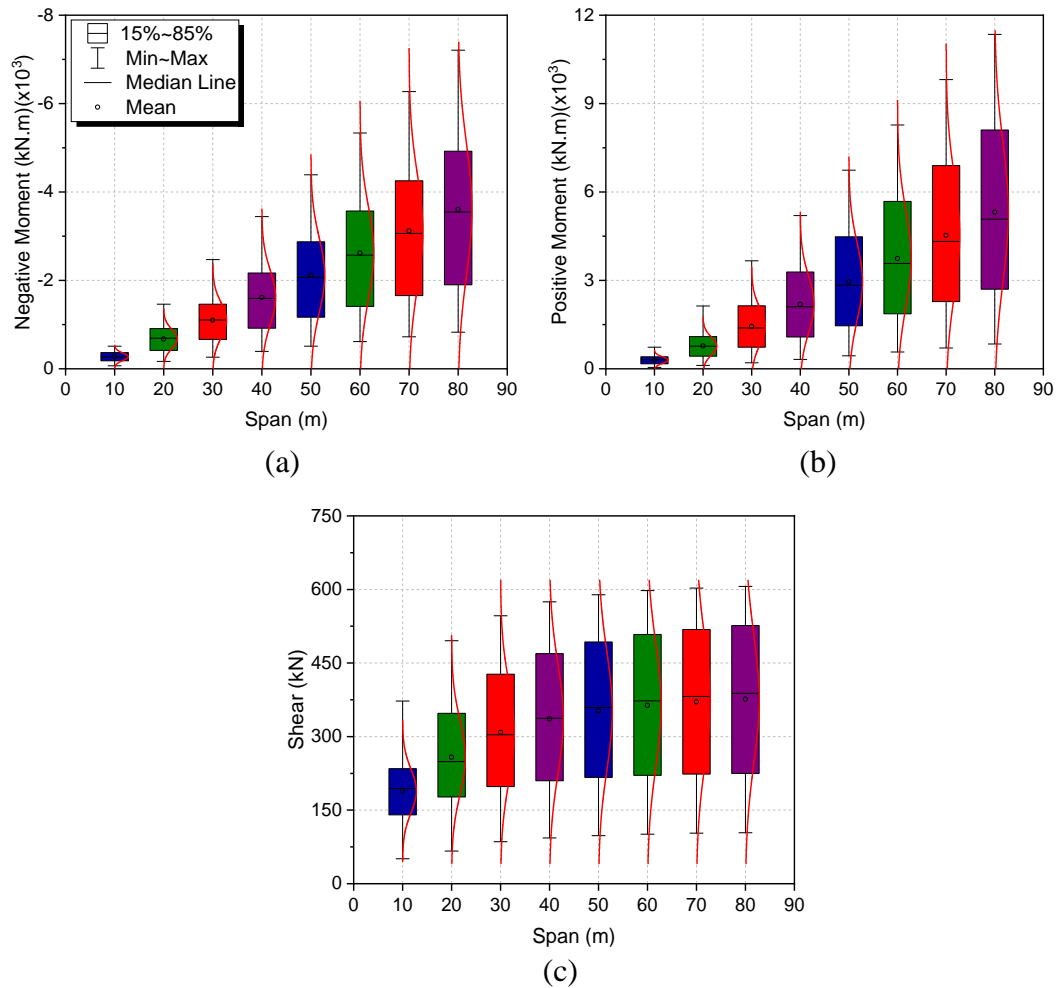


Figure 3.7: Statistical properties of maximum load effects of WIM vehicles: (a) negative moment; (b) positive moment; (c) shear force

The maximum load effects expected for this return period can be obtained directly from the normal probability plot by extending the upper most linear tail of the data to intercept with  $z_{75}$ , and reading the corresponding load effect ratio ( $LE_{75}$ ) from the abscissa. Figure

3.8 illustrates the negative moment ratio for a 50m FF bridge configuration on a normal probability plot and its respective  $LE_{75}$ . Although the data does not behave entirely as a straight line on the normal probability plot, the 15% upper most of the distribution does show a normal fit. Hence, it is a common practice to extrapolate the maximum load effect ratio using the upper tail of the distribution as depicted in Figure 2.8 with an obtained  $LE_{75} = 1.0963$ . Furthermore, the legal enforced weight limits and the truck population are assumed to remain the same over its 75-year design life.

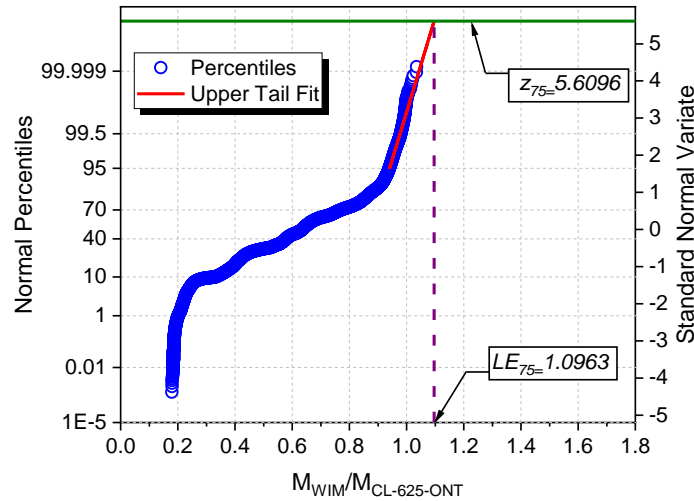


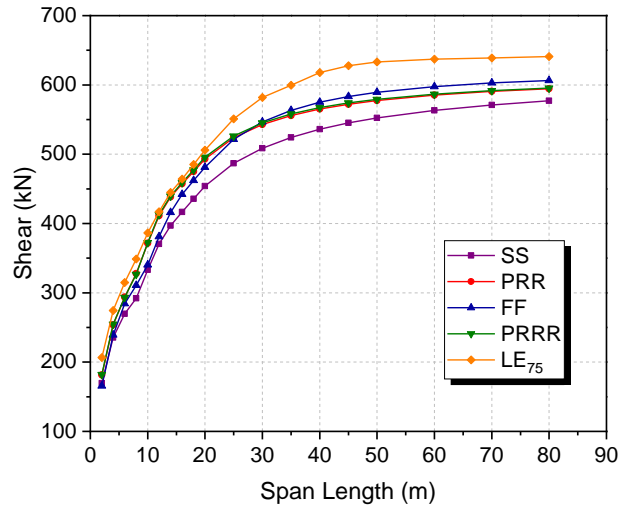
Figure 3.8: Upper tail extrapolation of negative moment for 50m FF bridge configuration on normal probability plot

Table 3.3 summarizes the maximum load effect ratios extrapolated for a 75-year lifespan in terms of the standard CL-625-ONT truck load model using the normal probability plot method. These values were later used as the load effect threshold to be enveloped by the proposed model.

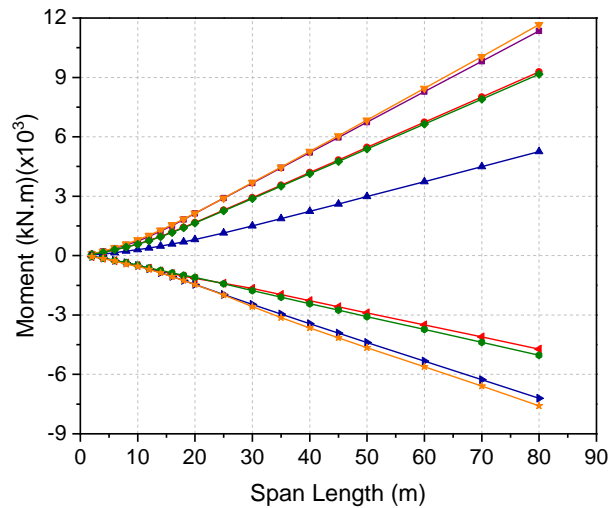
Table 3.3: Maximum load effects extrapolated for a 75-year lifespan

Span Length (m)	Extrapolated $LE_{75}$ Ratio		
	Positive Moment	Negative Moment	Shear
2	0.9797	1.1617	1.0598
4	1.0838	1.2047	1.1086
6	1.2110	1.2952	1.1674
8	1.2371	1.2703	1.1938
10	1.2236	1.2589	1.2286
12	1.2628	1.3186	1.2304
14	1.2880	1.3578	1.2199
16	1.2874	1.3067	1.2078
18	1.2608	1.3555	1.1868
20	1.2351	1.4043	1.1722
25	1.2076	1.3804	1.1621
30	1.1942	1.1728	1.1721
35	1.1716	1.1543	1.1828
40	1.1513	1.1321	1.1673
45	1.1363	1.1124	1.1565
50	1.1246	1.0963	1.1438
60	1.1082	1.0747	1.1228
70	1.0967	1.0643	1.1072
80	1.0883	1.0601	1.0959

Figure 3.9 shows the envelope for (a) shear force, and (b) positive and negative moment due to the WIM data representative of the normal traffic in New Brunswick for all bridge configurations considered in this study. This figure includes the maximum load effect  $LE_{75}$ , calculated by extrapolation for a 75-year service life.



(a)



(b)

Figure 3.9: Load envelope: (a) shear; (b) moment

### 3.4 Proposed Live Load Model

A multi-objective optimization-based approach was adopted in this study to develop an updated idealized live load model for New Brunswick. Over 150 optimized configurations were obtained and ultimately a five-axle truck model with the most optimal performance was chosen. The CL-625-ONT truck model was used as the base line model, and both axle

loads and axle spacing were chosen as the optimization parameters. Figure 3.10 shows this proposed idealized legal live load model. The CL-810-NB truck load consist of five axles with a GVW of 810kN and a base length of 17.1m. The wheel spacing and clearance envelope remain 1.8m and 3.0m, respectively, as outlined in the CAN/CSA-S6-14. As seen in this figure, the proposed model is heavier than the CL-625-ONT by approximately 30% and is 0.9m shorter than the existing model. The maximum axle load of the proposed model is 200kN, which in comparison with the CL-625-ONT is 25kN heavier.

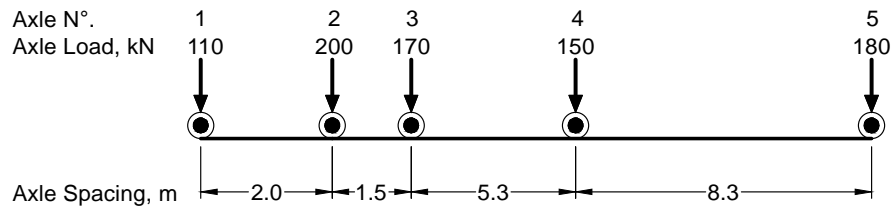


Figure 3.10: CL-810-NB idealized live load model

A performance indicator ( $PI_{Model}$ ) was selected to evaluate the efficiency of the proposed model in enveloping the WIM data load effects according to the following Equation (3.1):

$$PI_{Model} = \frac{LE_{Model}}{LE_{75}} \quad (3.1)$$

where  $LE_{Model}$  and  $LE_{75}$  are the load effects due to the proposed model and the extrapolated load effects for a design life of 75 years, respectively. Figure 3.11 depicts the performance of the CL-810-NB in terms of (a) negative moment, (b) positive moment and (c) shear, indicating that the model effectively envelopes the defined threshold for all bridge actions and bridge configurations considered in this study. As observed in this figure, the  $PI_{CL-810-NB}$  varies between 1.010 and 1.228 for negative moment, from 1.059 to 1.235 for positive

moment, and from 1.123 to 1.247 for shear. This also demonstrates a larger variation for negative moment for shorter spans up to 30m.

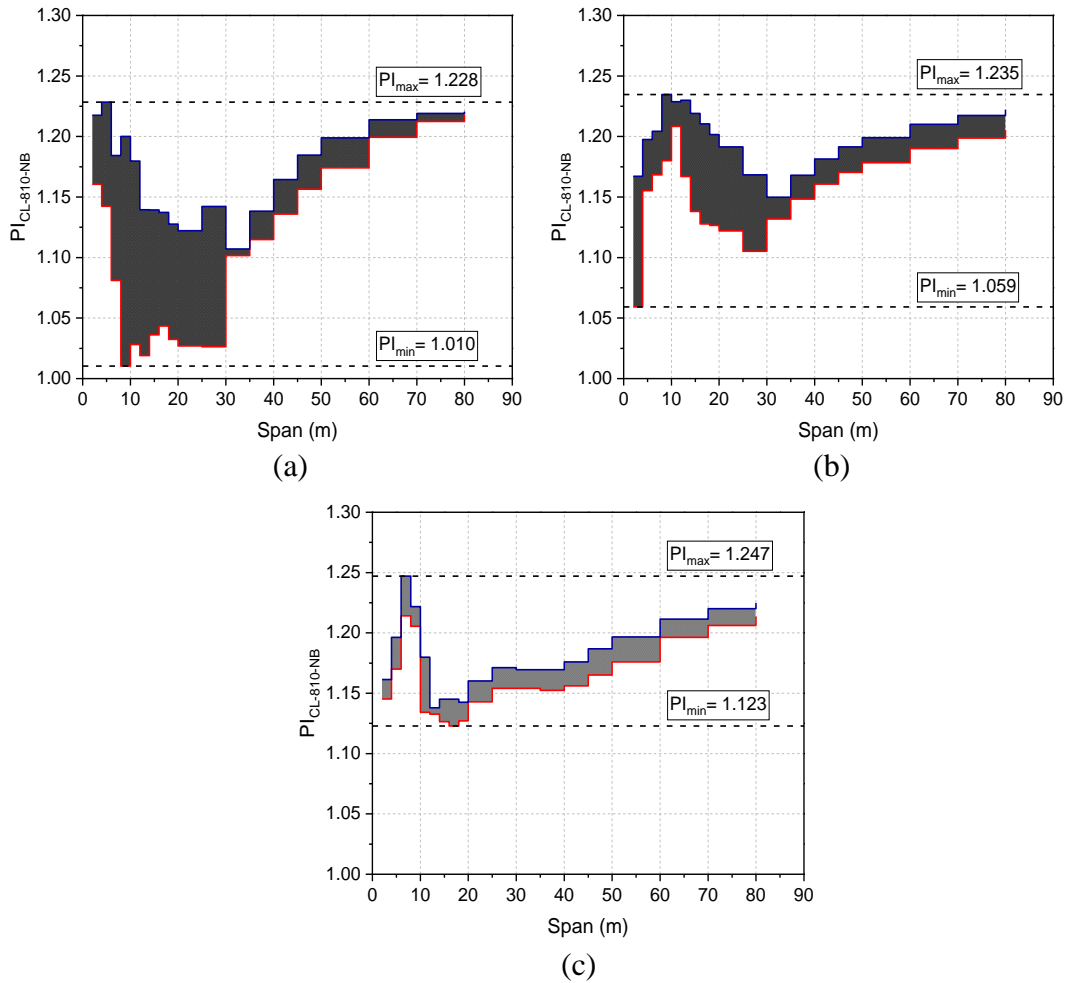


Figure 3.11: CL-810-NB performance indicator: (a) negative moment; (b) positive moment; (c) shear force

The New Brunswick normal traffic considered in this study and the proposed idealized live load model are also compared with the Ontario Bridge Formula (OBF) and with the Maximum Observed Load (MOL) in the province of Ontario during 1967 and 1975 (Agarwal 1988). OBF and MOL are the basis for the currently used live load models in the Ontario Highway Bridge Design Code and the CAN/CSA-S6 standards. Figure 3.12 shows

this comparison based on the relationship between the maximum load on an axle group and its equivalent base length. A significant number of vehicles exceeding the MOL for shorter equivalent base lengths are present in today's local traffic as evident in this figure. Furthermore, Figure 3.12 illustrates that the proposed CL-810-NB model effectively envelopes the axle group load and equivalent base length of the New Brunswick normal traffic database.

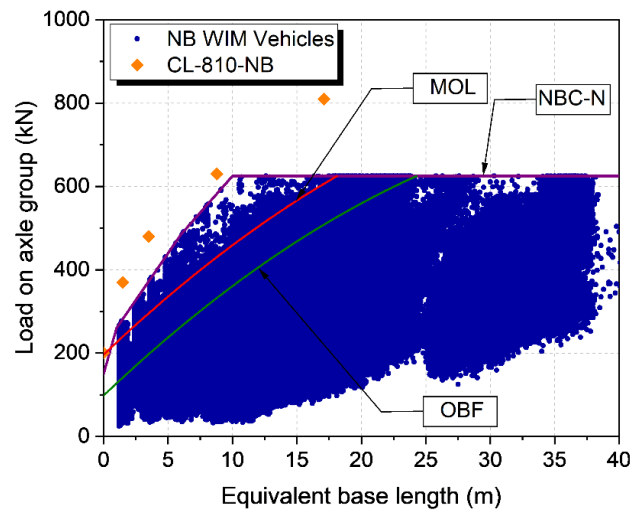


Figure 3.12: Comparison between NB normal traffic and OBF and MOL

This figure also shows the proposed New Brunswick Curve for normal traffic (NBC-N) which delineates the boundary used in this study to represent the relationship between the load on axle group and the respective equivalent base length for the traffic loads meeting the enforced provincial regulations. The vehicles falling outside these limits, which represented 0.08% of the filtered trucks, were considered to be nonconforming and were discarded from this study.

### 3.5 Performance of CL-625-ONT

The performance of the standard CL-625-ONT truck model to envelope the maximum load effects due to normal traffic extrapolated for a 75-year service life is depicted in Figure 3.13 in terms of (a) negative moment, (b) positive moment and (c) shear. As seen in this figure, the CL-625-ONT model underestimates the maximum load effects imposed upon the bridge structures in New Brunswick by approximately 29%, 22% and 19% for negative moment, positive moment and shear force, respectively. Although some of the filtered vehicles have the GVW lighter than the CL-625-ONT load model, their closely spaced axle configuration induces load effects substantially higher than the ones anticipated by the CAN/CSA-S6-14 Ontario load model. This also indicates that shorter spans are highly sensitive to the axle loads, whereas longer spans are more sensitive to the GVW. As seen in this figure, *PI* values vary between 0.712 and 1.015 for negative moment, from 0.776 to 1.022 for positive moment, and from 0.813 to 0.954 for shear. A comparison between the *PI* values for the CL-625-ONT and the  $LE_{75}$ , which accounts for the future traffic changes, shows that the currently used model is also underestimating the load effects due to today's traffic conditions.

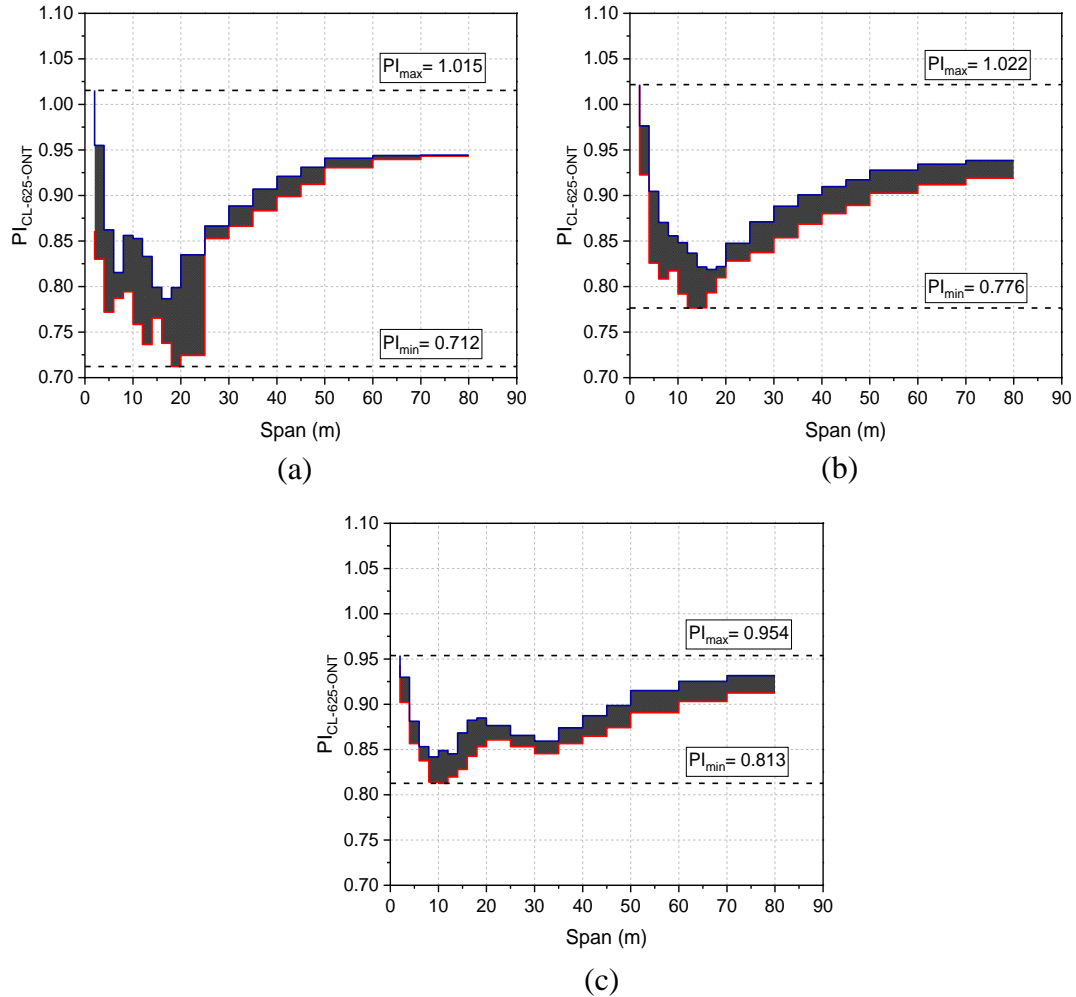


Figure 3.13: CAN/CSA-S6-14 CL-625-ONT truck load performance (a) negative moment; (b) positive moment; (c) shear force

### 3.6 Conclusions

The WIM data obtained from five sites in New Brunswick containing over 170,000 of the heaviest 5% vehicle configurations representative of normal traffic that were collected between 2014 and 2018 has been analyzed. The truck records were first filtered to remove any erroneous information and nonconforming vehicles that were not representative of the normal traffic in the province. Four bridge configurations were considered in this study

according to the provincial bridge inventory for spans ranging from 2m to 80m. The filtered vehicles were simulated as moving loads crossing the bridge configurations of interest in order to calculate the respective maximum load effects. The normal probability plot method was used to extrapolate the maximum load effects for a 75-year service life. The performance of the CL-625-ONT that is used by the NBDTI for design and evaluation of highway bridges in the province was evaluated. An updated idealized live load model (CL-810-NB) was developed using a multi-objective optimization-based approach to accurately reflect the increase in the live load spectra seen in the province that was insufficiently estimated by the CL-625-ONT truck load.

The proposed model consists of five axles with an overall GVW 30% heavier than the existing model with a shorter base length of 17.1m to account for the closely spaced heavily loaded axles. The proposed model may be adopted by the NBDTI for design and evaluation of medium and short span bridges in the province. Nonetheless, the findings from this study also emphasize the importance of assessing the site-specific truck loads, as these loads have significantly changed over the past few decades. The methodology outlined in this paper may also be adopted by other jurisdictions to effectively evaluate the nationwide or the site-specific traffic conditions and to develop the national agencies and updated bridge live load models that reflect the most up-to-date heavy truck loads.

## Notations

The following symbols are used in this chapter:

*AASHTO* = American Association of State Highway and Transportation Officials;

*CDF* = Cumulative distribution function;

*CL* = Canadian loading;

*FF* = Single span with fixed supports at both ends;

*FHWA* = Federal Highway Administration;

*GVW* = Gross vehicle weight;

*HPC* = High-performance computing;

*LE<sub>75</sub>* = Load effect ratio for a 75-year service life;

*LE<sub>Model</sub>* = Load effect due to live load model;

*LMI* = European load model 1;

*LPC* = License plate cameras;

*MOL* = Maximum observed loads in Ontario;

*MOU* = Memorandum of understanding;

*N* = Total number of vehicles;

*NBC-N* = New Brunswick curve for normal traffic;

*N<sub>75</sub>* = Total number of vehicles in a 75-year service life;

*NBDTI* = New Brunswick Department of Transportation and Infrastructure;

*NOA* = Number of axles;

*OHBDC* = Ontario highway bridge design code;

*OBF* = Ontario bridge formula;

*PI* = Performance indicator;

*PI<sub>CL-810-NB</sub>* = Performance indicator of CL-810-NB;

*PI<sub>Model</sub>* = Performance indicator of model;

*p<sub>i</sub>* = Cumulative probability;

*p<sub>75</sub>* = Cumulative probability for a 75-year service life;

*PRR* = Two-equal continuous spans;

*PRRR* = Three-equal continuous spans;

$SS$  = Simply supported span;

$SVC$  = Side view cameras

$T$  = Return period;

$WIM$  = Weigh-in-motion;

$z$  = Standard normal variate;

$z_{75}$  = Standard normal variate for a 75-year service life;

$\Phi^{-1}$  = Inverse of the standard normal distribution;

## References

- Agarwal, A. C. (1988). Permit vehicle control in Ontario. *Canadian Journal of Civil Engineering*, 15(5), 859-868.
- Code, O. H. B. D. (1983). Ministry of Transportation and Communications. Ontario.
- CSA (Canadian Standards Association). (2014). Canadian highway bridge design code. CAN/CSA-S6-14.
- Davis, J., Nassif, H. H., Nawy, E. G., Najm, H. S., & Tsakalakos, T. (2007). Live-load models for design and fatigue evaluation of highway bridges. *Language*, 10.
- Getachew, A., & O'Brien, E. J. (2007). Simplified site-specific traffic load models for bridge assessment. *Structure and Infrastructure Engineering*, 3(4), 303-311.
- Gindy, M., & Nassif, H. (2015). Effect of bridge live load based on 10 years of WIM data. In *Advances in Bridge Maintenance, Safety Management, and Life-Cycle Performance, Set of Book & CD-ROM* (pp. 755-756). CRC Press.
- Guide, T. M. (2001). Federal Highway Administration. US Department of Transportation, Washington, DC.
- Hanson, R., Executive, V. P., & COO, I. (2010). ITS Technologies for Commercial Vehicle Compliance in the Maritimes. In 2010 Annual Conference of the Transportation Association of Canada Halifax, Nova Scotia.

- Kozikowski, M. (2009). WIM based live load model for bridge reliability. *Civil Engineering Dissertations and Student Research*, 2.
- Leahy, C., O'Brien, E., & O'Connor, A. (2016). The effect of traffic growth on characteristic bridge load effects. *Transportation Research Procedia*, 14, 3990-3999.
- Luskin, D., & Walton, C. M. (2001). *Effects of truck size and weights on highway infrastructure and operations: A synthesis report* (No. FHWA/TX-0-2122-1,). Center for Transportation Research, Bureau of Engineering Research, University of Texas at Austin.
- Miao, T. J., & Chan, T. H. (2002). Bridge live load models from WIM data. *Engineering structures*, 24(8), 1071-1084.
- New Brunswick Department of Transportation and Infrastructure (2018). Highway Cameras. Retrieved from: <http://www.snb.ca/geonb1/e/map-prod/map-prod-E.asp>
- Nowak, A. S. (1999). Calibration of LRFD bridge design code (No. Project C12-33 FY'88-'92).
- Nowak, A. S. (1994). Load model for bridge design code. *Canadian Journal of Civil Engineering*, 21(1), 36-49.
- Nowak, A. S., & Collins, K. R. (2012). Reliability of structures. CRC Press.
- Nowak, A. S., & Hong, Y. K. (1991). Bridge live-load models. *Journal of Structural Engineering*, 117(9), 2757-2767.

Nowak, A. S., & Rakoczy, P. (2013). WIM-based live load for bridges. *KSCE Journal of Civil Engineering*, 17(3), 568-574.

Pelphrey, J., Higgins, C., Sivakumar, B., Groff, R. L., Hartman, B. H., Charbonneau, J. P., & Johnson, B. V. (2008). State-specific LRFR live load factors using weigh-in-motion data. *Journal of Bridge Engineering*, 13(4), 339-350.

Sivakumar, B., & Sheikh Ibrahim, F. I. (2007). Enhancement of bridge live loads using weigh-in-motion data. *Bridge Structures*, 3(3, 4), 193-204.

Southgate, H. F. (2001). Quality assurance of weigh-in-motion data. Federal Highway Administration.

Taplin, G., Deery, M., van Geldermalsen, T., Gilbert, J., & Grace, R. (2013). A new vehicle loading standard for road bridges in New Zealand (No. 539).

Tonias, D. E., & Zhao, J. J. (1995). *Bridge engineering: design, rehabilitation, and maintenance of modern highway bridges*. New York, NY: McGraw-Hill.

Vehicle Dimensions and Mass Regulation – Motor Vehicle Act. (2001). New Brunswick Regulation 2001-67. Retrieved from: <http://canlii.ca/t/535cs>

## **4 Permit Vehicle Live Load Model for Evaluation of Highway Bridges in the Province of New Brunswick**

**Diego Padilha<sup>1</sup>; Kaveh Arjomandi, Ph.D., P.Eng.<sup>2</sup>; and Tracy  
MacDonald, P.Eng.<sup>3</sup>**

<sup>1</sup>Research Assistant, Department of Civil Engineering, University of New  
Brunswick, Fredericton, NB, E3B 5A3, Canada. E-mail: dpadilha@unb.ca.

<sup>2</sup>Associate Professor, Department of Civil Engineering, University of New  
Brunswick, Fredericton, NB, E3B 5A3, Canada (corresponding author). E-mail:  
kaveh.arjomandi@unb.ca.

<sup>3</sup>Bridge Engineer, New Brunswick Department of Transportation and Infrastructure,  
Fredericton, NB, E3B 5H1, Canada. E-mail: tracy.macdonald@gnb.ca.

## **Abstract**

The Canadian Highway Bridge Design Code (CAN/CSA-S6-14) outlines the requirements for idealized live load models for the design and evaluation of highway bridges in Canada. These requirements are widely used by the provincial Departments of Transportation (DOT) nationwide. However, heavy traffic loads can vary substantially in different jurisdictions and over time depending upon factors such as the dominant industry, the economy and the population growth. As a result, several permits are issued yearly by the New Brunswick Department of Transportation and Infrastructure (NBDTI) to allow the operation of vehicles which do not comply with the provincial truck size and weight regulations. The study presented herein outlines the development of a permit truck live load model for evaluation of medium and short span bridges in New Brunswick. The model was developed using an optimization-based framework and a traffic database containing over 16,000 permit applications that was approved by the NBDTI between 2014 and 2018. Four governing bridge configurations with spans ranging from 2m to 80m were considered in this research. The proposed model was configured to envelope the maximum load effects due to 99.2% of the permit applicants. Finally, the performance of the standard CL-625-ONT live load model, which is currently used by the NBDTI for design and evaluation, is evaluated against the permit database and compared to the proposed permit truck load model. The proposed permit load model would allow the NBDTI to enhance their efficiency for bridge load rating practices of their designated heavy haul corridor.

## 4.1 Introduction

Highway bridges must be designed to withstand various load types including dead, live, wind, seismic, and thermal loads for an intended 75-year lifespan. Live load is often the governing loading scenario for short and medium span bridges (Tonias and Zhao 1995). Codes of practice outline the requirements for idealized live load models to represent the effects of heavy traffic loads on highway bridges. These loads are site-specific and can vary substantially over time depending upon local traffic characteristics influenced by factors such as the dominant industry, the economy, and the population growth.

The CAN/CSA-S6-14 specifies four categories of vehicles that can operate under a permit: Annual or project (PA), Bulk haul (PB), Controlled (PC), and Single trip (PS). The PAs represent the vehicles allowed to operate on either an annual basis or during a particular project. These vehicles may exceed the legal enforced axle load and Gross Vehicle Weight (GVW) and can be combined with normal traffic without any supervision. The PBs embody the bulk haul vehicles allowed by permit programs on an unlimited basis and are certified to operate simultaneously with normal traffic. PB permit holders may exceed the GVW, however, they shall comply with the individual legal enforced axle load. The PCs include the extremely heavy vehicle configurations allowed to operate under supervision and are subject to travel restrictions. The axle configuration of these vehicles shall be assessed upon the permit request, and they must not operate alongside normal traffic. Finally, the PSs account for vehicles allowed for a single trip that may exceed the legal enforced axle load and GVW and can operate freely with normal traffic.

In New Brunswick, vehicles that do not comply with the Vehicle Dimensions and Mass Regulations – Motor Vehicle Act (2001) are considered to be nonconforming, therefore, are required to obtain special permits in order to commute throughout the provincial highway bridge network. As a result, several permits are issued every year by the NBDTI to allow the operation of such nonconforming vehicles. A similar system to the CAN/CSA-S6-14 is adopted in New Brunswick, where oversize and overweight permits can be issued as either a seven-day (single-trip permit), or for extended periods of either three months or one year subject to permit restrictions in the vehicle GVW, dimensions, cargo and route. Figure 4.1 illustrates a typical vehicle layout with its respective dimensions controlled by the Motor Act (2001).

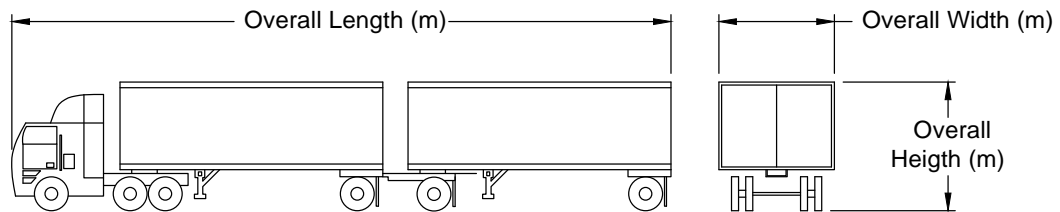


Figure 4.1: Typical vehicle dimensions controlled by NB – Motor Vehicle act (2001)

The overall limits for width and height are 2.60m and 4.15m, respectively, for any vehicle configuration specified in the act. However, the overall length, the axle load, and the GVW for legal vehicles in the province vary for different vehicle classes as summarized in Table 4.1, with the heaviest legal vehicle being the B-train configuration with a maximum allowed GVW of 613.1kN due to its greater stability.

Upon the submission of a permit application, the safety of the bridges located within the proposed route subject to the specific overweight truck load must be evaluated, and it is often necessary to perform the load rating of the respective bridges in accordance with the Chapter 14 of the CAN/CSA-S6-14. This is an extremely time-consuming task and creates a substantial amount of workload for DOTs, where a large number of permit applications are processed. In order to improve the efficiency of processing permit applications, many DOTs in the United States have developed permit live load models using their jurisdiction site-specific traffic load records. Examples include Pennsylvania (Laman and Shah 2016), Rhode Island (Da Lomba 2015), New Jersey (Lou et al. 2018) and Wisconsin (Zhao and Tabatabai 2011). The development of such updated overweight load models has proven to be crucial for the enhancement of the public safety in the respective jurisdictions as well as to improve the efficiency of bridge evaluation practices.

The province of New Brunswick currently does not use a standard permit live load model specific to the local traffic. Therefore, the significantly heavier loads that are permitted in the provincial highway network must be assessed on a case by case basis. This study outlines the efforts for the development of an idealized permit live load model for evaluation of medium and short span bridges in New Brunswick.

Table 4.1: Overall length, axle load, and gross vehicle weight limits in New Brunswick

Item	Vehicle Type						
	TTSM <sup>1</sup>	TTQST <sup>2</sup>	A-train	B-train	C-train	Coupled vehicles <sup>3</sup>	Bus
<b>Maximum axle load, kN</b>							
Steering axle	54.0	54.0	54.0	54.0	54.0	78.5	71.1
Single axle	89.3	89.3	89.3	89.3	89.3	89.3	89.3
Tandem axle	176.6	176.6	176.6	176.6	176.6	176.6	176.6
Tridem axle	255.1	274.7		235.4	235.4	206.0	
<b>Full vehicle</b>							
Gross weight, kN	485.6	544.5	524.8	613.1	573.9	524.8	247.7
Overall length, m	23.0	23.0	25.0	25.0	25.0	23.0	14.0

<sup>1</sup> Truck tractor and semi-trailer

<sup>2</sup> Truck tractor and quadrem axle semi-trailer

<sup>3</sup> Combination of vehicles coupled together that consists of more than one unit rather than train double vehicles. This includes truck - pony trailer, tandem steering axle truck – pony trailer, truck – full trailer and tandem steering axle truck – full trailer combinations.

The database containing over 16,000 permit applications issued by the NBDTI between 2014 and 2018 was analyzed. The applicants were classified based on the number of axles, and the statistical parameters of the vehicles pertaining to each class were calculated. Four governing bridge configurations were considered based on the provincial bridge inventory with spans ranging from 2m to 80m. The maximum load effects due to the large size permit database were calculated using parallel processing techniques. The statistical parameters of the load effects caused by the site-specific overweight vehicles are also described in detail. The proposed models were configured to envelope 99.2% of the permit database. The remaining 0.8% of the permits were substantially heavier vehicles that had a very low probability of occurrence and were assumed to be special escorted vehicles. Including these

vehicles was considered to result in the development of a noneconomic oversized permit load model.

## **4.2 Development of Permit Live Load Models**

According to the Commentary of the CAN/CSA-S6-14, the design live load should encompass a range of actual vehicle loads and bear a direct relationship to the legal loads on the highways in a jurisdiction. Several researchers have quantified the probabilistic nature of live loads and the uncertainties associated with these load patterns. The earliest efforts go back to the 19th century during the Industrial Revolution, when it was deemed necessary to reevaluate the bridge design specifications and to calibrate the live load models according to the increase in truck weight and volume (Taly 2014).

The CAN/CSA-S6-14 specifies the CL-625 truck loading (Figure 4.2a) as the minimum requirements to represent live loads for the design of a national highway network that is used for interprovincial transportation in Canada. This model was established based on the Memorandum of Understanding on Vehicle Weights and Dimensions (MOU), which consists of a set of regulations for interprovincial transportation signed by all Canadian provinces. The NBDTI uses the CL-625-ONT truck loading standards (Figure 4.2b) for design and evaluation of highway bridges in the province. The CL-625-ONT is a modified version of the CL-625 having a slightly different axle load distribution with heavier tandem axles (2 and 3) and a lighter rear axle, which was developed to account for overload trucks in Ontario.

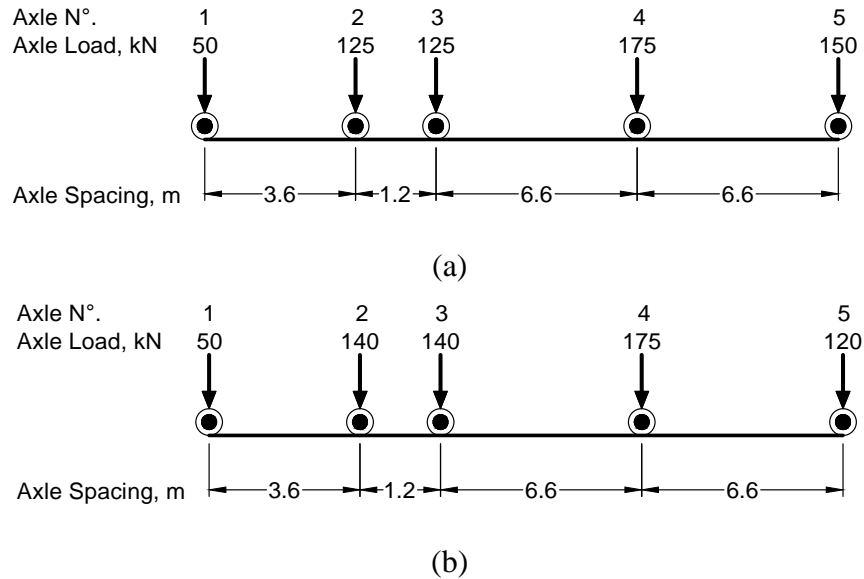


Figure 4.2: CAN/CSA-S6-14 live load models: (a) CL-625; (b) CL-625-ONT

The process for development and calibration of live load models for highway bridges using traffic database is well described in the literature (Novak 1994; Taplin et al. 2013; Davis et al. 2017; Leahy et al. 2016; Novak and Hong 1991). Novak (1994) used truck surveys conducted by the Ontario Ministry of Transportation in 1975 and 1988 to evaluate the adequacy of the Ontario Highway Bridge Design Code. He analyzed the performance of the standard live load model OHBDC-1983 to envelope the maximum moment and shear due to the truck database for simply supported spans. Upon completing the analysis, Novak (1994) proposed a new updated live load model in which the axle tandem of the OHBDC-1983 was increased to reflect the heavy vehicle configurations present in Ontario. In the literature, a general calibration approach has been adopted, where the site-specific traffic database vehicles were analyzed on different bridge configurations and the maximum load effects (i.e. moment and shear) were calculated. The extrapolated load effects were then compared to the ones caused by the respective standard live load model. Hence, depending

upon the adequacy to envelope the extrapolated maximum load effects due to the database vehicles, adjustments were applied to the axle configuration of the standard load model to establish a calibrated truck loading that adequately enveloped the database truck load effects for the respective site-specific loading spectra.

There is very limited literature describing the original development of permit live load models using traffic database with the absence of an existing standard truck loading as a base line model. Laman and Shah (2016) adopted a multi-step, multi-pronged approach to develop a new updated permit design vehicle (PA2016-13) for the state of Pennsylvania. In their study, Laman and Shah (2016) used a vehicle database containing 2508 combined overweight permit vehicle configurations. Upon reviewing the distribution of vehicles based on the number of axles, the dominant class within the permit database was thirteen-axle vehicles containing over 60% of the total truck database. Therefore, it was deemed necessary the construction of a thirteen-axle truck loading standard. This was achieved by maintaining the axle spacing within the average value and distributing the 95<sup>th</sup> percentile group weight equally to all axles pertaining to the group. The proposed PA2016-13 truck model was designed to envelope 98.3% of the permit vehicles, where the load effects due to the remaining 1.7% of the vehicles were considerably greater and were assumed to be special escorted vehicles.

Da Lomba (2015) adopted a different approach to develop overweight live load models using a traffic database containing over 44,000 permit applications approved by the Rhode Island Department of Transportation. In his study, several predetermined “trial models”

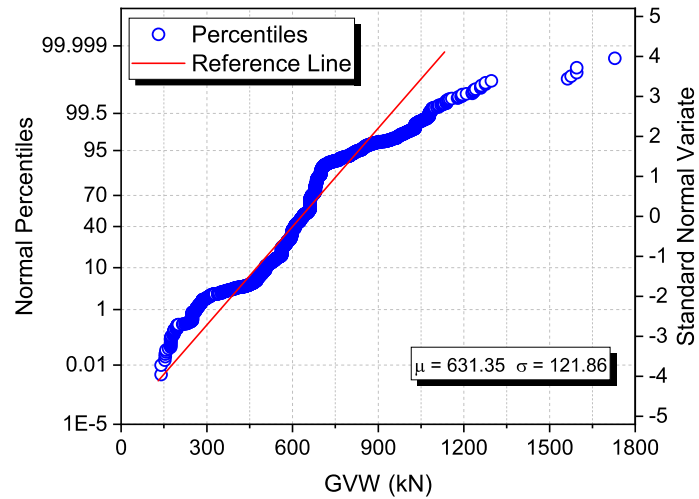
were created using the statistical parameters (i.e. average value, mode, standard deviation, 95<sup>th</sup> percentile) of the permit database including axle load, spacing, and GVW for vehicle configurations in a given class. The performance of each “trial model” was compared and the best model was selected. Finally, an iterative trial and error approach was used to adjust the axle configuration of the chosen case in order to meet the acceptable percent exceedance. In another study, Zhao and Tabatabai (2011) used a Weigh-In-Motion (WIM) database from Wisconsin to evaluate the performance of the existing standard permit vehicle for anticipating the maximum load effects caused by overloaded vehicles in the state. A short five-axle permit load model was proposed to supplement the standard permit vehicle for design and rating of shorter span bridges in Wisconsin. This was accomplished by using the 95<sup>th</sup> percentile of the axle loads while using the average values of the axle spacing. Tandem spacing was kept as 1.2m.

In all the previously mentioned studies, a multi-step framework was used for the development of permit live load models, in the absence of an existing standard truck model. In this framework, a base line model was created first according to the statistical properties of the permit database. Then the model was modified using an iterative approach in order to envelope the maximum load effects due to the permit vehicles in the respective jurisdictions.

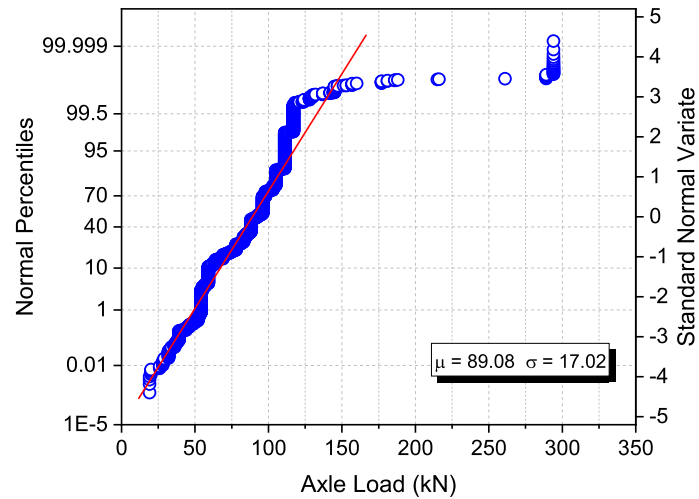
### **4.3 Statistical Analysis of New Brunswick Permit Database**

In this study, a traffic database containing 16,001 permit applications that were approved by the NBDTI from 2014 to 2018 was analyzed. The permit database contains the permit

vehicle parameters such as: permit number, type of vehicle, axle loads, axle spacing and GVW. Figure 4.3 presents the cumulative distribution function (CDF) of the permit vehicles in terms of (a) GVW, and (b) axle load on a normal probability plot. Figure 4.3a reveals that the majority of the database (99.78%) consists of vehicles weighing up to 1100kN with a mean value of 631.35kN and a standard deviation of 121.86kN. This also confirms the presence of particular heavier vehicles weighing close to 1600kN, which is more than two times heavier than the standard CL-625-ONT that is used for design and evaluation of highway bridges in New Brunswick. However, these extremely heavy vehicles represent only 0.11% of the permit database and were assumed to be operated with special escorts, therefore, were omitted in this study. Figure 4.3b demonstrates that most of the permit database (99.68%) comprises of axle loads weighing up to 150kN with a mean value of 89.08kN and a standard deviation of 17.02kN. This also reveals that only 0.32% of the vehicles have axle loads exceeding 150kN with the heaviest being close to 300kN. The latter is due to either the two-axle mobile cranes or other particular PC configurations that are only allowed to operate under supervision subject to travel restrictions.



(a)



(b)

Figure 4.3: NB permit database cumulative distribution functions for: (a) GVW; (b) axle load

The New Brunswick bridge inventory consists of a variety of structure types. The most common bridge types are steel/wood stringer (32.3%), prestressed concrete girder (22.6%), conventional reinforced concrete slab/beam (13.9%), concrete rigid frame (8.1%) and steel plate girder (5.2%), representing 82.1% of the provincial bridge network. Figure 4.4 shows the CDF for span length of all bridge types in New Brunswick on a lognormal probability

plot. As seen in this graph, the majority of bridges in the inventory (99.2%) have a span length up to 80m, with the mean value of 17.85m and standard deviation of 18.06m.

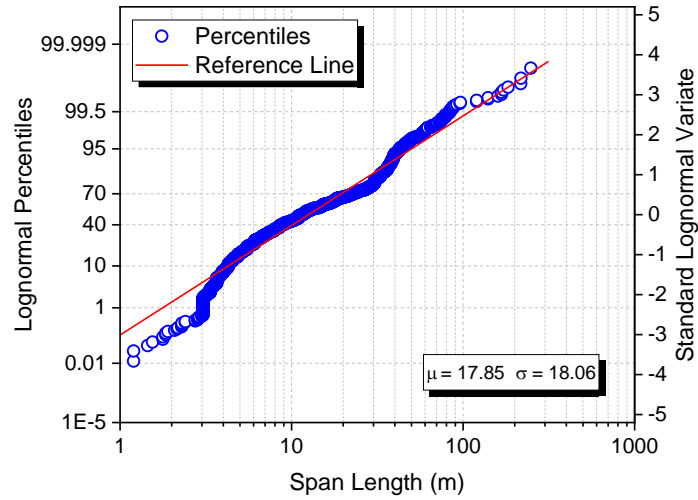


Figure 4.4: Cumulative distribution function of New Brunswick bridge inventory

Table 4.2 summarizes the distribution of the most common bridge types in the province in terms of the number of spans. According to this table, most of the bridges have 1 to 3 spans representing 94.0% of the bridge network. Bridges with a number of spans larger than 3 represent 6.0% of the provincial bridge inventory.

Table 4.2: Distribution of New Brunswick bridge inventory in terms of number of spans

Number of Spans	Number of Bridges	%
1	1923	75.29
2	160	6.26
3	318	12.45
> 4	153	6.00

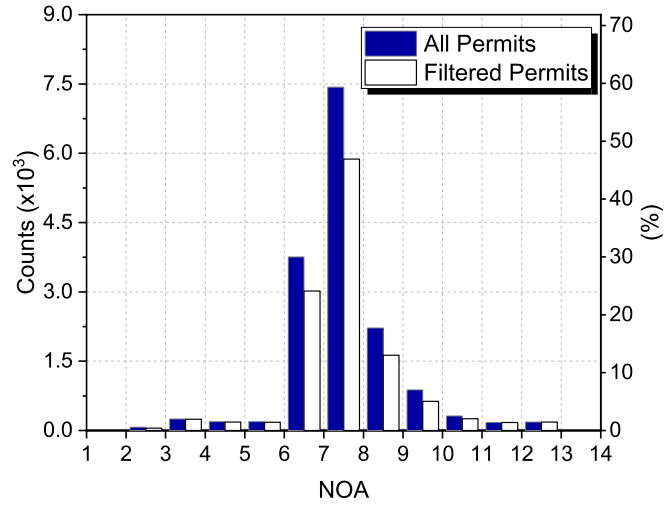
A data quality check was deemed necessary prior to the analysis of the permit database in order to remove any particular permit applicant containing erroneous information. This

was also used to discard the mobile cranes and the PC configurations that embody only 0.43% of the permit database as illustrated previously in Figure 4.3. The following criteria were used to filter the permit database:

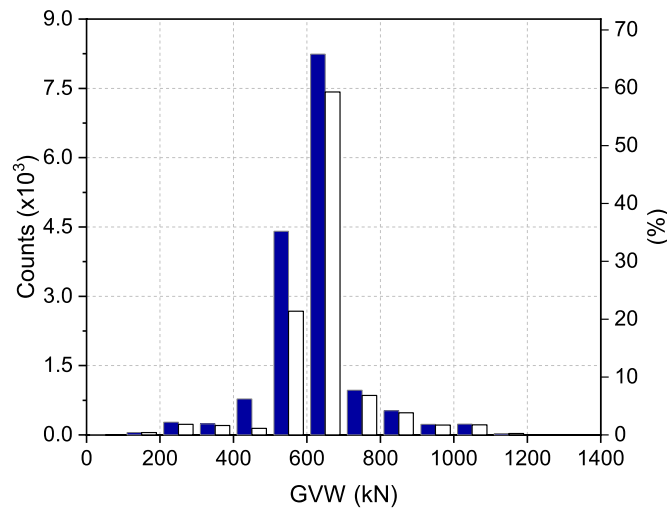
- i. Maximum axle load is limited to 150kN. Some vehicles have individual axle load exceeding 500kN. These permits were assumed to be an input error or to be related to trucks that can operate under restrictions and must be approved on a case by case basis. Figure 3 shows that 99.68% of the permit database vehicles have axle loads weighing up to 150kN.
- ii. Axle spacing is between 1m and 100m. Spacing falling outside these bounds were assumed to be either impractical or an input error.
- iii. Maximum GVW is limited to 1100kN. Vehicles exceeding this limit represents only 0.22% of the permit database, which were assumed to be special escorted vehicles.
- iv. Number of axles (NOA) must match with the counts of axle loads.
- v. Number of spacing must match with the counts of spacing.

Criteria *iv* and *v* were used to identify input errors observed in some of the permit applications. As a result, a total of 12,459 permit applications successfully passed through the data quality check, therefore, proceeding to the truck load simulation. Figure 4.5 shows the distribution of the permit database prior and after the data quality check in terms of (a) NOA, and (b) GVW. Figure 4.5a indicates that the seven-axle configuration is the dominant vehicle class representing 46.9% of the filtered permits. In addition, the majority

of the filtered vehicles (59.2%) weighs between 600kN and 700kN as shown in Figure 4.5b.



(a)



(b)

Figure 4.5: Distribution of permit vehicles: (a) NOA; (b) GVW

## 4.4 Permit Live Load Development

An optimization-based framework was adopted in this study to develop an idealized permit live load model for New Brunswick: the NB P10-1300. The proposed model was configured to envelope the structural responses of 99.2% of the permit database. First, the statistical properties (i.e. the mean, maximum, mode, minimum, 15<sup>th</sup> and 85<sup>th</sup> percentile values) of the permit database were determined. A data quality check was carried out to filter the permit database. The maximum load effects (i.e. shear and moment) on the governing bridge configurations were then calculated using parallel processing techniques. An initial model was established by selecting the vehicle configuration that had the most governing load effects. Finally, the initial model was optimized to envelope the load effects due to all filtered permit trucks within the database. The latter was achieved by optimizing the axle spacing and loads of the model in order to minimize the difference between the maximum load effects due the database vehicles and the ones due to the proposed model.

### 4.4.1 Permit Vehicle Group

In lieu of developing a live load model for each vehicle class, which would result in twelve load models, the permit vehicles were combined into one group based on the number of axles. For the purpose of this study, the vehicle's axle loads and axle spacing were numbered as depicted in Figure 4.6. In this figure,  $F_n$  is the axle load for the  $n^{\text{th}}$  axle, and  $S_j$  is the  $j^{\text{th}}$  spacing between  $F_n$  and  $F_{n+1}$ .

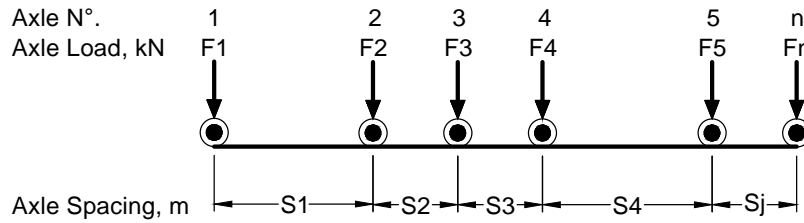
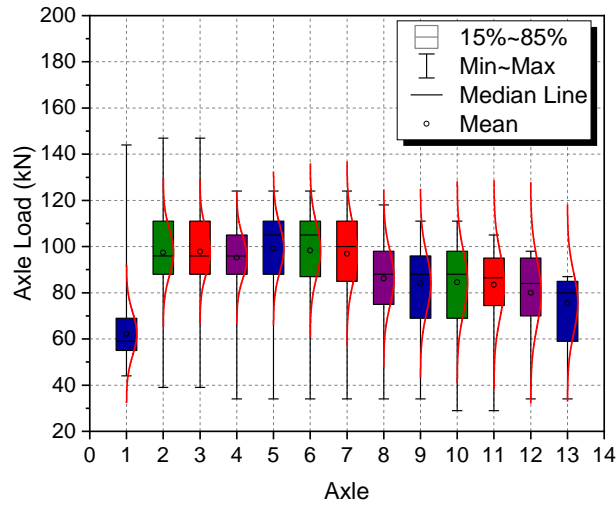
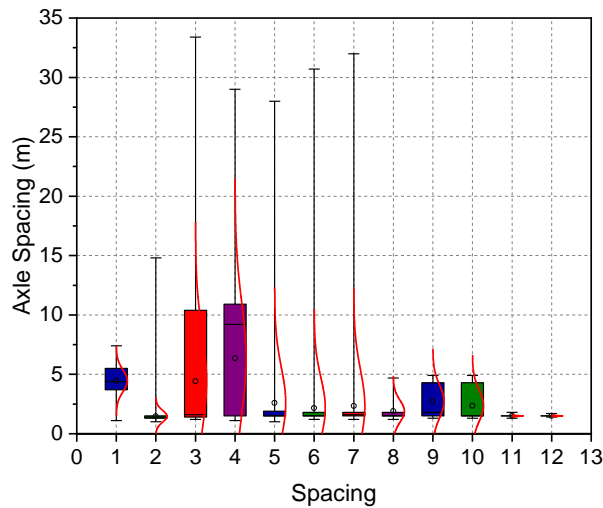


Figure 4.6: Permit vehicles axle load and spacing numbering

The filtered database consists of permit vehicles containing two to thirteen axles. Figure 4.7 presents the distribution of the axle loads and the axle spacing for all vehicles considered in this study. As seen in Figure 4.7a, on average, the steering axle has the lightest axle load with a mean value of 62kN while the mean value of the remaining axles varies between 76kN and 99kN. However, the variation of axle loads is the highest among the first three axles varying between 39kN and 147kN. In addition, axles 5, 6 and 7 show a relatively identical distribution. Figure 4.7b indicates that the axle spacing has the highest variation in spacing 3 and 4, in which varies between 1.1m to 33.4m. This also confirms that axle spacing 8, 11 and 12 are typically tandem axles, while spacing 9 and 10 have a similar distribution varying between 1.2m to 4.9m.



(a)



(b)

Figure 4.7: Distribution of New Brunswick permits: (a) axle load; (b) axle spacing

#### 4.4.2 Permit Truck Load Simulation

The linear direct stiffness method for beam analysis was implemented in a MATLAB code for load analysis of the filtered permit vehicles. Trucks were simulated as moving loads crossing the bridge configurations of interest and the maximum load effects (i.e. shear, positive and negative moment) were calculated. Four governing bridge configurations were

considered in this study based on the provincial bridge inventory: simply supported span (SS), two-equal continuous spans (PRR), three-equal continuous spans (PRRR) and single span with fixed supports on both ends (FF). Spans ranged from 2m to 80m with the following increments: 2m from 2m to 20m, 5m from 20m to 50m, and 10m from 50m to 80m. Due to the extremely intensive computational power required to perform the moving load simulations of the permit database as well as to perform the optimization, a High Performance Computing (HPC) infrastructure using a cluster of computers (nodes) in a parallel manner was employed to distribute the computational work load. This enables a much better performance than one could obtain from a single conventional desktop computer to perform analysis with high level of complexity. In this study, the CEDAR network, that currently offers over 58,000 CPUs and over 584 GPUs (WestGrid 2016) and is part of the Compute Canada clusters, was used.

Figure 4.8 illustrates the moving load analysis results and the statistical properties of the load effects for the boundary conditions of interest, at 10m span increments. In this analysis, the multiple presence of permit vehicles simultaneously on a bridge was not considered. As seen in this figure, different bridge types govern for different load effects depending on the bridge span and the vehicle configuration. The maximum positive moment always governs for the SS configuration as expected, since there is not rotational restraint at the supports. Figure 4.8b presents the negative moments for only PRR, FF and PRRR configurations, since simply supported spans do not experience any negative moment. It is evident that the PRR configuration often governs for shorter spans for negative moment, whereas the FF configuration results in the worst-case scenario for

longer spans. The latter is due to the randomness of the axle configuration of the vehicles pertaining to the database.

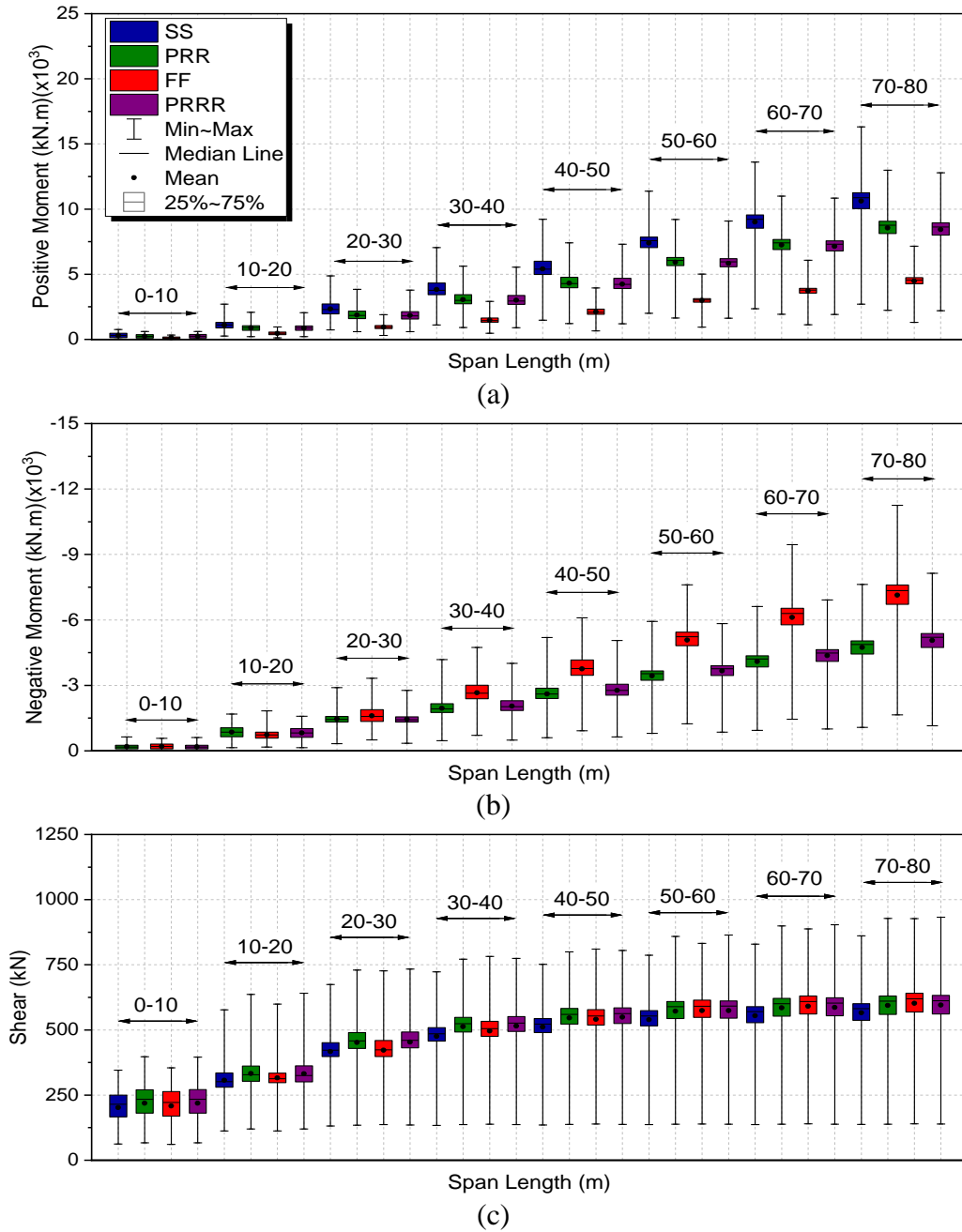


Figure 4.8: Load effects distribution of permit vehicles: (a) positive moment; (b) negative moment; (c) shear force

As shown in Figure 4.8c, the PRR and PRRR configurations generally dictate the most critical effects for shorter spans up to 30m and spans longer than 50m, whereas the FF configuration governs for spans between 30m and 50m. Furthermore, conversely to the positive moment effects, the SS configuration does not govern for shear in any span.

Figure 4.9 summarizes the distribution of the maximum load effects for the permit vehicles in terms of (a) negative moment, (b) positive moment and (c) shear force. As seen in this figure, the maximum negative moment varies between 638kN.m and 11255kN.m, the maximum positive moment varies between 754kN.m and 16314kN.m, and the maximum shear force varies between 397kN and 932kN for 10m and 80m spans, respectively. It is evident that the shear effects show significant less variation as the span increases in comparison to the bending moments. This is due to the direct relationship between the weight on the axle group and the shear effects. Conversely, in addition to the weight on the axle group, the moment effects are also affected by the moment arm created as a function of the bridge span.

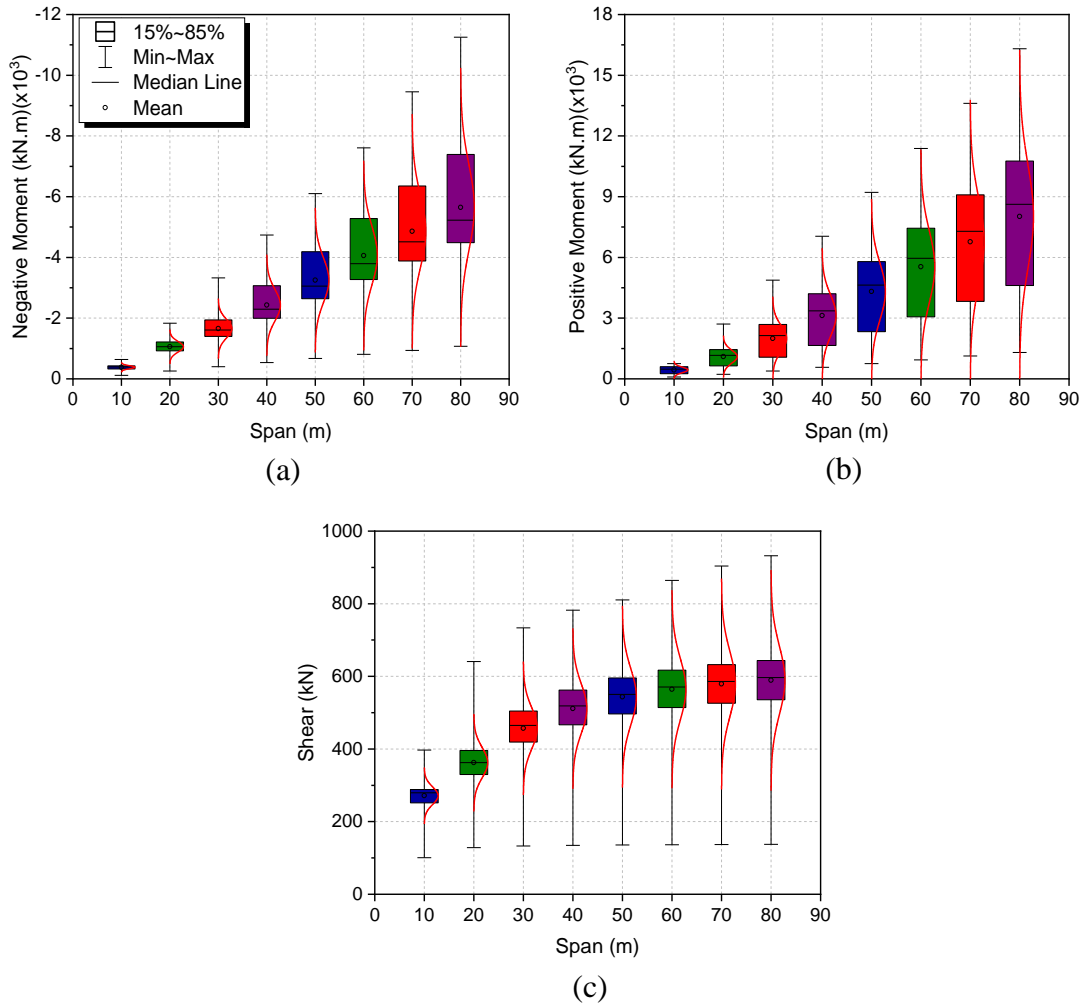
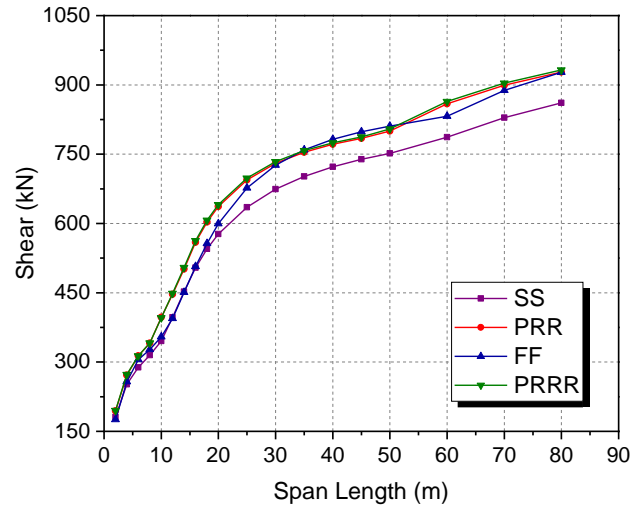
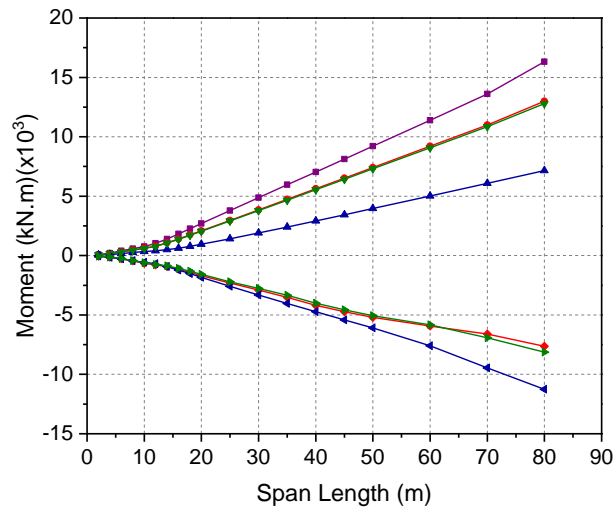


Figure 4.9: Statistical properties of load effects due to permits: (a) negative moment; (b) positive moment; (c) shear force

The maximum values were chosen as the threshold required to be enveloped by the proposed model. Figure 4.10 illustrates the maximum (a) shear force, and (b) positive and negative moment due to the New Brunswick permit vehicles. This figure also represents the load effects for each bridge configuration, indicating that different boundary conditions govern for different actions and in different spans.



(a)



(b)

Figure 4.10: Load effects envelope: (a) shear; (b) moment

### 4.5 Proposed Model

The proposed permit live load model described herein was developed using an optimization-based framework. First, an actual vehicle configuration that governed the most was selected as an initial model. The axle loads and spacing were then optimized to envelope the maximum load effects due to all permit vehicles. The optimization objective

was to minimize the difference between the load effects due to the proposed model and the specified threshold leading to the optimal vehicle configuration.

Figure 4.11 shows the proposed idealized permit live load model for New Brunswick. The NB P10-1300 permit load model consists of ten axles with a GVW of 1300kN and a base length of 34.6m. The wheel spacing and clearance envelope remain 1.8m and 3.0m, respectively, as outlined in the CAN/CSA-S6-14. This load model was configured to envelope the maximum load effects due to all permit trucks considered herein. As seen in this figure, the steering and rear axles are identical to the existing CL-625-ONT truck load model. This also indicates that the maximum axle load of the proposed model only exceeds the heaviest axle load of the CL-625-ONT model by 5kN.

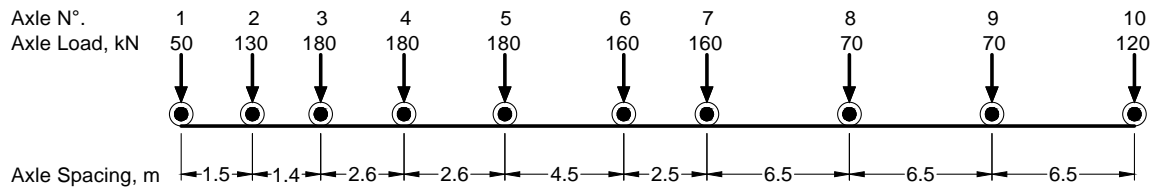


Figure 4.11: NB P10-1300 idealized permit live load model

The adequacy of the proposed model was measured in terms of a performance indicator ( $PI_{Model}$ ), which can be expressed according to Equation (4.1) as the ratio of the load effects (shear, positive and negative moment) caused by the idealized model,  $LE_{Model}$ , over the threshold defined for the respective vehicle group  $LE_{Threshold}$ .

$$PI_{Model} = \frac{LE_{Model}}{LE_{Threshold}}; \quad (4.1)$$

Figure 4.12 illustrates the performance of the NB P10-1300 permit live load model in enveloping the maximum load effects due to the New Brunswick permit vehicles in terms of (a) negative moment, (b) positive moment, and (c) shear. A  $PI_{Model}$  greater than unit confirms that the proposed model is successfully enveloping the maximum bridge responses due to all permit vehicles for all boundary conditions considered in this study. As seen in this figure, the  $PI_{NB\ P10-1300}$  varies between 1.021 and 1.327 for negative moment, from 1.003 to 1.309 for positive moment, and from 1.064 to 1.339 for shear. This also confirms the variation is the highest for negative moment longer spans ranging between 20m and 60m.

A comparison of the New Brunswick permit database along with the proposed permit model is presented in Figure 4.13 in terms of the equivalent base length and the maximum load on an axle group, with the Ontario Bridge Formula (OBF) and with the Maximum Observed Load (MOL) in Ontario during load surveys carried out in 1967 and 1975 (Agarwal 1988). These are the basis for the currently used live load models in the Ontario Highway Bridge Design Code as well as the CAN/CSA-S6-14 standards. As seen in this figure, the maximum axle group weights permitted in the province today are substantially heavier than the MOL in Ontario. This also indicates that the axle group weights of the proposed models are adequately enveloping the New Brunswick permit database.

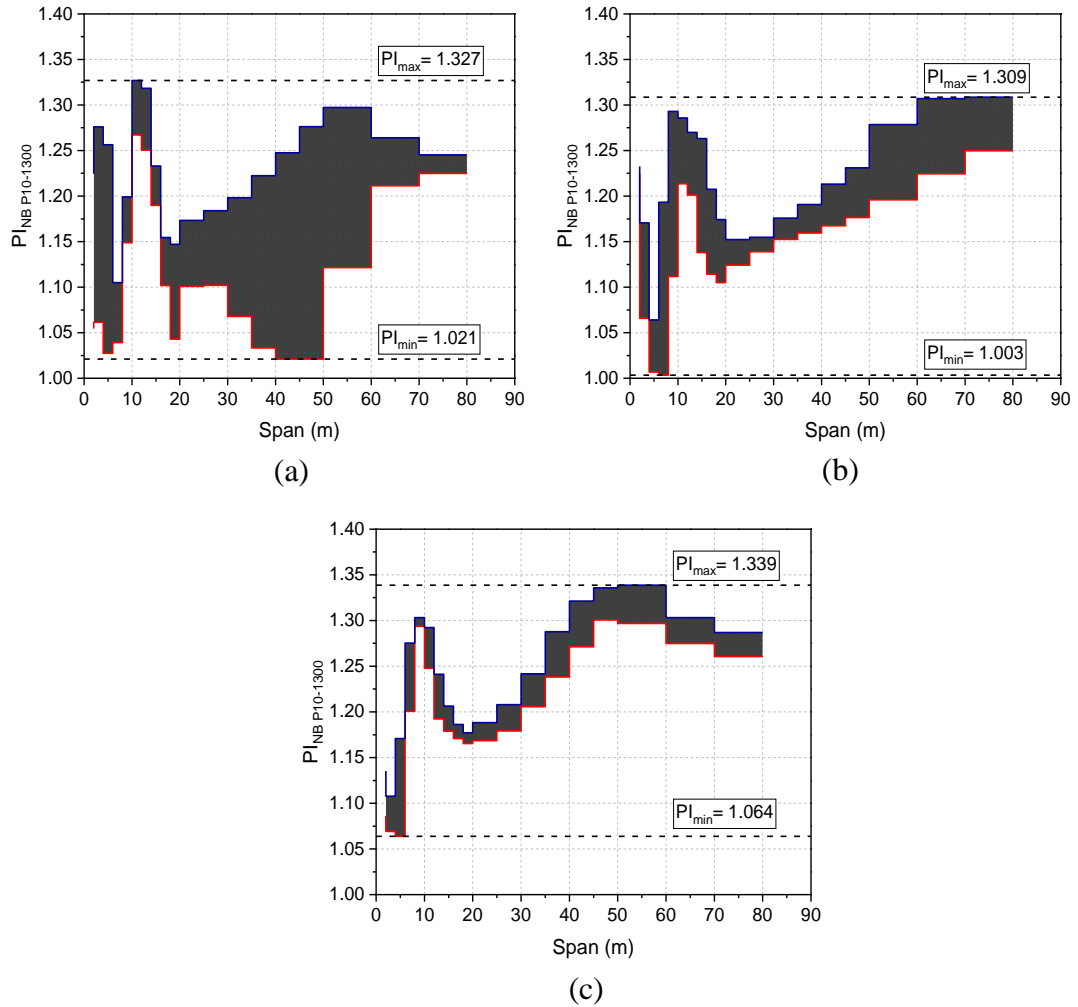


Figure 4.12: Performance of NB P10-1300: (a) negative moment; (b) positive moment; (c) shear force

Figure 4.13 also shows the proposed New Brunswick Curve for permit vehicles (NBC-P), which defines the boundary for the relationship between the load on axle group and vehicle base length of the permit vehicles allowed in the province. Any vehicle configuration falling outside this boundary was considered to be *PCs* that represented only 0.8% of the truck database. As a result, the proposed NB P10-1300 model 99.2% of the permit vehicles that are within the NBC-P curve.

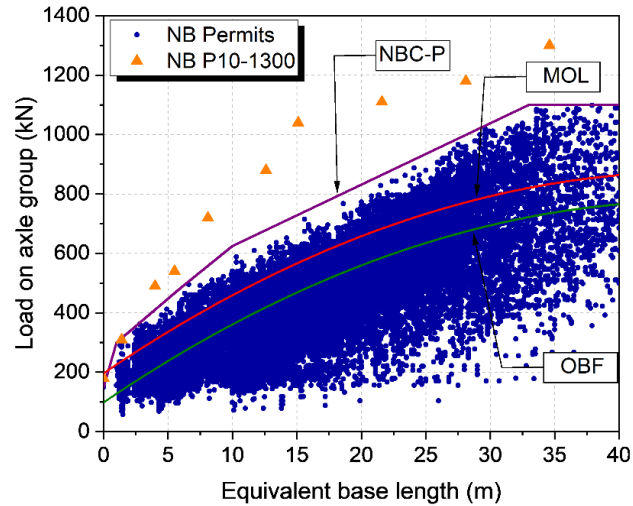


Figure 4.13: Comparison between NB permits and OBF and MOL

#### 4.6 Standard CL-625-ONT Performance

The performance of the Ontario standard live load model in comparison to the envelope of the maximum load effects caused by the permit vehicles, is represented in terms of PIs in Figure 4.14 in terms of (a) negative moment, (b) positive moment and (c) shear. As seen in this figure, the standard CL-625-ONT truck loading significantly underestimates the load effects due to the permits allowed in New Brunswick in almost every boundary condition. Only the maximum positive moment and shear force for a 2m span is enveloped with *PIs* varying between 1.062 and 1.190. The latter is due to the considerably heavier axle load 4 (175kN) for positive moment, and due to the tandem axles 2 and 3 (140kN/axle) for shear. This also indicates the axle loads dictates the load effects on shorter spans, whereas the GVW have greater influence for longer spans. Nonetheless, this reconfirms that the nonconforming overweight vehicles cause substantially larger structural responses that can be estimated using the proposed idealized permit live load model.

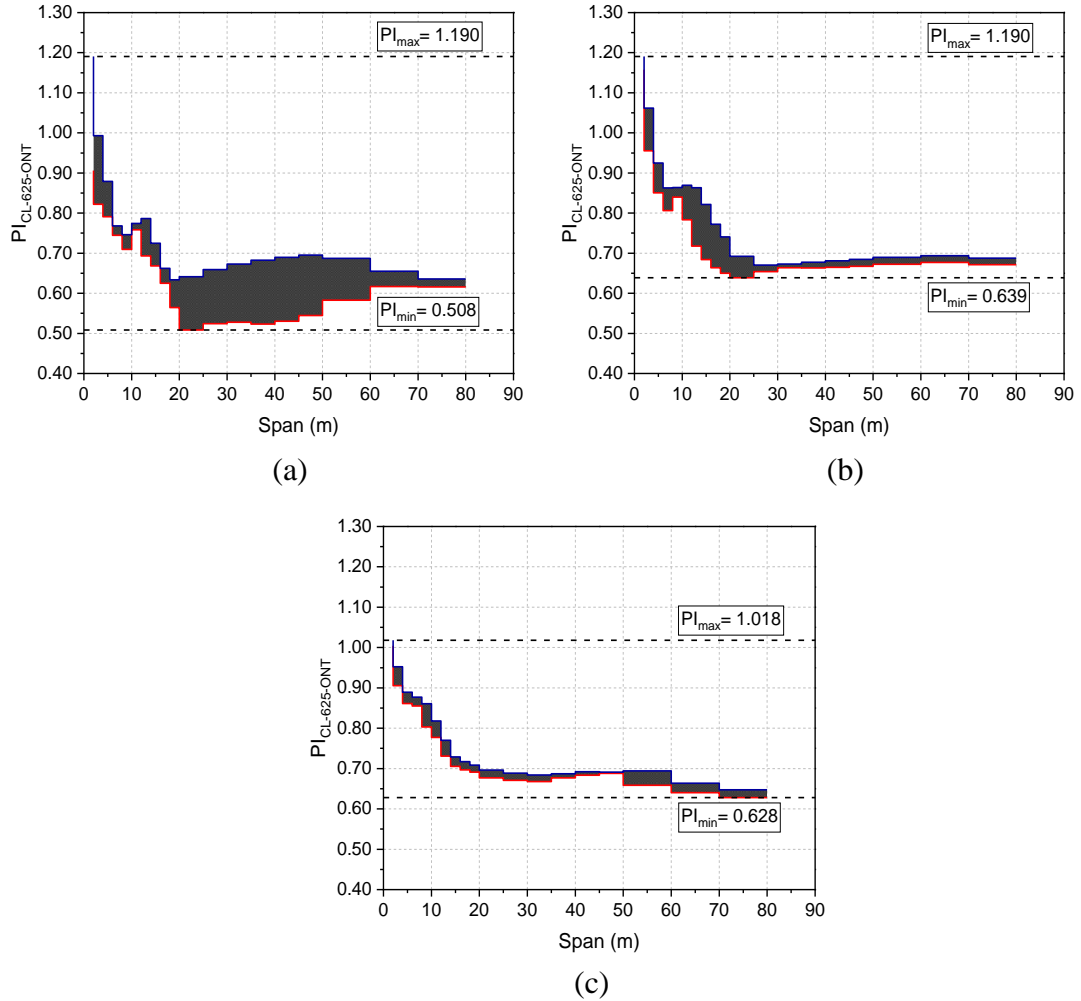


Figure 4.14: Performance of CL-625-ONT truck load model: (a) negative moment; (b) positive moment; (c) shear force

## 4.7 Conclusions

In this study, the New Brunswick permit truck database containing over 16,000 permit applications approved by the NBDTI from 2014 to 2018 was analyzed. The traffic database was filtered to remove any vehicle application comprising erroneous information as well as the mobile cranes and uncommon PC configurations that only represent 0.8% of the database and are allowed to operate only under supervision subject to travel restrictions.

The statistical characteristics of the permits were evaluated, and the filtered database was used to calculate the maximum load effects on bridges. For this purpose, moving load simulations were performed on four bridge configurations based on the provincial bridge inventory with spans ranging from 2m to 80m. An optimization-based approach was adopted to establish an idealized permit live load model that accurately accounts for the structural responses of the site-specific nonconforming overweight permits. The performance of the proposed models was discussed in detail. Furthermore, the performance of the current standard CL-625-ONT truck loading was evaluated against the New Brunswick permit truck database. The latter analysis reveals that the CL-625-ONT significantly underestimates the load effects due to the overweight vehicles. The proposed live load model in this study can be used by the NBDTI to improve the assessment of designated heavy haul corridor in New Brunswick, therefore, enhancing the safety of the provincial highway network. The results of this study can also be used by other jurisdictions as a model to develop their site-specific idealized permit truck models. Finally, this study also reveals the importance of reevaluating the up to date site-specific live load spectra, and the currently used live load model outlined by the CAN/CSA-S6-14, as this model does not represent a significant portion of traffic operating on the highway bridge network today.

## Notations

The following symbols are used in this chapter:

*CDF* = Cumulative distribution function;

*CL* = Canadian loading;

*DOT* = Department of transportation;

$F_n$  = Axle load for the  $n^{\text{th}}$  axle;

*FF* = Single span with fixed supports at both ends;

*GVW* = Gross vehicle weight;

*HPC* = High-performance computing;

*LE<sub>Model</sub>* = Load effect due to live load model;

*LE<sub>Threshold</sub>* = Load effect threshold;

*MOL* = Maximum observed loads in Ontario;

*MOU* = Memorandum of understanding;

*NBC-P* = New Brunswick curve for permit;

*NBDTI* = New Brunswick Department of Transportation and Infrastructure;

*NOA* = Number of axles;

*OHBDC* = Ontario highway bridge design code;

*OBF* = Ontario bridge formula;

*PA* = Annual or project permit;

*PB* = Bulk haul permit;

*PC* = Controlled permit;

*PI* = Performance indicator;

*PI<sub>NB P10-1300</sub>* = Performance indicator of NB -P10-1300;

*PI<sub>Model</sub>* = Performance indicator of model;

*PRR* = Two-equal continuous spans;

*PRRR* = Three-equal continuous spans;

*PS* = Single trip permit;

$S_j$  = Axle spacing;

*SS* = Simply supported span;

## References

- Agarwal, A. C. (1988). Permit vehicle control in Ontario. *Canadian Journal of Civil Engineering*, 15(5), 859-868.
- Baldwin, S. (2012). Compute Canada: advancing computational research. In *Journal of Physics: Conference Series* (Vol. 341, No. 1, p. 012001). IOP Publishing.
- CSA (Canadian Standards Association). (2014). Canadian highway bridge design code. CAN/CSA-S6-14.
- CSA (Canadian Standards Association). (2014). Commentary on CAN/CSA-S6-14, Canadian highway bridge design code (CHBDC). CAN/CSA-S6. 1-14
- Code, O. H. B. D. (1983). Ministry of Transportation and Communications. Ontario.
- Da Lomba, T. (2015). Development of state legal and overweight live load models (Doctoral dissertation, University of Rhode Island).
- Davis, J., Nassif, H. H., Nawy, E. G., Najm, H. S., & Tsakalagos, T. (2007). Live-load models for design and fatigue evaluation of highway bridges. *Language*, 10.
- Jung, F. W., & Wilecki, A. A. (1971). Determining the maximum permissible weights of vehicles on bridges.
- Laman, J. A., & Shah, M. (2016). Assessment of Current Design Loads for Permit Vehicles (No. FHWA-PA-2016-003-PSU WO 16). Pennsylvania. Dept. of Transportation.

Leahy, C., OBrien, E., & O'Connor, A. (2016). The effect of traffic growth on characteristic bridge load effects. *Transportation Research Procedia*, 14, 3990-3999.

Lou, P., Nassif, H., & Truban, P. (2018). Development of Live Load Model for Strength II Limit State in AASHTO LRFD Design Specifications. *Transportation Research Record*, 0361198118756874.

Nowak, A. S. (1994). Load model for bridge design code. *Canadian Journal of Civil Engineering*, 21(1), 36-49.

Nowak, A. S., & Collins, K. R. (2012). Reliability of structures. CRC Press.

Nowak, A. S., & Hong, Y. K. (1991). Bridge live-load models. *Journal of Structural Engineering*, 117(9), 2757-2767.

Steeves, W. H. (2005). Bill 19 An Act to Amend the Motor Vehicle Act. 3rd Session, 55th Legislature. New Brunswick. 54-55 Elizabeth II, 2005-2006.

Taly, N. (2014). Highway bridge superstructure engineering: LRFD approaches to design and analysis. CRC Press.

Taplin, G., Deery, M., van Geldermalsen, T., Gilbert, J., & Grace, R. (2013). A new vehicle loading standard for road bridges in New Zealand (No. 539).

The Highway Traffic Act and Certain Regulations (1978). MTC, Downsview, Ontario.

Tonias, D. E., & Zhao, J. J. (1995). *Bridge engineering: design, rehabilitation, and maintenance of modern highway bridges*. New York, NY: McGraw-Hill.

Vehicle Dimensions and Mass Regulation – Motor Vehicle Act. (2001). New Brunswick Regulation 2001-67. Retrieved from: <http://canlii.ca/t/535cs>

WestGrid (2016). Cedar Technical Specifications. Retrieved from: <https://www.westgrid.ca/support/systems/Cedar>

Zhao, J., & Tabatabai, H. (2011). Evaluation of a permit vehicle model using weigh-in-motion truck records. *Journal of Bridge Engineering*, 17(2), 389-392.

## 5 Summary and Conclusions

The study outlined in this thesis focused on evaluating the heavy truck loads imposed upon the highway bridge infrastructure in New Brunswick today, as well as assessing the adequacy of the currently used CAN/CSA-S6-14 CL-625-ONT truck load model for anticipating the maximum load effects due to the local traffic conditions. An extensive WIM database obtained from five sites across the province along with a truck database containing permit applications approved by the New Brunswick Department of Transportation and Infrastructure (NBDTI) between 2014 and 2018 were analyzed. Four bridge configurations were considered according to the provincial bridge inventory, with spans ranging from 2m to 80m. Based upon the findings of this study, it is observed that the live load spectra to which bridges are subjected in New Brunswick has substantially increased over the years leading to overstress of primary structural members, thus, compromising the integrity of these structures. It is also confirmed that the CL-625-ONT live load model significantly underestimates the maximum load effects due to the current normal traffic demands.

A multi-objective optimization-based approach was adopted in this study for the development of two idealized live load models that addresses the current traffic load in New Brunswick: CL-810-NB and NB P10-1300. The CL-810-NB consists of five axles with a GVW of 810kN and a base length of 17.1m, which is approximately 30% heavier than the CL-625-ONT. The proposed model effectively envelopes the maximum load effects due to the normal traffic that are insufficiently estimated by the CL-6256-ONT

model. The NB P10-1300 consists of ten axles weighing 1300kN with a base length of 34.6m and was configured to envelope the maximum load effects due to the nonconforming configurations that are permitted in New Brunswick under special permits. The proposed models may be used by the NBDTI for the design and evaluation of highway bridges and to improve the assessment of designated heavy haul corridor in the province. Nonetheless, this study emphasizes the importance of reevaluating the current live loads imposed upon bridge structures, and the standard load models outlined by codes of practice, as they found to be outdated. Finally, the methodology outlined in this thesis may be implemented by other jurisdictions nationwide to develop their own live load models representative of their site-specific traffic conditions.

The following conclusions are drawn based on the findings outlined in this thesis:

- (1) The live load spectra imposed upon highway bridges in New Brunswick have substantially changed over the past few decades, and primary structural members may be overstressed.
- (2) The currently used CAN/CSA-S6-14 CL-625-ONT live load model is no longer representative of the local traffic conditions in New Brunswick, as the load effects anticipated by this model are significantly underestimated.
- (3) Multi-Objective-Optimization have proven to be a powerful tool for developing live load models for highway bridges.

- (4) Two idealized live load models were developed to effectively account for the current site-specific live load demand in New Brunswick and can further assist the NBDTI for design and evaluation of highway bridges in the province: The CL-810-NB and the NB P10-1300.
- (5) This study emphasizes the importance of reevaluating the current live loads to which bridges are subjected to, and the adequacy of standard load models outlined by codes of practice.
- (6) The methodology outlined in this thesis may be adopted by other jurisdictions to develop their own updated live load models representative of their site-specific traffic conditions.

## **6 Recommendations for Future Work**

The author would like to make the following recommendations for future work:

- (1) Perform reliability analysis and calibrate the load factors based on the distribution of traffic data.
- (2) Consider the multiple presence of vehicles on a bridge.
- (3) Extend the study using a national traffic database.
- (4) Investigate other multi-objective optimization algorithms that could be used for further optimization of load models.

## References

- Agarwal, A. C. (1988). Permit vehicle control in Ontario. *Canadian Journal of Civil Engineering*, 15(5), 859-868.
- Baldwin, S. (2012). Compute Canada: advancing computational research. In *Journal of Physics: Conference Series* (Vol. 341, No. 1, p. 012001). IOP Publishing.
- Bridge Integration System (BRDG 2018). Information and Technology – *Production Internet Applications*. New Brunswick Department of Transportation and Infrastructure.
- Code, O. H. B. D. (1983). Ministry of Transportation and Communications. Ontario.
- Chen, Y. L., & Liu, C. C. (1994). Multiobjective VAR planning using the goal-attainment method. *IEE Proceedings-Generation, Transmission and Distribution*, 141(3), 227-232.
- Cortés-Borda, D., Ruiz-Hernández, A., Guillén-Gosálbez, G., Llop, M., Guimerà, R., & Sales-Pardo, M. (2015). Identifying strategies for mitigating the global warming impact of the EU-25 economy using a multi-objective input–output approach. *Energy Policy*, 77, 21-30.
- CSA (Canadian Standards Association). (2014). Canadian highway bridge design code. *CAN/CSA-S6-14*.
- CSA (Canadian Standards Association). (2014). Commentary on CAN/CSA-S6-14, Canadian highway bridge design code (CHBDC). CAN/CSA-S6. 1-14.

Da Lomba, T. (2015). Development of state legal and overweight live load models (Doctoral dissertation, University of Rhode Island).

Davis, J., Nassif, H. H., Nawy, E. G., Najm, H. S., & Tsakalakos, T. (2007). Live-load models for design and fatigue evaluation of highway bridges. *Language*, 10.

Fathi, H., & Afshar, A. (2010). GA-based multi-objective optimization of finance-based construction project scheduling. *KSCE Journal of Civil Engineering*, 14(5), 627-638.

Gembicki, F., & Haimes, Y. (1975). Approach to performance and sensitivity multiobjective optimization: The goal attainment method. *IEEE Transactions on Automatic control*, 20(6), 769-771.

Getachew, A., & O'Brien, E. J. (2007). Simplified site-specific traffic load models for bridge assessment. *Structure and Infrastructure Engineering*, 3(4), 303-311.

Gindy, M., & Nassif, H. (2015). Effect of bridge live load based on 10 years of WIM data. In *Advances in Bridge Maintenance, Safety Management, and Life-Cycle Performance, Set of Book & CD-ROM* (pp. 755-756). CRC Press.

Guide, T. M. (2001). Federal Highway Administration. US Department of Transportation, Washington, DC.

Hanson, R., Executive, V. P., & COO, I. (2010). ITS Technologies for Commercial Vehicle Compliance in the Maritimes. In 2010 Annual Conference of the Transportation Association of Canada Halifax, Nova Scotia.

Hibbeler, R. C. (2015). *Structural analysis ninth edition*. Pearson Prentice Hall.

Hwang, C. L., & Masud, A. S. M. (2012). *Multiple objective decision making methods and applications: a state-of-the-art survey* (Vol. 164). Springer Science & Business Media.

Jung, F. W., & Wilecki, A. A. (1971). Determining the maximum permissible weights of vehicles on bridges.

Kozikowski, M. (2009). WIM based live load model for bridge reliability. *Civil Engineering Dissertations and Student Research*, 2.

Laman, J. A., & Shah, M. (2016). Assessment of Current Design Loads for Permit Vehicles (No. FHWA-PA-2016-003-PSU WO 16). Pennsylvania. Dept. of Transportation.

Leahy, C., O'Brien, E., & O'Connor, A. (2016). The effect of traffic growth on characteristic bridge load effects. *Transportation Research Procedia*, 14, 3990-3999.

Lou, P., Nassif, H., & Truban, P. (2018). Development of Live Load Model for Strength II Limit State in AASHTO LRFD Design Specifications. *Transportation Research Record*, 0361198118756874.

Luskin, D., & Walton, C. M. (2001). *Effects of truck size and weights on highway infrastructure and operations: A synthesis report* (No. FHWA/TX-0-2122-1,). Center for Transportation Research, Bureau of Engineering Research, University of Texas at Austin.

MATLAB and Statistics Toolbox Release 2018a (2018), The MathWorks, Inc., Natick, Massachusetts, United States.

Miao, T. J., & Chan, T. H. (2002). Bridge live load models from WIM data. *Engineering structures*, 24(8), 1071-1084.

New Brunswick Department of Transportation and Infrastructure (2018). Highway Cameras. Retrieved from: <http://www.snb.ca/geonb1/e/map-prod/map-prod-E.asp>

Nowak, A. S. (1999). Calibration of LRFD Bridge Design Code (No. Project C12-33 FY'88-'92).

Nowak, A. S. (1994). Load model for bridge design code. *Canadian Journal of Civil Engineering*, 21(1), 36-49.

Nowak, A. S., & Collins, K. R. (2012). Reliability of structures. CRC Press.

Nowak, A. S., & Hong, Y. K. (1991). Bridge live-load models. *Journal of Structural Engineering*, 117(9), 2757-2767.

Nowak, A. S., & Rakoczy, P. (2013). WIM-based live load for bridges. *KSCE Journal of Civil Engineering*, 17(3), 568-574.

Pelphrey, J., Higgins, C., Sivakumar, B., Groff, R. L., Hartman, B. H., Charbonneau, J. P., & Johnson, B. V. (2008). State-specific LRFR live load factors using weigh-in-motion data. *Journal of Bridge Engineering*, 13(4), 339-350.

Przemieniecki, J. S. (1985). *Theory of matrix structural analysis*. Courier Corporation.

SAP2000. (2018). Integrated finite element analysis and design of structures, Computers and Structures, Berkeley, CA.

Sivakumar, B., & Sheikh Ibrahim, F. I. (2007). Enhancement of bridge live loads using weigh-in-motion data. *Bridge Structures*, 3(3, 4), 193-204.

Southgate, H. F. (2001). Quality assurance of weigh-in-motion data. Federal Highway Administration.

Steeves, W. H. (2005). Bill 19 An Act to Amend the Motor Vehicle Act. 3rd Session, 55th Legislature. New Brunswick. 54-55 Elizabeth II, 2005-2006.

Taly, N. (2014). Highway bridge superstructure engineering: LRFD approaches to design and analysis. CRC Press.

Taplin, G., Deery, M., van Geldermalsen, T., Gilbert, J., & Grace, R. (2013). A new vehicle loading standard for road bridges in New Zealand (No. 539).

The Highway Traffic Act and Certain Regulations (1978). MTC, Downsview, Ontario.

Timoshenko, S. P. (1921). On the correction for shear of the differential equation for transverse vibrations of prismatic bars. *Phil. Mag.*, 41, 744-746.

Tonias, D. E., & Zhao, J. J. (1995). Bridge engineering: design, rehabilitation, and maintenance of modern highway bridges. New York, NY: McGraw-Hill.

Vehicle Dimensions and Mass Regulation – Motor Vehicle Act. (2001). New Brunswick Regulation 2001-67. Retrieved from: <http://canlii.ca/t/535cs>

Wang, J. J., Jing, Y. Y., Zhang, C. F., & Zhao, J. H. (2009). Review on multi-criteria decision analysis aid in sustainable energy decision-making. *Renewable and sustainable energy reviews*, 13(9), 2263-2278.

WestGrid (2016). Cedar Technical Specifications. Retrieved from: <https://www.westgrid.ca/support/systems/Cedar>

Zavala, G., Nebro, A. J., Luna, F., & Coello, C. A. C. (2016). Structural design using multi-objective metaheuristics. Comparative study and application to a real-world problem. *Structural and Multidisciplinary Optimization*, 53(3), 545-566.

Zhao, J., & Tabatabai, H. (2011). Evaluation of a permit vehicle model using weigh-in-motion truck records. *Journal of Bridge Engineering*, 17(2), 389-392.

# **Appendix A: Direct Stiffness Method for Moving Load Analysis**

## A.1 Code Description

The following self-prepared MATLAB code was developed to analyze 2D beam elements under a series of moving point loads using the direct stiffness method. Timoshenko beam theory is used when determining the element stiffness matrices, which accounts for shear deformations. The SAP2000 software (SAP2000 2018) also uses Timoshenko beam theory and it was used to validate the code presented herein.

### A.1.1 Variables

Table A.1 describes the variables used in the code script including the variable name, size and description. The units are in  $N$  and  $m$ .

Table A.1: Variables used in the code.

VARIABLES	SIZE	DESCRIPTION
$N_{\text{elems}}$	1 x 1	Number of elements
$N_{\text{nodes}}$	1 x 1	Number of nodes
$L_{\text{beam}}$	1 x 1	Total length of beam (m)
$\text{beam\_incr}$	1 x 1	Length of finite element (m)
nodes	$N_{\text{nodes}} \times 2$	Matrix with nodes coordinate
	Column 1	Node x coordinate
	Column 2	Node y coordinate
elements	$N_{\text{elems}} \times 2$	Matrix with elements coordinates
	Column 1	Initial node number
	Column 2	End node number

E	$N_{\text{elems}} \times 1$	Array with modulus of elasticity for each element ( $\text{N/m}^2$ )
A	$N_{\text{elems}} \times 1$	Array with cross sectional area of each element ( $\text{m}^2$ )
I	$N_{\text{elems}} \times 1$	Array with moment of inertia about of each element ( $\text{m}^4$ )
G	$N_{\text{elems}} \times 1$	Array with shear modulus of each element ( $\text{N/m}^2$ )
bcs	Number of constrained DOF x 3	Matrix with defined constrained boundary conditions
	Column 1	Joint index where boundary condition is applied
	Column 2	Applied restrains (1 for translation; 2 for rotation).
	Column 3	Initial displacement applied to respective joint)
$S_i$	$1 \times 1$	Spacing between $A_i$ and $A_n$
$A_i$	$1 \times 1$	Position of axle i moving from node 1 to node n
loads	Number of loads x 3	Matrix with defined loads
	Column 1	Joint index where point load is applied
	Column 2	DOF (1 for force; 2 for moment)
	Column 3	Load magnitude (N; N.m)
K	$(2 \times N_{\text{nodes}})^2$	Global stiffness matrix
u	$2 \times N_{\text{nodes}} \times 1$	Array with nodal displacements (m)
f	$2 \times N_{\text{nodes}} \times 1$	Array with nodal forces

all_dofs	$1 \times (2 \times N_{\text{elems}})$	Two DOF per joint (1 for translation; 2 for rotation)
dofspec	$1 \times \text{Size}(\text{bcs},1)$	Restrained DOFs at support
thisdof	$1 \times 1$	Index or restrained DOFs
doffree	$1 \times [2 \times N_{\text{nodes}} - \text{length}(\text{dofspec})]$	Unrestrained DOFs
K_element	$4 \times 4$	Element stiffness matrix
k_elem	$N_{\text{elems}} \times 1$ cell	Cell with individual element stiffness matrix
u1_	$N_{\text{elems}} \times 1$ cell	Cell with individual nodal displacement
f_	$N_{\text{elems}} \times 1$ cell	Cell with individual nodal forces
f__	$(4 \times N_{\text{elems}}) \times 1$	Nodal forces for each element
M_maxx	$(2 \times N_{\text{elems}}) \times 1$	Array with nodal moment (N.m)
M_max	$1 \times 1$	Maximum negative moment
M_maxx_vector	$1 \times (2 \times \text{Number of DOF}+1)$	Array with maximum nodal moment at specific location
Maximum_negative_moment	$1 \times 1$	Absolute maximum moment at point of interest
Momento	$N_{\text{nodes}} \times 1$	Array with nodal displacement
Momento__	$N_{\text{nodes}} \times \text{sum}(S)$	Matrix with moments for all loading cases
V_maxx	$(2 \times N_{\text{elems}}) \times 1$	Array with shear forces at each joint (N)
V_max	$1 \times 1$	Maximum shear force
V_maxx_vector	$1 \times (2 \times \text{Number of DOF}+1)$	Array with maximum shear at all joints
Maximum_shear	$1 \times 1$	Absolute maximum shear
Shear	$N_{\text{nodes}} \times 1$	Array with nodal shear
Shear__	$N_{\text{nodes}} \times \text{sum}(S)$	Matrix with nodal shear for all loading cases

moment_envelope_min	$N_{nodes} \times 1$	Array with negative moment envelope
moment_envelope_max	$N_{nodes} \times 1$	Array with positive moment envelope
Shear_envelope_min	$N_{nodes} \times 1$	Array with negative shear envelope
Shear_envelope_max	$N_{nodes} \times 1$	Array with positive shear envelope

### A.1.2 Define System Parameters

The first step is to define the total length,  $L_{beam}$ , of the system as shown in Figure A.1

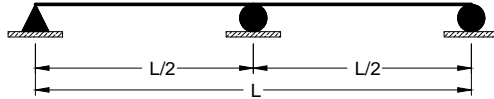


Figure A.1: Beam layout

A beam array *beam*, with the total length divided into increments 0.1m long is created. Therefore, every node is 0.1m apart from each other. The node and element matrices are then generated, and material and section properties are assigned to the elements. Finally, the arrays defining the section properties are created as depicted in Figure A.2.

```

%% Define System Parameters [Input]
L_beam = 12; %length of entire beam [m]
beam_incr = 0.1; %divide the beam into elements
0.1 m long each
beam = 0:beam_incr:L_beam; %create a beam array
nodes = zeros(length(beam),2); %create a zero matrix for the
nodes
nodes(:,1)=0:beam_incr:L_beam; %node coordinates (x,y)
elements = zeros((length(beam)-1),2); %defining the elements (node
initial; node end)
elements(:,1)=1:length(beam)-1; %element initial node
elements(:,2)=2:length(beam); %element end node
%% Define Material Properties
E = zeros(length(elements),1);E(:,1)=1.999e11; %modulus of elasticity
of each member [N/m2]
A = zeros(length(elements),1);A(:,1)=7.526e-4; %cross sectional area of
each member [m2]
I = zeros(length(elements),1);I(:,1)=7.047e-7; %moment of inertia about
strong axis of each member [m4]
G = zeros(length(elements),1);G(:,1)=7.69e10; %shear modulus of each
member [N/m2]

```

Figure A.2: System parameters

### A.1.3 Define Boundary Conditions

The boundary conditions *bcs*, are used to define the restrained DOFs at the support locations. The first column represents the node number, the second is used to specify the restrained DOF (1 for translation; 2 for rotation). The third column is used to determine any initial nodal displacement. In case of fixed support, both translation and rotation must be defined for the same joint separately. The boundary conditions are then applied at support locations. The variable *dofspec* and *doffree* corresponds to the constrained and unconstrained nodes along the beam, respectively. These parameters are used to partition the system and to solve for displacement later. Figure A.3 shows the script describing this step.

```

%% Define Boundary Conditions
bcs = [1 ((length(beam)+1)/2) length(beam); 1 1 1; 0 0 0]'; %BCS: (node
#; dof; displacement)>>DOFs 1 and 2 for translation and rotation
respect.
N_elems = size(elements,1); %Number of elements
N_nodes = size(nodes,1); %Number of nodes
all_dofs = 1:2*N_nodes; %All DOFS (2DOFs per
node for displacement and rotation)
dofspec = []; %DOF restrained
for ii = 1:size(bcs,1)
    thisdof = 2*(bcs(ii,1)-1)+bcs(ii,2);
    dofspec = [dofspec thisdof]; %specified dof where
there is support
    u(thisdof) = bcs(ii,3);
end
doffree = all_dofs;
doffree(dofspec) = []; %delete specified dofs
from all

```

Figure A.3: Boundary conditions

#### A.1.4 Global Stiffness Matrix

The element stiffness matrix  $K_{el}^{(i)}$ , is calculated for each member using the function *element\_stiff\_timo.m*, as shown in Figure A.4, in which shear deformation is considered based on Timoshenko beam theory as given in Equation A.1.

$$K_{el}^{(i)} = \frac{EI}{L^3(1 + \beta_s)} \begin{bmatrix} 12 & 6L & -12 & 6L \\ 6L & L^2(4 + \beta_s) & -6L & L^2(2 - \beta_s) \\ -12 & -6L & 12 & -6L \\ 6L & L^2(2 - \beta_s) & -6L & L^2(4 + \beta_s) \end{bmatrix} \quad (\text{A.1})$$

Where:

- The coefficient  $\beta_s = \frac{12EI f_s}{GAL^2}$
- $E$  is the modulus of elasticity of the element in (N/m<sup>2</sup>)
- $I$  is the moment of inertia about the strong axis in (m<sup>4</sup>)
- $L$  is the length of the element in (m)

- $G$  is the shear modulus in (N/m<sup>2</sup>)
- $A$  is the cross-sectional area of the beam in (m<sup>2</sup>)
- $f_s$  is the shape factor = 1.2002 for rectangular shape

```
function [K_el] = element_stiff_timo(nodexy, E, A, I, G)
%This matrix is in the global coordinates
E1 = [(nodexy(2,1)-nodexy(1,1)) ...
      (nodexy(2,2)-nodexy(1,2))];
L = norm(E1);
E1 = E1/L;
E2 = [-E1(2) E1(1)];
fs = 1.2002; % for rectangular section
beta = 12*E(1,1)*I(1,1)*fs/(G(1,1)*A(1,1)*L^2);
K_el = [...
          12*E*I/((L^3)*(1+beta))    6*E*I/((L^2)*(1+beta))    -
12*E*I/((L^3)*(1+beta))    6*E*I/((L^2)*(1+beta)) ; ...
          6*E*I/((L^2)*(1+beta))    (4+beta)*E*I/(L*(1+beta))    -
6*E*I/((L^2)*(1+beta))    (2-beta)*E*I/(L*(1+beta))    ; ...
          -12*E*I/((L^3)*(1+beta))   -6*E*I/((L^2)*(1+beta))
12*E*I/((L^3)*(1+beta))   -6*E*I/((L^2)*(1+beta)) ; ...
          6*E*I/((L^2)*(1+beta))    (2-beta)*E*I/(L*(1+beta))    -
6*E*I/((L^2)*(1+beta))    (4+beta)*E*I/(L*(1+beta))    ];
```

Figure A.4: Element stiffness matrix

The global matrix  $K$  is created by assembling all the element stiffness matrices together using superposition, as shown in Figure A.5.

```

%% Calculate global stiffness matrix
K = zeros(2*N_nodes); %initialize global
stiffness matrix
for i_elem = 1:N_elems
    el_nodes = elements(i_elem, 1:2); %creating an array with
the element and its respective nodes
    nodexy = nodes (el_nodes, :);
    % Create global stiffness matrix
    [K_element] = element_stiff_timo(nodexy, E(i_elem), A(i_elem),
I(i_elem), G(i_elem));
    k_elem{i_elem,1} = K_element; %element matrix
    % Group the element stiffness matrix into the global stiffness
matrix
    el_dofs = 2*(el_nodes(1)-1)+1:2*el_nodes(1);
    el_dofs = [el_dofs 2*(el_nodes(2)-1)+1:2*el_nodes(2)];
    K(el_dofs,el_dofs) = K(el_dofs, el_dofs) + K_element;
end
%% Calculate inverse of global stiffness matrix
K_inv=inv(K(doffree,doffree)); %Inverse of global
stiffness matrix

```

Figure A.5: Global stiffness matrix

### A.1.5 Defining Moving Load

The spacing  $S_i$  between each axle load is first defined and the axle loads  $A_i$  are then defined as a series of point loads as shown in Figure A.6. The series of moving point loads move from the left to the right starting at joint  $i$  (*start\_location*) and ends when the last point load exists the beam. The respect script is shown in Figure A.7.

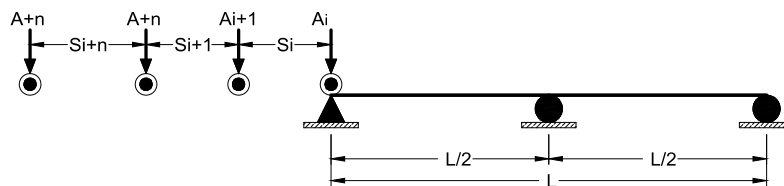


Figure A.6: Moving load layout

```

%% Define the axle spacing
S1=round(3.6/beam_incr,1); %space between axle 1 and 2 [m]
S2=round(1.2/beam_incr,1); %space between axle 2 and 3 [m]
S3=round(6.6/beam_incr,1); %space between axle 3 and 4 [m]
S4=round(6.6/beam_incr,1); %space between axle 4 and 5 [m]
S5=round(1.0/beam_incr,1); %space between axle 5 and 6 [m]
S6=round(1.2/beam_incr,1); %space between axle 6 and 7 [m]
S7=round(1.2/beam_incr,1); %space between axle 7 and 8 [m]
S8=round(1.2/beam_incr,1); %space between axle 8 and 9 [m]
S9=round(1.3/beam_incr,1); %space between axle 9 and 10 [m]
S10=round(1.0/beam_incr,1); %space between axle 10 and 11 [m]
S11=round(1.0/beam_incr,1); %space between axle 10 and 11 [m]
S12=round(1.0/beam_incr,1); %space between axle 10 and 11 [m]
S13=round(1.0/beam_incr,1); %space between axle 10 and 11 [m]
%% Calculate load effect envelope for the moving load
for
start_location=0:1:(L_beam/beam_incr)+S13+S12+S11+S10+S9+S8+S7+S6+S5+
S4+S3+S2+S1 %truck starts with AXW 1 at joint 1, and finishes with last
AXW at last joint
    A1=start_location; %position of AX1 at joint 1
    A2=A1-S1; %position of AX2 from AX1
    A3=A2-S2; %position of AX3 from AX2
    A4=A3-S3; %position of AX4 from AX3
    A5=A4-S4; %position of AX5 from AX4
    A6=A5-S5; %position of AX6 from AX5
    A7=A6-S6; %position of AX7 from AX6
    A8=A7-S7; %position of AX8 from AX7
    A9=A8-S8; %position of AX9 from AX8
    A10=A9-S9; %position of AX10 from AX9
    A11=A10-S10; %position of AX11 from AX10
    A12=A11-S11; %position of AX12 from AX11
    A13=A12-S12; %position of AX13 from AX12
    A14=A13-S13; %position of AX14 from AX13
loads = [A1 A2 A3 A4 A5 A6 A7 A8 A9 A10 A11 A12 A13 A14; 1 1 1 1 1 1 1
1 1 1 1 1 1; -50000 -125000 -125000 -175000 -150000 -0 -0 -0 -0 -0 -
0 -0 -0 -0]'; % Nodal loads [N] with respective coordinate (node #,
dof, specified load)

```

Figure A.7: Defining series of moving point loads

### A.1.6 Applying Loads and Calculating Displacement and Support Reactions

The displacement  $u$  and force  $f$  arrays are initialized, and the external loads are applied to  $f$ , as shown in Figure A.8.

```

%% Initialize zero matrices for the following parameters
u = zeros(2*N_nodes,1); % zero displacement vector
f = zeros(2*N_nodes,1); % zero force vector
%% Nodal loads
for ii = 1:size(loads,1)
    if (loads(ii,1)>=0 && loads(ii,1)<=L_beam/beam_incr) % specify
the point load limits until last AXW is at last joint
        f(2*(loads(ii,1)) + loads(ii,2))= loads(ii,3); % external
nodal loads applied to the beam
    end
end
end

```

Figure A.8: Applying external loads

The global force vector  $F$  can then be related to its global stiffness matrix  $K$ , and the displacement vector  $D$  can be calculated using the following equations:

$$\{F\} = [K]\{D\} \xrightarrow{yields} \{D\} = [K]^{-1}\{f\} \quad (A.2)$$

$$\begin{Bmatrix} m_i \\ fy_i \\ m_{i+1} \\ fy_{i+1} \\ \vdots \\ m_{i+n} \\ fy_{i+n} \end{Bmatrix}_{nx1} = \begin{bmatrix} K11 & K12 & K13 & \dots & K1n \\ \vdots & K22 & K23 & \dots & K2n \\ \vdots & \vdots & K33 & \dots & K3n \\ \vdots & \vdots & \vdots & \ddots & \vdots \\ K1n & K2n & K3n & \dots & Knn \end{bmatrix}_{nxn} * \begin{Bmatrix} \phi_i \\ u_i \\ \phi_{i+1} \\ u_{i+1} \\ \vdots \\ \phi_{i+n} \\ u_{i+n} \end{Bmatrix}_{nx1} \quad (A.3)$$

where  $F$  and  $D$  consist of the known and unknown externally applied loads and nodal displacements, respectively. Equation A.3 can be portioned as given in Equation A.4 to group the known and the unknown DOFs together.

$$\begin{Bmatrix} F_{Known} \\ F_{Unknown} \end{Bmatrix} = \begin{bmatrix} K_{11} & K_{12} \\ K_{21} & K_{22} \end{bmatrix} \begin{Bmatrix} D_{Unknown} \\ D_{Known} \end{Bmatrix} \quad (A.4)$$

Expanding Equation A.1.4 yields the two following equations:

$$F_{Known} = K_{11}D_{Unknown} + K_{12}D_{Known} \quad (A.5)$$

$$F_{Unknown} = K_{21}D_{Unknown} + K_{22}D_{Known} \quad (A.6)$$

Therefore,  $D_{Unknown}$  can be determined directly from Equation A.5, and the support reactions  $F_{Unknown}$  can be consecutively calculated according to Equation A.6. Figure A.9 shows the script describing this step.

```

%% Calculate Nodal displacements and reaction forces
u(doffree) = K_inv*f(doffree);           % Nodal displacements
after applying boundary conditions
f(dofspec) = K(dofspec,:) * u;         % Support reactions

```

Figure A.9: Nodal displacement and support reactions

Once the nodal displacements and reaction forces are determined, the internal forces  $f^{(i)}$  for each element can be calculated using the following equation:

$$\{f^{(i)}\} = [K_{el}^{(i)}] * \{u^{(i)}\} \quad (A.7)$$

Figure A.10 shows the script used to calculate element forces  $f_{-}$ , where  $kl_{-}$  and  $ul_{-}$  are the elements stiffness matrix and nodal displacements for the element, respectively.

```

%% Calculate element forces
Ndof = length(all_dofs); %number of DOF
for i = 1:N_elems
    ii= 0:N_elems-1;
    iii = 0:2:Ndof-2;
    u1_{i,1} = u((i+ii(1,i)): (4+iii(1,i))), 1 ); %nodal
    displacement
    f_{i,1}= k_elem{i,1}* u1_{i,1}; %member forces
    (shear and moment)
end

```

Figure A.10: Element forces

### A.1.7 Maximum Load Effect Envelope

The maximum moment and shear envelopes are calculated upon the passage of the moving loads, where the positive and negative moment envelopes are stored in the *moment\_envelop\_min* and *moment\_envelop\_max*, respectively. The positive and negative shear envelopes are stored in the *shear\_envelop\_min* and *shear\_envelop\_max*, respectively. The load envelope as well as the maximum load effects are generated as shown in Figures A.11 and A.12.

```

%% Extracting load effects for members
f__=cell2mat(f_); %convert cell containing load effects to mat
M_maxx = zeros((length(f__))/2,1); %initialize matrix for moment
V_maxx = zeros((length(f__))/2,1); %initialize matrix for shear
ii=0;
% Separate moment and shear and store in their respective matrices
for i=1:length(f__)/2
    M_maxx(i,1) = f__(2*i,1); %element moments
    V_maxx(i,1) = f__(i+ii,1); %element shear
    ii=i;
end
M_maxx_vector(start_location+1)= max(M_maxx);
M_minx_vector(start_location+1)= min(M_maxx);
V_maxx_vector(start_location+1)= max(V_maxx);
%% Extracting maximum load effects at each node
ii=0;
Momento=zeros(length(M_maxx)/2+1,1); %initialize moment matrix
Shear = zeros(length(V_maxx)/2+1,1); %initialize shear matrix
for i=1:length(M_maxx)/2
    Momento(i,1)=M_maxx(i+ii,1); %extracted nodal moment
    Shear(i,1) = V_maxx(i+ii,1); %extracted nodal shear
    ii=i;
end
Momento(length(M_maxx)/2+1,1)= -M_maxx(length(M_maxx),1);
Shear(length(V_maxx)/2+1,1) = -V_maxx(length(V_maxx),1);
Momento__(:,start_location+1) = Momento; %Moment envelope
Shear__(:,start_location+1) = Shear; %Shear envelope
x =zeros(length(Momento),1);
end

```

Figure A.11: Maximum load effect envelope

```

%% Display Moment and shear envelopes
% Defining envelopes
for dd = 1:length(beam)
    momento_envelope_min(dd,1) = min(Momento__(dd,:)); % positive
moment envelope
    momento_envelope_max(dd,1) = max(Momento__(dd,:)); % negative
moment envelope
    shear_envelope_min(dd,1) = min(Shear__(dd,:)); %positive shear
envelope
    shear_envelope_max(dd,1) = max(Shear__(dd,:)); %negative shear
envelope
end
%% Moment Envelope
subplot(2,1,1)
% Plot beam
plot(beam*10,x,'--r' , 'linewidth',2.5); hold on
% %Plot Moment Diagram
plot(round(beam*10,0),1*momento_envelope_min,'-b' , 'linewidth',2.0);
hold on %Maximum negative Moment [N-m]
plot(round(beam*10,0),1*momento_envelope_max,'-b' , 'linewidth',2.0)
%Maximum positive Moment [N-m]
ylabel('Moment [N.m]','fontsize',14, 'fontweight','bold')
xlabel('Span length [m * 10-1] ','fontsize',14, 'fontweight','bold')
title('Bending Moment Envelope','fontsize',16, 'fontweight','bold');
grid on
%% Shear envelope
subplot(2,1,2)
%Plot Beam
plot(beam*10,x,'--r' , 'linewidth',2.5); hold on
%Plot beam diagram
plot(beam*10,-1*shear_envelope_min,'-b' , 'linewidth',2.0); hold on
%Maximum negative shear [N]
plot(beam*10,-1*shear_envelope_max,'-b' , 'linewidth',2.0)
%Maximum positive shear [N]
ylabel('Shear [N]','fontsize',14, 'fontweight','bold')
xlabel('Span length [m * 10-1] ','fontsize',14, 'fontweight','bold')
title('Shear Diagram','fontsize',16, 'fontweight','bold'); grid on
%% Display maximums
disp(['Maximum negative moment = ', num2str(-
1*max(momento_envelope_max)), ' N-m'])
disp(['Maximum positive moment = ', num2str(-
1*min(momento_envelope_min)), ' N-m'])
disp(['Maximum shear force = ', num2str(max(V_maxx_vector)), ' N'])

```

Figure A.12: Load effect diagrams

### A.1.8 Code Validation

The SAP2000 software was used to validate the code used in this study. The following problem was solved using both resources to calculate the maximum shear and moment for a 12m long rectangular steel two-continuous equal span beam (Figure A.13) subjected to a seven-axle truck moving load (Figure A.14). The beam properties are:

- Width,  $w = 0.0071$  m
- Height,  $h = 0.106$  m
- Modulus of elasticity,  $E = 1.99E^{11}$  N/m<sup>2</sup>
- Cross sectional area,  $A = 7.526E^{-4}$  m<sup>2</sup>
- Moment of inertia about strong axis,  $I = 7.047E^{-7}$  m<sup>4</sup>
- Shear modulus,  $G = 7.69E^{10}$  N/m<sup>2</sup>
- Shape factor,  $f_s=1.2002$  (Timoshenko beam theory)

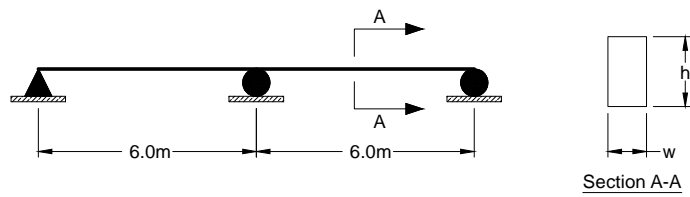


Figure A.13: Beam problem validation

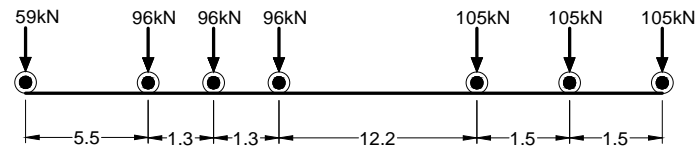


Figure A.14: Moving load

The results obtained from each both methods are shown in Figures A.15 and A.16. As seen in these figures, the results from both resources show agreement.

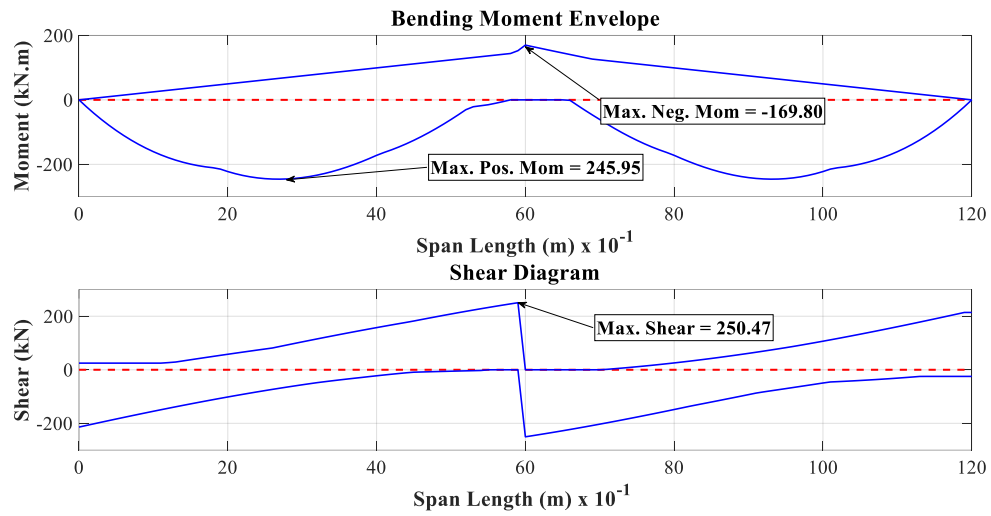


Figure A.15: MATLAB results

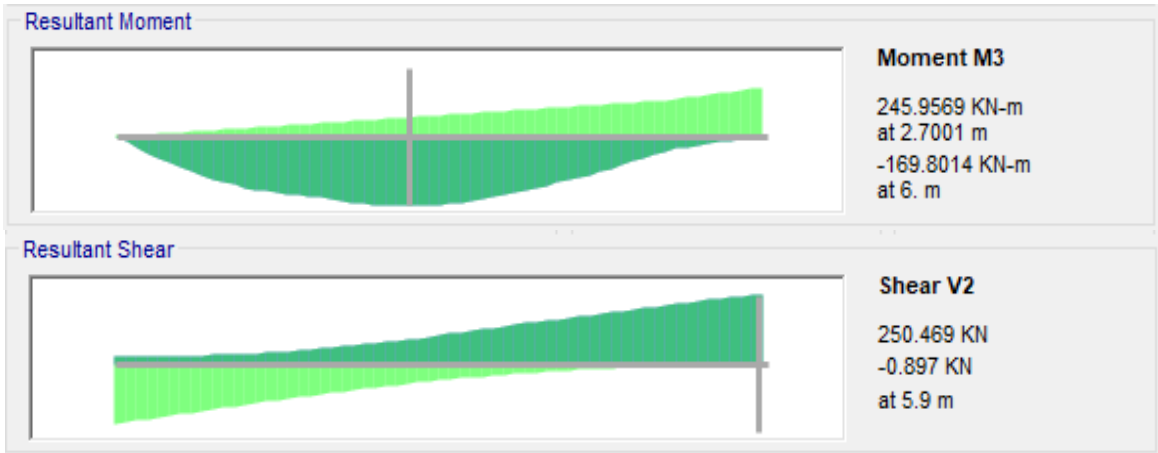


Figure A.16: SAP2000 results

## **Appendix B: WIM Quality Assurance**

The WIM system records the traffic loads in real time as the vehicles move over the tracking sensors, and calibration must be conducted on a regular basis to ensure the adequate operation of the system. Several factors may impact the calibration of a WIM system including the effects from temperature, calibration drift over, improper installation, poor maintenance, and stiffness of flexible asphalt (Southgate 2001). Therefore, a data quality check was performed to the WIM data using the calibration assurance technique proposed by Southgate (2001). This technique assesses the calibration of the WIM systems using a logarithmic regression of the first axle spacing ( $S_1$ ) and steering axle load ( $A_1$ ) of Class 9 vehicles only. The sample size was limited to one day only, as recommended, due to the effects caused by the temperature. English units must be used for compatibility, where axle load and spacing are in *ft* and *lb*, respectively. The data quality check was conducted according to the following procedure:

- I. One day records containing Class 9 vehicles were considered.
- II. The regression equations for  $X = \text{Log}_{10}(S_1)$  and  $Y = \text{Log}_{10}(A_1/S_1)$  were calculated.
- III. A linear regression was determined for  $y = mx + b$ .
- IV. The regression equation  $R = 10^{[b+m*\text{Log}_{10}(S_1)]}$  was calculated.
- V. The reference regression equation  $RE = 10^{[3.925361-0.952182*\text{Log}_{10}(S_1)]}$  was calculated.
- VI. The upper and lower bounds regression equations  $UB = 12000\text{lb}/(S_1 + 50\text{lb}/\text{ft})$  and  $LB = 10^{[3.942369-1.07509*\text{Log}_{10}(S_1)]}$  were calculated.

VII. The following parameters were plotted:  $A_1/S_1$ ,  $R$ ,  $RE$ ,  $UB$ , and  $LB$  vs  $S_1$  for each record.

Figures B.1 through B.5 show the results obtained from the WIM data quality assurance performed for the five sites of New Brunswick. As seen in this figure, most of the recorded data are within the lower and upper bounds. This observation indicates that the WIM systems demonstrate satisfactory calibration and the WIM data used in this study are reliable.

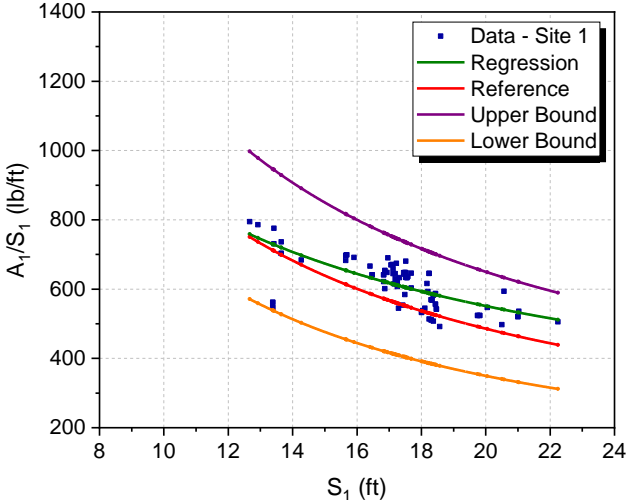


Figure B.1: WIM quality assurance of Deerwood Site

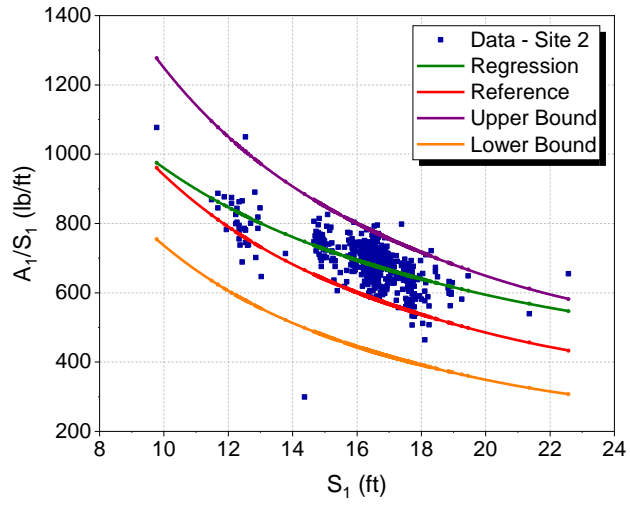


Figure B.2: WIM quality assurance of Longscreek Site

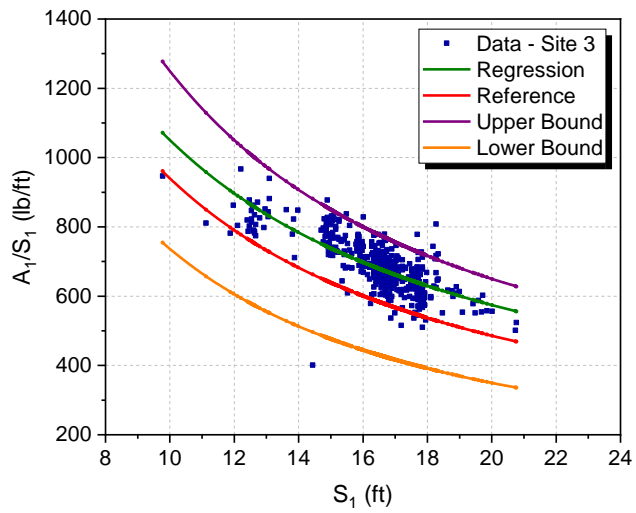


Figure B.3: WIM quality assurance of Waweig Site

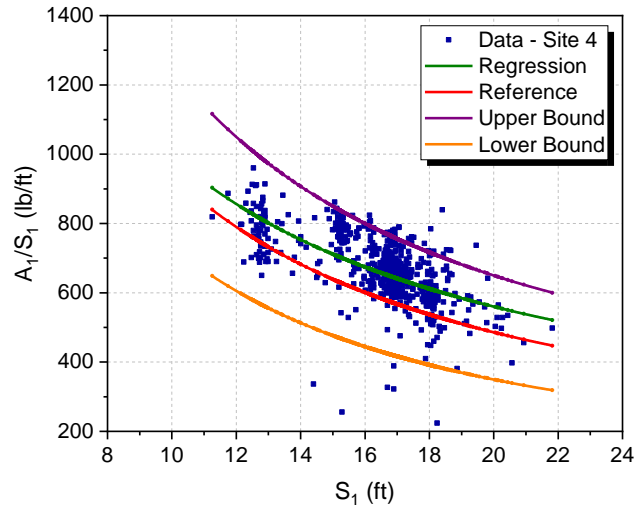


Figure B.4: WIM assurance of Salisbury Eastbound

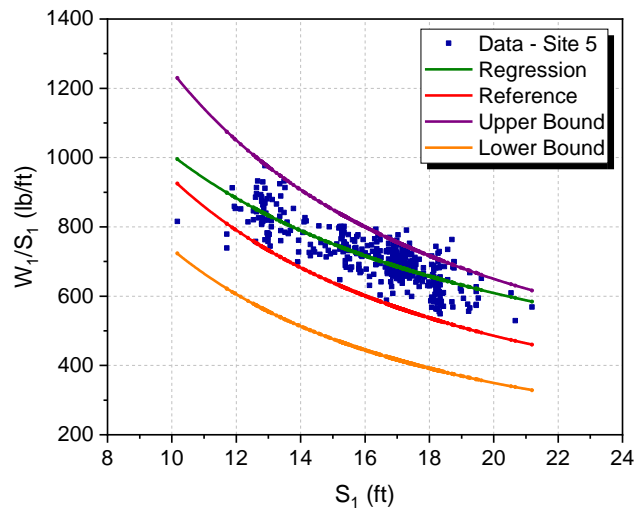


Figure B.5: WIM assurance of Salisbury Westbound

## **Appendix C: Raw WIM Database Sample**

Figures C.1 through C.5 show a sample sheet of the raw WIM database containing 17 vehicles obtained from Waweig site, where there are 37 columns describing each vehicle recorded by the WIM system.

Year	Month	Day	Hour	Minute	Seconds	Vehicle Number	Record Type	Lane	Speed (km/h)	Vehicle Class	Vehicle Type
14	6	23	18	22	43	63706	11	1	96	12	27
14	6	23	18	40	13	63762	11	1	96	9	20
14	6	23	18	41	52	63770	11	1	97	9	20
14	6	23	18	42	9	63772	11	1	108	5	3
14	6	23	18	49	47	63806	11	1	97	9	20
14	6	23	18	50	36	63809	11	1	96	12	27
14	6	23	19	7	58	63878	11	1	106	9	21
14	6	23	19	11	3	63890	11	1	106	8	17
14	6	23	19	21	30	63932	11	1	92	12	27
14	6	23	19	21	50	63935	11	1	104	9	20
14	6	23	19	22	56	63943	11	1	88	9	20
14	6	23	19	25	45	63953	11	1	84	9	20
14	6	23	19	28	23	63962	11	1	104	9	20
14	6	23	19	35	29	63989	11	1	114	10	25
14	6	23	19	40	42	64010	11	1	103	10	25
14	6	23	19	40	47	64011	11	1	110	9	20
14	6	23	19	54	20	64038	11	1	93	9	20

Figure C.1: WIM raw data from Waweig site. Columns 1 – 12

Length (cm)	FrontBumper Space (cm)	RearBumper Space (cm)	GVW (kg)	ESAL	AxleWeight (kg)	Axle Group	SpacingToNext Axle (cm)
2199	76	203	20881	0.2835	5085	1	537
2334	98	254	30232	1.7565	5120	1	623
2166	52	236	29400	1.7025	5466	1	534
615	76	151	9999	0.273	4460	1	388
2319	134	305	23062	0.709	5225	1	486
2413	103	109	31564	1.115	5288	1	470
2200	53	192	23833	0.578	5093	1	512
1242	111	82	10019	0.1719	3518	1	419
2222	62	156	23330	0.449	5141	1	526
1734	93	50	20891	0.384	5206	1	550
2217	64	276	18410	0.3055	5174	1	574
2173	42	309	33763	2.9215	5203	1	524
2257	90	287	32595	2.6075	4851	1	555
2271	93	234	41483	4.9715	4790	1	554
1771	94	86	48164	8.3615	4782	1	553
1807	40	79	40900	7.146	5421	1	532
2153	44	198	34577	3.216	5427	1	524

Figure C.2: WIM raw data from Waweig site. Columns 13 – 20

AxleWeight (kg)	Axle Group	SpacingToNext Axle (cm)	AxleWeight (kg)	Axle Group	SpacingToNext Axle (cm)	AxleWeight (kg)	Axle Group
3940	2	131	3700	2	889	2641	1
6502	2	129	6800	2	1107	5619	2
6836	2	130	6755	2	1090	5081	2
5539	1	0	0	0	0	0	0
5505	2	130	5506	2	1142	3594	2
5165	2	132	5175	2	597	5938	1
4939	2	133	4752	2	1126	4606	1
5176	1	544	639	2	86	686	2
4828	2	131	4626	2	983	2815	1
4557	2	149	4207	2	761	3272	2
4080	2	132	3918	2	1046	2517	2
7418	2	131	7088	2	1043	6872	2
7114	2	131	7275	2	1071	6561	2
8798	2	131	8820	2	1012	6127	3
9104	2	131	9145	2	652	9507	3
8289	2	140	8634	2	891	8953	2
7750	2	131	7676	2	1131	6832	2

Figure C.3: WIM raw data from Waweig site. Columns 21 – 28

SpacingToNext Axle (cm)	AxleWeight (kg)	Axle Group	SpacingToNext Axle (cm)	AxleWeight (kg)	Axle Group	ExternalDataItemTag
181	2660	1	182	2855	1	IMAGE_FN
123	6191	2	0	0	0	IMAGE_FN
124	5262	2	0	0	0	IMAGE_FN
0	0	0	0	0	0	IMAGE_FN
122	3232	2	0	0	0	IMAGE_FN
298	5038	1	704	4960	1	IMAGE_FN
184	4443	1	0	0	0	IMAGE_FN
0	0	0	0	0	0	IMAGE_FN
183	2868	1	181	3052	1	IMAGE_FN
131	3649	2	0	0	0	IMAGE_FN
125	2721	2	0	0	0	IMAGE_FN
124	7182	2	0	0	0	IMAGE_FN
123	6794	2	0	0	0	IMAGE_FN
123	6180	3	124	6768	3	IMAGE_FN
128	8337	3	127	7289	3	IMAGE_FN
125	9603	2	0	0	0	IMAGE_FN
125	6892	2	0	0	0	IMAGE_FN

Figure C.4: WIM raw data from Waweig site. Columns 29 – 35

ExternalDataItemInfo	Temperature (C°)
Image077776_0	20
Image077794_0	20
Image077796_0	20
Image077797_0	20
Image077808_0	20
Image077809_0	20
Image077831_0	20
Image077835_0	20
Image077848_0	20
Image077849_0	20
Image077852_0	20
Image077855_0	20
Image077858_0	20
Image077866_0	20
Image077873_0	20
Image077874_0	20
Image077882_0	20

(e)

Figure C.5: WIM raw data from Waweig site. Columns 36 – 37

## **Appendix D: Raw Permit Database Sample**

Figures D.1 through D.3 show a sample sheet of the raw permit database containing 16 permit applications approved by the NBDTI, where there are 30 columns describing each permit vehicle.

Permit Number	Truck Type	Truck Type Description	Axle weights (kN)				
			1	2	3	4	5
2014-10013	CG 23-2	5-AXLE MOBILE CRANE AND 2-AXLE DOLLY	101	101	93	93	93
2014-10026	13S3	4-AXLE TRACTOR - 3-AXLE SEMITRAILER	59	96	96	96	105
2014-10029	13S3	4-AXLE TRACTOR - 3-AXLE SEMITRAILER	61	96	96	96	92
2014-10035	CG 122-2	5-AXLE MOBILE CRANE AND 2-AXLE DOLLY	104	93	93	93	93
2014-10046	13S3	4-AXLE TRACTOR - 3-AXLE SEMITRAILER	59	96	96	96	105
2014-10047	12S3	3-AXLE TRACTOR AND 3-AXLE SEMITRAILER	59	117	117	96	96
2014-10058	12S3	3-AXLE TRACTOR AND 3-AXLE SEMITRAILER	59	111	111	105	105
2014-10078	13S3	4-AXLE TRACTOR - 3-AXLE SEMITRAILER	59	96	96	96	105
2014-10093	12S3	3-AXLE TRACTOR AND 3-AXLE SEMITRAILER	71	117	117	105	105
2014-10097	13S4	4-AXLE TRACTOR AND 4-AXLE SEMITRAILER	64	96	96	96	83
2014-10109	12S3	3-AXLE TRACTOR AND 3-AXLE SEMITRAILER	62	96	96	96	96
2014-10144	12S4	3-AXLE TRACTOR AND 4-AXLE SEMITRAILER	60	111	111	83	83
2014-10170	13S3	4-AXLE TRACTOR - 3-AXLE SEMITRAILER	59	96	96	96	105
2014-10173	12S3	3-AXLE TRACTOR AND 3-AXLE SEMITRAILER	59	111	111	96	96
2014-10190	13S3	4-AXLE TRACTOR - 3-AXLE SEMITRAILER	59	96	96	96	105
2014-10193	13S3	4-AXLE TRACTOR - 3-AXLE SEMITRAILER	59	96	96	96	105

Figure D.1: Permit database. Columns 1 – 8

Axle weights (kN)								Distance from Previous Axle (m)				
6	7	8	9	10	11	12	13	1	2	3	4	5
78	78	0	0	0	0	0	0	0	2.7	1.7	2	1.7
105	105	0	0	0	0	0	0	0	3.8	1.4	1.4	10.9
92	92	0	0	0	0	0	0	0	5.4	1.4	1.4	12
88	88	0	0	0	0	0	0	0	2.6	1.9	2.1	1.9
105	105	0	0	0	0	0	0	0	3.8	1.4	1.4	10.9
96	0	0	0	0	0	0	0	0	5.5	1.4	11.8	1.3
105	0	0	0	0	0	0	0	0	5.4	1.4	13.5	1.5
105	105	0	0	0	0	0	0	0	4.2	1.4	1.4	10.9
105	0	0	0	0	0	0	0	0	4.6	1.4	10.7	1.5
83	83	83	0	0	0	0	0	0	5.4	1.4	1.4	11.9
96	96	0	0	0	0	0	0	0	4.4	1.4	1.3	10.7
83	83	0	0	0	0	0	0	0	5.6	1.4	19	1.5
105	105	0	0	0	0	0	0	0	4.2	1.4	1.4	10.9
96	0	0	0	0	0	0	0	0	3.2	1.4	7.2	1.2
105	105	0	0	0	0	0	0	0	4.1	1.5	1.5	9.2
105	105	0	0	0	0	0	0	0	4.2	1.4	1.4	10.9

Figure D.2: Permit database. Columns 9 – 21

Distance from Previous Axle (m)								GVW (kN)
6	7	8	9	10	11	12	13	
4.7	1.4	0	0	0	0	0	0	637
1.5	1.5	0	0	0	0	0	0	662
1.8	1.8	0	0	0	0	0	0	625
4.5	1.2	0	0	0	0	0	0	652
1.5	1.5	0	0	0	0	0	0	662
1.3	0	0	0	0	0	0	0	581
1.5	0	0	0	0	0	0	0	596
1.5	1.5	0	0	0	0	0	0	662
1.5	0	0	0	0	0	0	0	620
1.5	1.5	1.5	0	0	0	0	0	684
1.4	1.4	0	0	0	0	0	0	638
1.5	1.8	0	0	0	0	0	0	614
1.5	1.5	0	0	0	0	0	0	662
1.2	0	0	0	0	0	0	0	569
1.5	1.5	0	0	0	0	0	0	662
1.5	1.5	0	0	0	0	0	0	662

Figure D.3: Permit database. Columns 22 – 30

# **Curriculum Vitae**

## **Candidate's full name:**

Diego Gomes Padilha

## **Universities attended:**

University of New Brunswick, B.Sc.E (Civil Engineering), 2013-2017

## **Publications:**

Padilha, D., Araki, Y., Arjomandi, K., & McGinn, J. (2017, September). Vibration Testing of Scaled Cable-Stayed Bridges. In IABSE *Symposium* Report. International Association for Bridge and Structural Engineering.